

## Chapter 4:

# Results and Discussion

This study is a continuation of our ongoing project in physics department (faculty of science, Al-Azher university, Assuit branch, Egypt) related to the measurement of specific activity of  $^{226}\text{Ra}$ ,  $^{232}\text{Th}$  and  $^{40}\text{K}$  in environmental samples from Upper Egypt using a gamma-ray spectrometric technique and estimation of the gamma dose rate from these radionuclides, to obtain the background baseline naturally occurring radionuclides for investigating the environmental impact of anthropogenic radioactive sources. Our present work is focused on measuring the activity concentration of above natural radionuclides in sediment samples in different cities along Red sea coastline, Egypt. The main aim of the radiation protection view point is to study the activity concentrations of naturally occurring radionuclides and the extent of their exposure to population. Radionuclides present in the environmental media are generally found in low concentration. Detection and intensity measurements of weak gamma activities are more and more playing a vital role in physics experiments and industrial investigation. The most important naturally occurring radionuclides present in sediment are not uniformly distributed; the knowledge of their distribution in sea sediments plays an important role in radiation protection and measurement. In minerals, the incorporation of uranium and thorium into the crystal lattice depends on the abundance of these elements in the sediments during crystallization and on the matching of the chemicals properties and the atomic radii of hosts and substitutes. (Huy and Luyen, 2006). The isotopes to interests are  $^{226}\text{Ra}$ ,  $^{232}\text{Th}$  and  $^{40}\text{K}$ .  $^{226}\text{Ra}$  is chosen because the external exposure to the population is mostly by gamma rays emitted from its main daughters  $^{214}\text{Pb}$  and  $^{214}\text{Bi}$ . The contribution of these gamma rays to external dose encompasses  $\sim 98\%$  of all  $\gamma$ -rays from all nuclides in the  $^{238}\text{U}$  series (Huy and Luyen, 2006).

## 1 Activity Concentrations:

### 1.1 Radionuclide Activity Concentrations in Qusier City.

A total of twenty-Seven sediment samples collected from three-areas in **Qusier City** (6 from El-Edua area, 14 from Quseir Harbor and 7 from North Flaminko Village) have been analyzed for the natural radionuclides  $^{226}\text{Ra}$ ,  $^{232}\text{Th}$  and  $^{40}\text{K}$  using ( $\gamma$ -ray spectrometry). The activity concentrations and their corresponding total uncertainties for samples under investigation were listed in Table (3.1): As we can note from Table (3.1): that, the specific activity for  $^{226}\text{Ra}$ ,  $^{232}\text{Th}$  and  $^{40}\text{K}$  of investigated samples from **El-Edua Area** ranged from  $17\pm 2$  to  $38\pm 3$  from  $12\pm 2$  to  $26\pm 3$  and  $89\pm 5$  to  $378\pm 21$  BqKg<sup>-1</sup>, respectively. While its values in **Quseir Harbor Area** ranged from  $5\pm 0.4$  to  $58\pm 5$ , from  $4\pm 1$  to  $47\pm 11$  and from  $15\pm 1$  to  $628\pm 35$  respectively. In the other side, we found the specific radioactivity of natural radionuclide in

**N.FlaminkoVillage** ranged from  $1.8\pm 0.1$  to  $52\pm 6$ , from  $4\pm 1$  to  $35\pm 6$  and from  $34\pm 3$  to  $153\pm 9$ , respectively. The average values of all samples are lower than the corresponding worldwide average values, which are 35, 30 and 400 Bqkg<sup>-1</sup> for <sup>226</sup>Ra, <sup>232</sup>Th and <sup>40</sup>K respectively, (UNSCEAR, 2000).

**Table 3.1:** Activity concentrations of <sup>226</sup>Ra, <sup>232</sup>Th and <sup>40</sup>K (Bqkg<sup>-1</sup>) found in Qusier City.

Samples Location	Sample Name	Activity concentrations(Bqkg <sup>-1</sup> )			Total	contribution%		
		<sup>226</sup> Ra	<sup>232</sup> Th	<sup>40</sup> K		Ra	Th	K
south (El-Edua area)	Q1	32±2	26±3	350±20	408	8	6	86
	Q2	19±2	16±2	104±6	138	14	12	75
	Q3	29±2	26±3	181±10	236	12	11	77
	Q4	38±3	25±3	263±15	325	12	8	81
	Q5	20±2	21±2	378±21	419	5	5	90
	Q6	17±2	12±2	275±15	304	6	4	90
	Q7	19±1	12±1	89±5	119	16	10	74
Middle (Quscir Harbor)	Q8	17±1	19±5	394±23	430	4	5	92
	Q9	27±2	19±2	342±19	388	7	5	88
	Q10	34±2	22±4	325±18	381	9	6	85
	Q11	33±3	13±2	298±17	344	10	4	87
	Q12	29±2	23±2	628±35	680	4	3	92
	Q13	17±1	15±2	267±15	299	6	5	89
	Q14	27±2	17±2	115±7	158	17	10	73
	Q15	28±2	25±3	212±12	265	11	9	80
	Q16	17±1	13±2	101±6	131	13	10	77
	Q17	58±5	33±3	101±6	192	30	17	53
	Q18	5±0.4	4±1	15±1	27	19	15	66
	Q19	35±4	47±11	613±36	695	5	7	88
	Q20	13±1	14±2	447±25	474	3	3	94
Q21	21±2	23±5	355±21	398	5	6	89	
North(N.Fla- minko Village)	Q22	28±2	35±6	153±9	215	13	16	71
	Q23	30±2	30±3	139±8	198	15	15	70
	Q24	52±6	34±5	89±5	174	30	19	51
	Q25	2±0.1	4±1	34±3	39	3	10	87
	Q26	29±2	19±2	126±7	175	17	11	72
	Q27	15±2	14±1	98±6	127	12	11	77
MIN		1	4	18	27	1	0.2	51
MAX		58	47	628	692	30	19	99
AVEG		26	21	240	287	11	9	80
STDEV		12	10	163	169	7	5	12
S.E		2	2	31	32	1	1	2
SKEWNESS		0.59	0.64	0.83	0.78	1.25	0.64	-1.05
KURTOSIS		1.29	0.98	0.24	0.54	1.65	-0.42	0.87

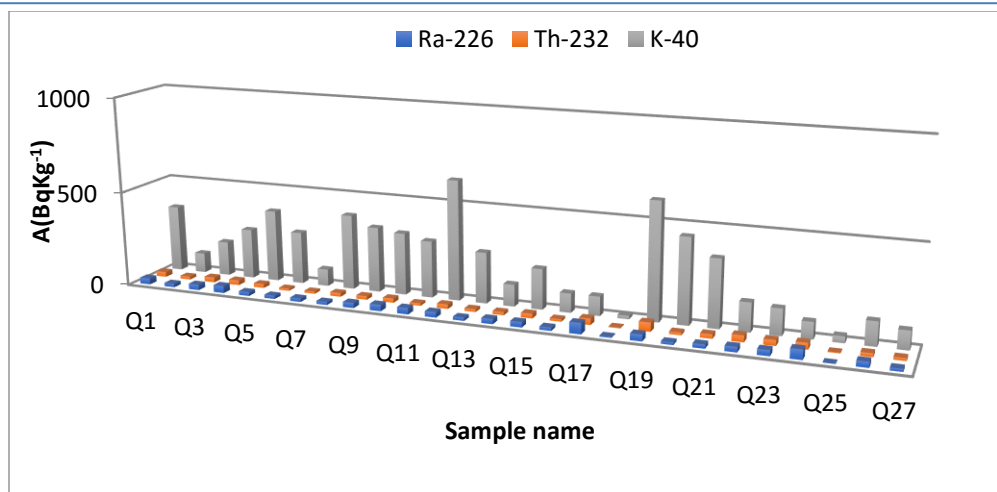


**Figure 3.1:** Activity concentrations of the radioelements ( $Bqkg^{-1}$ ) found in Quseir City samples.

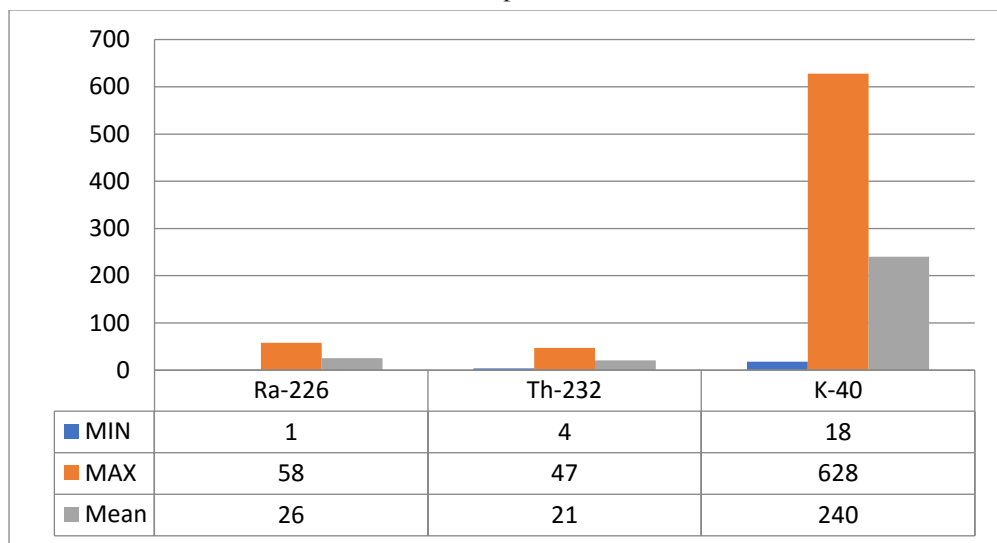


**Figure 3.2:** Distribution of (Mean, Max and Min) of  $^{226}Ra$ ,  $^{232}Th$  and  $^{40}K$  in Quseir City

Figures, 3.1 and 3.2 show the activity concentrations and (Mean, Max and Min) Distribution of  $^{226}Ra$ ,  $^{232}Th$  and  $^{40}K$  in graphical form for the sediment samples in **Quseir City**. From the obtained result, it is evident that activity concentration of  $^{40}K$  is much higher than that of other radionuclides; this is a common occurrence in normal geological materials. Average values concentration of  $^{40}K$  in samples under investigation are somewhat lower than the world average value,  $400 Bqkg^{-1}$ (UNSCEAR, 2000; Merdanoğlu and Altınsoy, 2006). Thorium series activities are lower than Uranium series activities this may be due to thorium is less abundant in nature than uranium, and thorium is largely transported in insoluble resistant minerals. (UNSCEAR, 2000)

The frequency distributions of activity concentration of all the radionuclides were analyzed, and the histograms are given in Figures 3.3 and 3.5. The graphs of  $^{226}\text{Ra}$  and  $^{232}\text{Th}$  show that these radionuclides demonstrate a normal (bell-shape) distribution. But  $^{40}\text{K}$  exhibited some degree of multi-modality. This multi-modal feature of the radioelements demonstrates the complexity of Quseir samples.

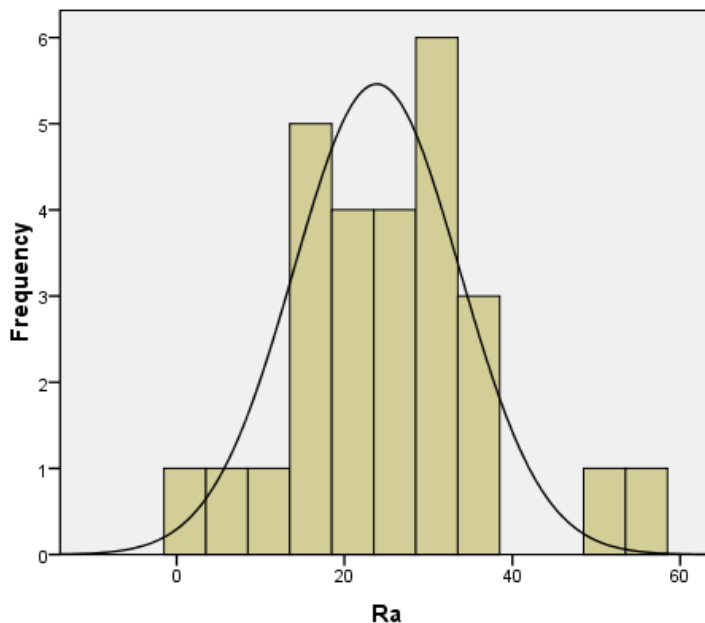


**Figure 3.3:** The frequency distributions of Ra-226 found in Quseir City samples

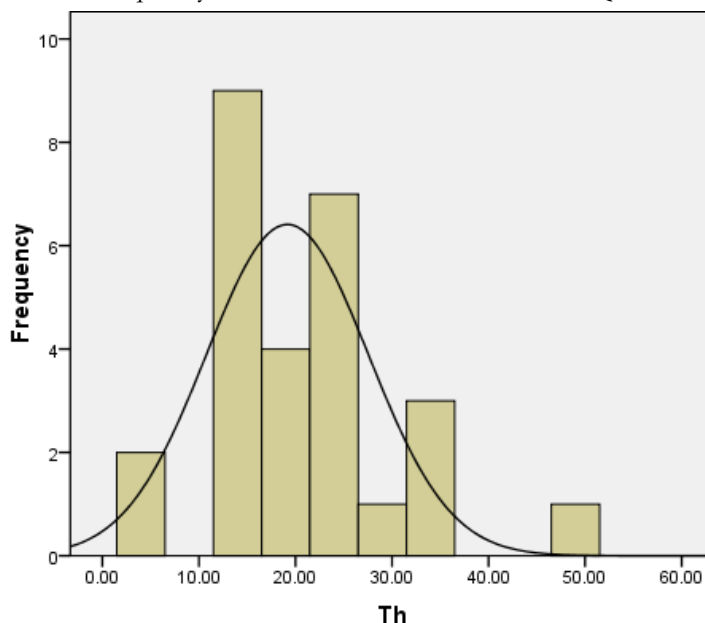


**Figure 3.4:** The frequency distributions of Th-232 found in Quseir City samples

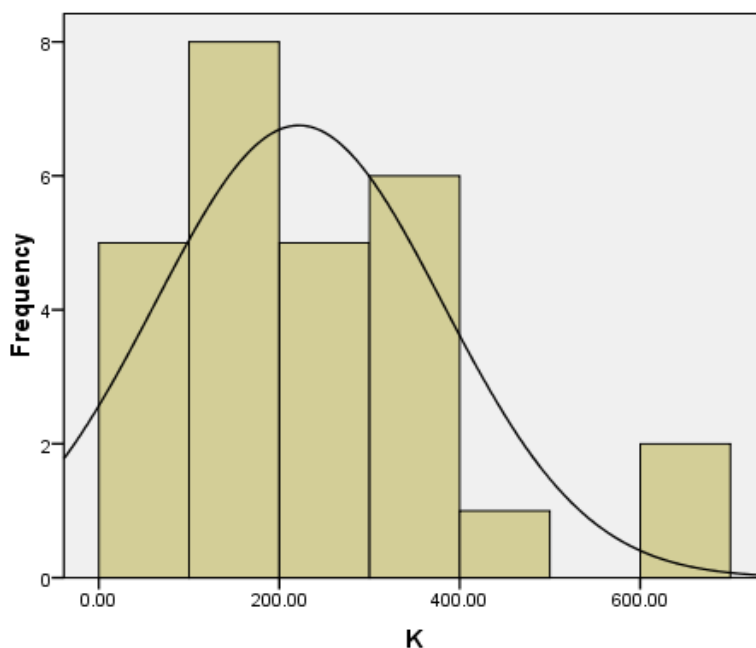


**Figure 3.5:** frequency distributions of K-40 found in Quseir City samples

Table 3.1: presents the basic statistics were used to describe the statistical characteristics of the radionuclide activities. SKEWNESS is a measure of the asymmetry of the probability distribution of a real-valued random variable. The normal distribution has a skewness of zero. However, in reality, data points may not be perfectly symmetric. Therefore, an understanding of the skewness of the data set indicates whether deviations from the mean are likely to be positive or negative. Skewness characterizes the degree of asymmetry of a distribution around its mean (Groeneveld and Meeden, 1984). Positive skewness indicates a distribution with an asymmetric tail extending towards values that are more positive. Negative skewness indicates a distribution with an asymmetric tail extending towards values that are more negative. Lower skewness values indicate generally normal distributions. The skewness values of activity concentrations of  $^{226}\text{Ra}$ ,  $^{232}\text{Th}$  and  $^{40}\text{K}$  in Qusier city are 0.59 and 0.64 and 0.83 respectively; these small skewness values in Table (3.1), indicate that the distributions of activity concentrations  $^{226}\text{Ra}$ ,  $^{232}\text{Th}$  and  $^{40}\text{K}$  are asymmetric in nature

Kurtosis is a measure of the peakedness of the probability distribution of a real-valued random variable. It characterizes the relative peakedness or flatness of a distribution compared with the normal distribution (Ravisankar, at al., 2014). Positive kurtosis indicates a relatively peaked distribution, as in case of  $^{226}\text{Ra}$ ,  $^{232}\text{Th}$  and  $^{40}\text{K}$ . Higher kurtosis means that more of the variance is the result of infrequent extreme deviations, as opposed to frequent modestly sized deviations; this appears in case of  $^{226}\text{Ra}$ .

### 1.1.1 Correlation and Concentration Ratio of Natural Radionuclides in Sediment Samples from Qusier City

From the activity concentration of  $^{226}\text{Ra}$ ,  $^{232}\text{Th}$  and  $^{40}\text{K}$  values, which have been listed in Table (3.1), the relationships between these radionuclides in sediments samples under investigation were computed in Table (3.2)

**Table 3.2:** Activity ratios between natural radionuclides in sediment samples from Qusier city, Egypt.

Sample	$^{232}\text{Th}/^{226}\text{Ra}$	$^{232}\text{Th}/^{40}\text{K}$	$^{226}\text{Ra}/^{40}\text{K}$
Q1	0.80	0.07	0.09
Q2	0.85	0.15	0.18
Q3	0.90	0.14	0.16
Q4	0.67	0.10	0.14
Q5	1.01	0.05	0.05
Q6	0.69	0.04	0.06
Q7	0.62	0.13	0.21
Q8	1.17	0.05	0.04
Q9	0.69	0.06	0.08
Q10	0.66	0.07	0.10
Q11	0.39	0.04	0.11
Q12	0.80	0.04	0.05
Q13	0.90	0.06	0.06
Q14	0.62	0.14	0.23
Q15	0.88	0.12	0.13
Q16	0.75	0.13	0.17
Q17	0.57	0.33	0.57
Q18	0.75	0.22	0.29
Q19	1.36	0.08	0.06
Q20	1.04	0.03	0.03
Q21	1.08	0.06	0.06
Q22	1.26	0.23	0.18
Q23	1.00	0.21	0.21
Q24	0.66	0.38	0.58
Q25	3.01	0.11	0.04
Q26	0.65	0.15	0.23
Q27	0.96	0.15	0.15
Minimum	0.39	0.03	0.03
Maximum	3.01	0.38	0.58
Average	0.92	0.12	0.16

The ratio of  $^{232}\text{Th}/^{226}\text{Ra}$ ,  $^{232}\text{Th}/^{40}\text{K}$  and  $^{226}\text{Ra}/^{40}\text{K}$  for all samples under investigation are 0.92, 0.12 and 0.16 respectively. In Figure 3.6 (a, b and c), show  $^{232}\text{Th}/^{226}\text{Ra}$ ,  $^{232}\text{Th}/^{40}\text{K}$  and  $^{226}\text{Ra}/^{40}\text{K}$  activity concentration ratios. From the values of  $^{232}\text{Th}/^{226}\text{Ra}$  we can conclude that there is a good correlation between  $^{232}\text{Th}$  and  $^{226}\text{Ra}$ . On other sides for ratio values of  $^{232}\text{Th}/^{40}\text{K}$  and  $^{226}\text{Ra}/^{40}\text{K}$  indicate that the  $^{40}\text{K}$  concentration always high.

Figure 3. (7-a): shows moderate correlation between  $^{232}\text{Th}$  and  $^{226}\text{Ra}$  with correlation factor ( $R=0.748$ ), while we found weak correlation between  $^{232}\text{Th}$  and  $^{40}\text{K}$  with correlation coefficients ( $R=0.363$ ), in Figure 3. (7-b). Also the correlation between  $^{226}\text{Ra}$  and  $^{40}\text{K}$  are weak with correlation coefficient ( $R=0.346$ ) as shown in Figure 3. (7-c).

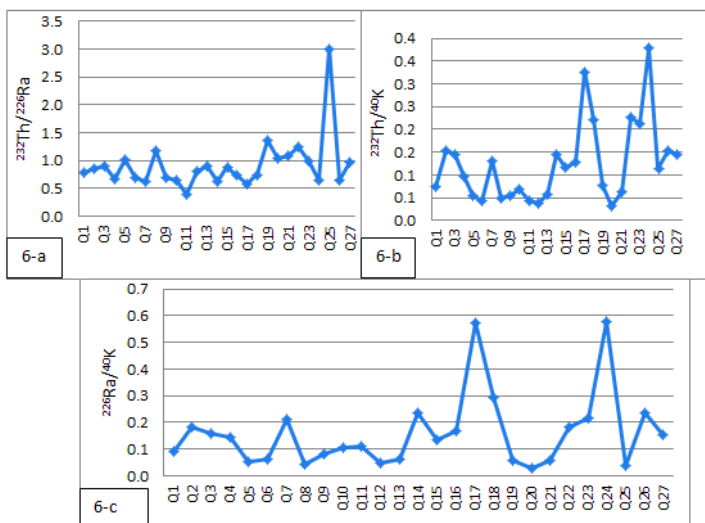


Figure 3.7:  $^{232}\text{Th} / ^{226}\text{Ra}$ ,  $^{232}\text{Th} / ^{40}\text{K}$  and  $^{226}\text{Ra} / ^{40}\text{K}$  in sediment samples from Qusier, Egypt.

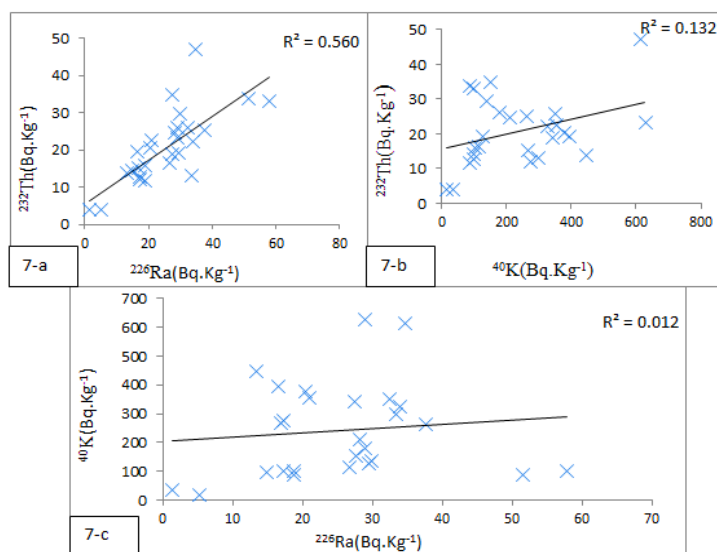


Figure 3.6: Correlation between natural radionuclides in sediment samples from Qusier city

## 1.2 Radionuclide Activity Concentrations in Safaga City

The measured activity concentrations of  $^{226}\text{Ra}$ ,  $^{232}\text{Th}$  and  $^{40}\text{K}$  in sediment samples from Safaga City are presented in Table (3.3). It shows that, the highest values for the specific activities of  $^{226}\text{Ra}$ ,  $^{232}\text{Th}$  are  $53\pm 4$  and  $34\pm 3$  in (Abu Tartour Harbour), while the highest value of  $^{40}\text{K}$  ( $821\pm 46$  Bqkg $^{-1}$ ), found in Touristic Harbour respectively. The lowest observed values of the specific activities of the same radionuclides are  $7\pm 1$ ,  $6\pm 1$  and  $196\pm 11$  Bqkg $^{-1}$  in (Km 17 Mangrove area), respectively. As it appear from Table (3.3), the activity of  $^{226}\text{Ra}$  varies from 7 to 53 Bqkg $^{-1}$  with average equal 22 Bqkg $^{-1}$ . The activity concentration values of  $^{232}\text{Th}$  ranged from 6 to 34 Bqkg $^{-1}$ , and it is average value is 19 Bqkg $^{-1}$ . The activity concentration of  $^{40}\text{K}$  varies from 196 to 821 Bqkg $^{-1}$ , and the average is 478 Bqkg $^{-1}$ .

**Table 3.3:** Activity concentrations of the radioelements of  $^{226}\text{Ra}$ ,  $^{232}\text{Th}$  and  $^{40}\text{K}$  (Bqkg $^{-1}$ ) found in Safaga City

Samples Location	Sample Name	Activity concentrations(Bqkg $^{-1}$ )			Total	contribution%		
		$^{226}\text{Ra}$	$^{232}\text{Th}$	$^{40}\text{K}$		Ra	Th	K
South(Km 17 Mangrove area)	S1	14±1	24±3	339±19	377	4	6	90
	S2	7±1	6±1	196±11	209	4	3	93
	S3	17±1	19±2	481±27	517	3	4	93
	S4	13±1	22±4	604±34	639	2	3	95
	S5	19±1	17±2	288±16	325	6	5	89
	S6	14±1	13±2	207±20	234	6	6	88
Middle (Abu-Tartour Harbour)	S7	53±4	34±3	511±29	598	9	6	85
	S8	32±3	14±2	386±22	432	7	3	89
	S9	24±1	21±2	398±22	444	5	5	90
	S10	15±1	18±2	378±21	410	4	4	92
	S11	43±3	17±2	515±29	575	7	3	90
	S12	14±1	18±2	390±22	422	3	4	93
North (Touristic Harbour)	S13	31±3	20±2	644±37	694	4	3	93
	S14	25±2	32±3	635±35	692	4	5	92
	S15	15±1	15±3	736±41	765	2	2	96
	S16	14±1	17±2	821±46	852	2	2	96
	S17	15±1	16±2	740±42	771	2	2	96
	S18	35±3	23±5	327±18	386	9	6	85
MIN		7	6	196	209	2	2	85
MAX		53	34	821	852	9	6	96
AVEG		22	19	478	519	5	4	91
STDEV		12	6	186	189	2	1	3
S.E		3	2	44	45	1	0.3	1
SKEWNESS		1.3	0.7	0.3	0.1	0.6	0.1	-0.3
KURTOSIS		1.1	1.4	-0.9	-1.0	-0.7	-1.1	-0.5



The average values of activity concentrations of  $^{226}\text{Ra}$  and  $^{232}\text{Th}$  are lower than the corresponding worldwide average values, ( $35$  and  $30 \text{ Bqkg}^{-1}$ ) while, the average value of  $^{40}\text{K}$  is higher than the corresponding worldwide average values, which  $400 \text{ Bqkg}^{-1}$ , (UNSCEAR, 2000). Figures 3.8 and 3.9: show the activity concentrations and (Mean, Max and Min) distribution of  $^{226}\text{Ra}$ ,  $^{232}\text{Th}$  and  $^{40}\text{K}$  for the sediment samples in Safaga City in graphical form.

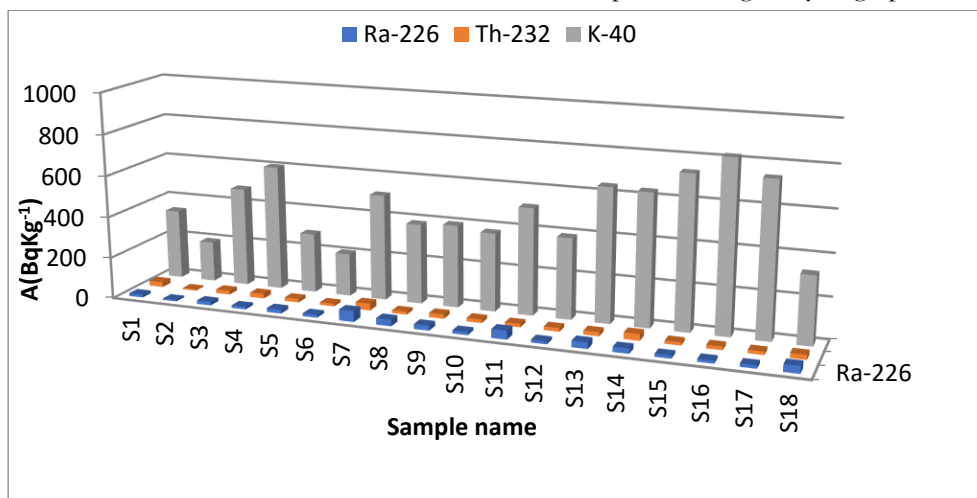


**Figure 3.8:** Activity concentrations of the radioelements ( $\text{Bqkg}^{-1}$ ) found in Safaga City samples

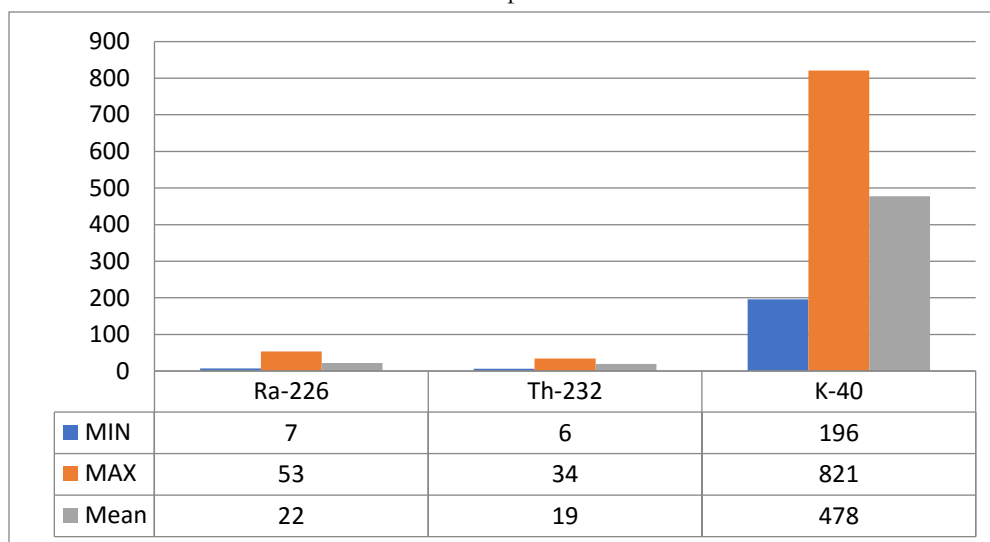


**Figure 3.9:** Distribution of  $^{226}\text{Ra}$ ,  $^{232}\text{Th}$  and  $^{40}\text{K}$  in Safaga City

The frequency distributions of all the radionuclides in sediments samples were analyzed, and the histograms are given in Figures (3.10) to (3.12). The graphs of  $^{226}\text{Ra}$ ,  $^{232}\text{Th}$  and  $^{40}\text{K}$  show that these radionuclides demonstrate a normal (bell-shape) distribution.

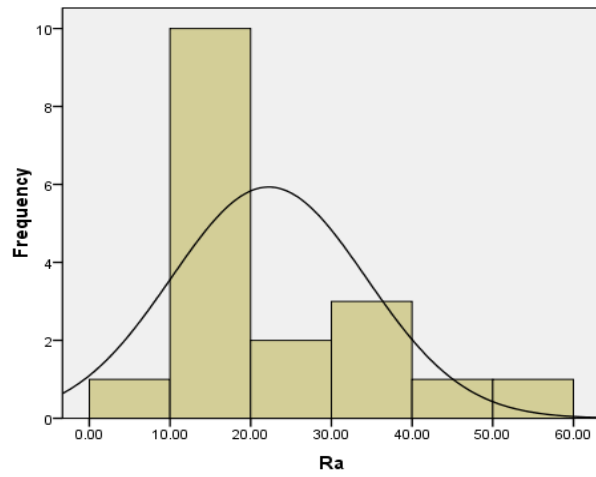


Figure 3.10: The frequency distributions of Ra-226 of Safaga City samples

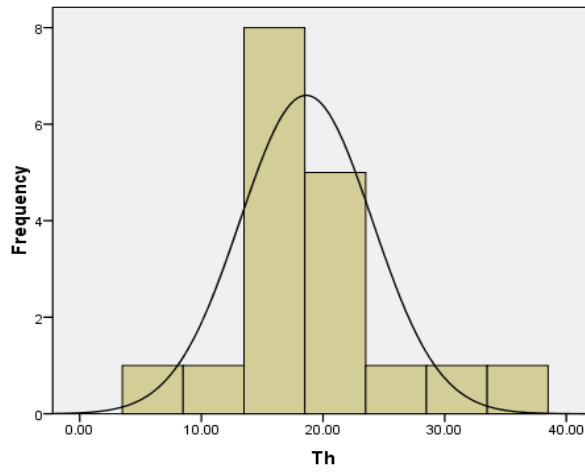


Figure 3.11: The frequency distributions of Th-232 found in Safaga City samples

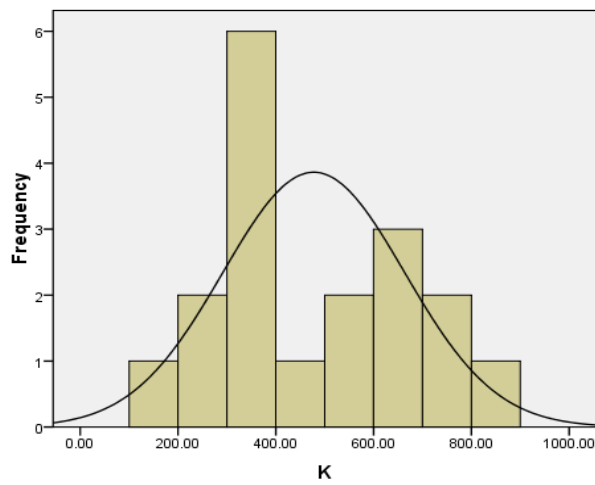


Figure 3.12: Frequency distributions of K-40 found in Safaga City samples

Table 3.3: presents the Positive skewness in Safaga samples, which, indicates a distribution with an asymmetric tail extending towards values that are more positive. The activity concentrations of  $^{226}\text{Ra}$ ,  $^{232}\text{Th}$  and  $^{40}\text{K}$  in this Safaga city are 1.3, 0.7 and 0.3, respectively; small skewness values Table (3.3), which indicate that the distributions are asymmetric in nature. In Safaga city, the  $^{226}\text{Ra}$ , and  $^{232}\text{Th}$  have positive kurtosis value Table (3.3), indicating peaked distribution. While the  $^{40}\text{K}$  distributions have negative kurtosis values indicating flat distributions.

### 1.2.1 Correlation and Concentration Ratio of Natural Radionuclides in Sediment Samples from Safaga City

From the activity concentration of  $^{226}\text{Ra}$ ,  $^{232}\text{Th}$  and  $^{40}\text{K}$  given in Table 3.3, the relationships between these radionuclides in sediments samples under investigation were computed and diagrammatically plotted as shown in Table 3.4, and Figure 3.13. Figure 3. (13-a) shows moderate correlation between  $^{232}\text{Th}$  and  $^{226}\text{Ra}$  with Correlation Coefficient ( $R=0.541$ ), while correlation coefficients is weak between  $^{232}\text{Th}$  and  $^{40}\text{K}$  with Correlation Coefficient ( $R=0.251$ ) in figure 3. (13-b). Also we found no correlation between  $^{40}\text{K}$  and  $^{226}\text{Ra}$  with factor ( $R=0.054$ ) figure 3. (13-c).

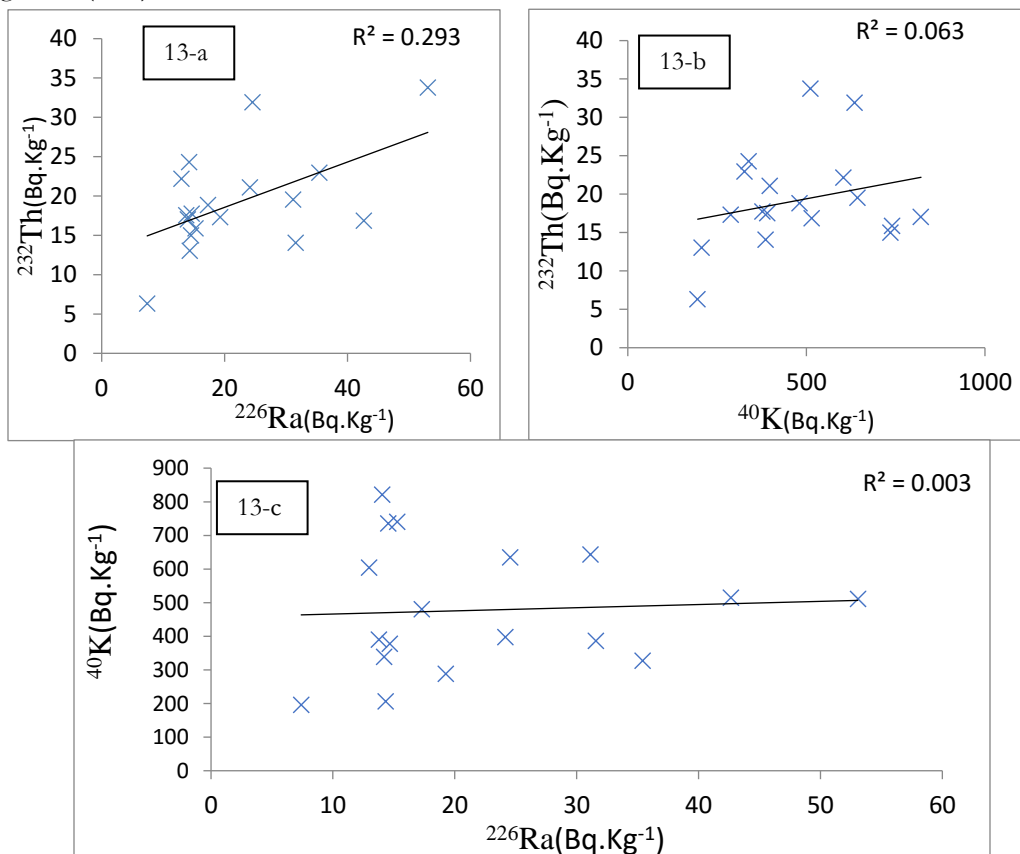


Figure 3.13. Correlation between natural radionuclides in sediment samples from Safaga

The mean values of  $^{232}\text{Th}/^{226}\text{Ra}$ ,  $^{232}\text{Th}/^{40}\text{K}$  and  $^{226}\text{Ra}/^{40}\text{K}$  ratios for all samples under investigation are 0.99, 0.04 and 0.05 respectively. In Figure 3.14 show  $^{232}\text{Th}/^{226}\text{Ra}$ ,  $^{232}\text{Th}/^{40}\text{K}$  and  $^{226}\text{Ra}/^{40}\text{K}$  activity concentration ratios.

**Table 3.4:** Activity ratios between natural radionuclides in sediment samples from Safaga city, Egypt.

sample	$^{232}\text{Th}/^{226}\text{Ra}$	$^{232}\text{Th}/^{40}\text{K}$	$^{226}\text{Ra}/^{40}\text{K}$
S1	1.71	0.07	0.04
S2	0.86	0.03	0.04
S3	1.09	0.04	0.04
S4	1.71	0.04	0.02
S5	0.90	0.06	0.07
S6	0.91	0.06	0.07
S7	0.64	0.07	0.10
S8	0.45	0.04	0.08
S9	0.87	0.05	0.06
S10	1.21	0.05	0.04
S11	0.40	0.03	0.08
S12	1.28	0.05	0.04
S13	0.63	0.03	0.05
S14	1.30	0.05	0.04
S15	1.03	0.02	0.02
S16	1.21	0.02	0.02
S17	1.04	0.02	0.02
S18	0.65	0.07	0.11
Minimum	0.40	0.02	0.02
Maximum	1.71	0.07	0.11
Average	0.99	0.04	0.05

From the values of  $^{232}\text{Th}/^{226}\text{Ra}$  we can conclude that there is a good correlation between  $^{232}\text{Th}$  and  $^{226}\text{Ra}$ . On other sides for ratio values of  $^{232}\text{Th}/^{40}\text{K}$  and  $^{226}\text{Ra}/^{40}\text{K}$  indicate that the  $^{40}\text{K}$  concentration always high.

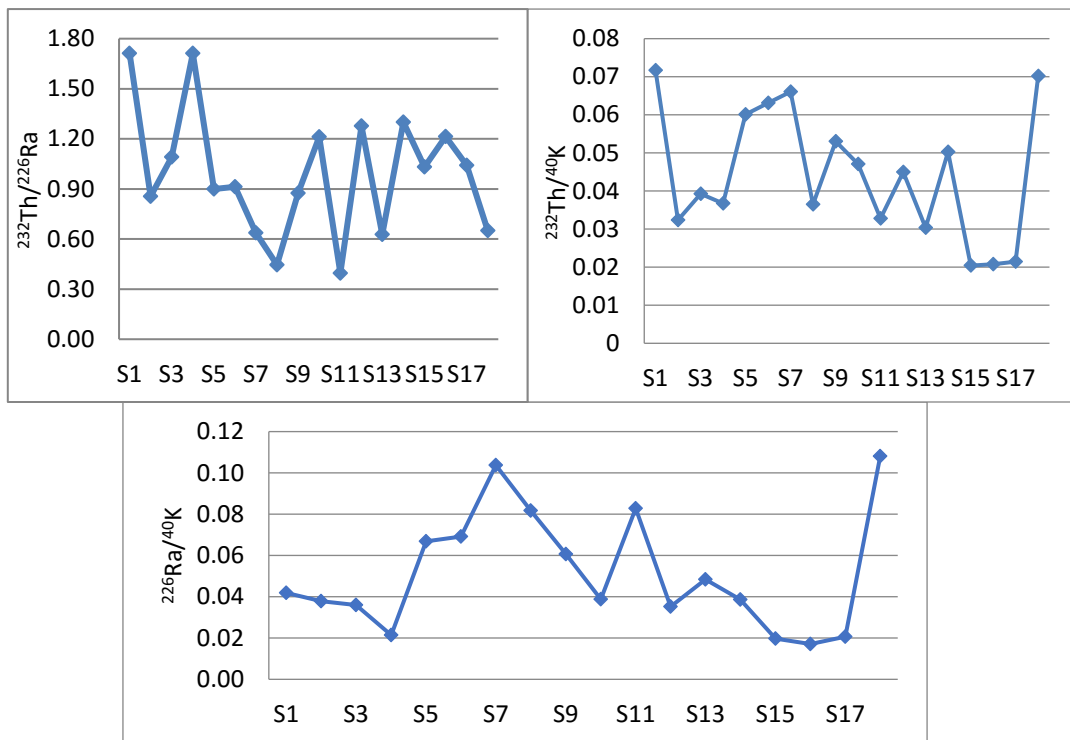


**Figure 3.14:**  $^{232}\text{Th} / ^{226}\text{Ra}$ ,  $^{232}\text{Th} / ^{40}\text{K}$  and  $^{226}\text{Ra} / ^{40}\text{K}$  ratios in sediment samples from Safaga, Egypt.

### 1.3 Radionuclide Activity Concentrations in Hurghada City

The measured activity concentrations of  $^{226}\text{Ra}$ ,  $^{232}\text{Th}$  and  $^{40}\text{K}$  in sediment samples from Hurghada City are presented in Table 3.5. It shows that, the highest values observed for the specific activities of  $^{226}\text{Ra}$ ,  $^{232}\text{Th}$  and  $^{40}\text{K}$  are  $53 \pm 4$ ,  $32 \pm 6$  and  $1120 \pm 63$  Bqkg<sup>-1</sup> in (NIOF area), respectively, while the lowest observed values of the specific activities of the same radionuclides are  $5 \pm 1$ ,  $2 \pm 1$  and  $36 \pm 2$  Bqkg<sup>-1</sup> in (Hurghada Harbor), respectively. As it appears in table 3.5, the activity of  $^{226}\text{Ra}$  varies from 5 to 53 Bqkg<sup>-1</sup> with average equal 19 Bqkg<sup>-1</sup>. The activity concentration of  $^{232}\text{Th}$  varies from 2 to 32 Bqkg<sup>-1</sup>, and it's average is 15 Bqkg<sup>-1</sup>. The activity concentration of  $^{40}\text{K}$  ranged from 36 to 1120 Bqkg<sup>-1</sup>, and it's average is 432 Bqkg<sup>-1</sup>.

**Table 3.5:** Activity concentrations of the radioelements of  $^{226}\text{Ra}$ ,  $^{232}\text{Th}$  and  $^{40}\text{K}$  ( $\text{Bqkg}^{-1}$ ) found in Hurghada City.

Samples Location	Sample Name	Activity concentrations( $\text{Bqkg}^{-1}$ )			Total	contribution%		
		$^{226}\text{Ra}$	$^{232}\text{Th}$	$^{40}\text{K}$		Ra	Th	K
South( north Safir Hotel	H1	7±1	7±1	167±11	181	4	4	93
	H2	12±1	10±2	240±13	262	4	4	92
	H3	27±2	26±3	431±24	484	5	5	89
	H4	13±1	22±3	598±34	633	2	3	94
	H5	11±1	6±1	323±20	341	3	2	95
	H6	10±1	14±2	287±16	312	3	5	92
Middle Hurghada Harbor	H7	26±2	15±1	429±26	470	6	3	91
	H8	5±1	2±1	36±2	43	12	4	84
	H9	8±1	7±1	118±7	134	6	5	89
	H10	11±1	8±2	950±53	969	1	1	98
	H11	15±1	21±2	731±41	767	2	3	95
	H12	17±2	23±2	672±38	712	2	3	94
North NIOF area	H13	21±2	15±3	384±22	419	5	3	91
	H14	20±2	21±4	293±17	334	6	6	88
	H15	8±1	11±2	247±14	266	3	4	93
	H16	39±3	32±6	431±25	502	8	6	86
	H17	53±4	14±2	1120±63	1187	4	1	94
	H18	15±1	12±1	410±23	438	4	3	94
	H19	38±3	30±3	498±28	566	7	5	88
	H20	22±2	6±1	376±21	405	6	2	93
	H21	22±2	16±3	329±19	367	6	4	90
MIN		5	2	36	43	1	1	84
MAX		53	32	1120	1187	12	6	98
AVEG		19	15	432	466	5	4	92
STDEV		12	8	263	273	2	2	3
S.E		3	2	57	60	1	0.3	1
SKEWNESS		1.4	0.5	1.1	1.1	1.2	-0.1	-0.5
KURTOSIS		1.8	-0.4	1.4	1.4	2.6	-0.5	0.01

The average values of activity concentrations of  $^{226}\text{Ra}$  and  $^{232}\text{Th}$  are less than the corresponding worldwide average values, which are 35 and 30  $\text{Bqkg}^{-1}$  for  $^{226}\text{Ra}$ ,  $^{232}\text{Th}$ , respectively, except average value of  $^{40}\text{K}$  is higher than 400  $\text{Bqkg}^{-1}$ , which is the corresponding worldwide average values, (UNSCEAR, 2000). Figure 3.15 and 3.16 shows the activity concentrations and (Mean, Max and Min) distribution of  $^{226}\text{Ra}$ ,  $^{232}\text{Th}$  and  $^{40}\text{K}$  for the sediment samples in Hurghada City.

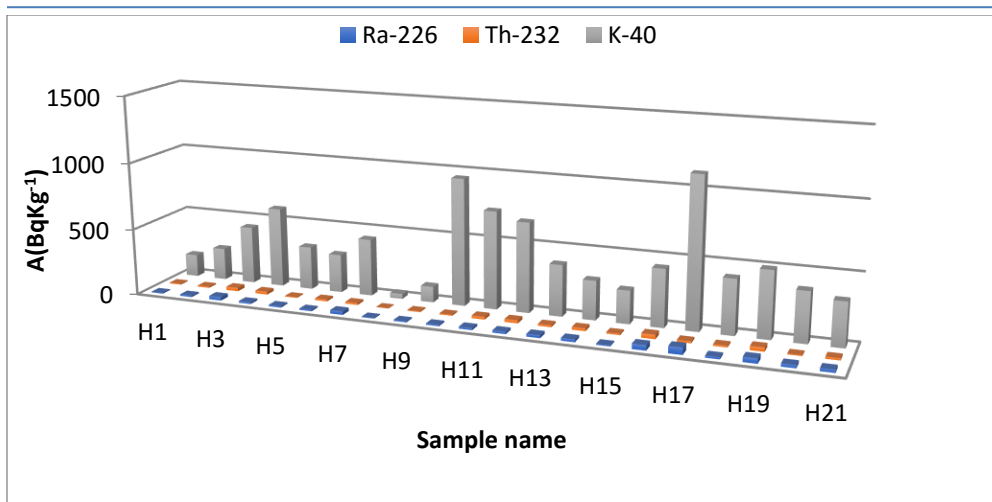


Figure 3.15: Activity concentrations of the radioelements ( $Bqkg^{-1}$ ) found in Hurchada City samples.

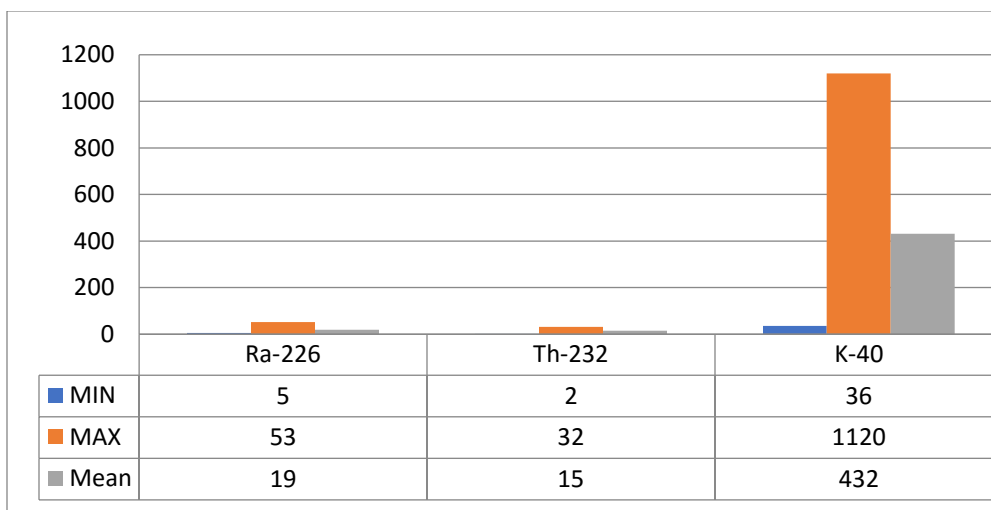


Figure 3.16: Distribution of  $^{226}Ra$ ,  $^{232}Th$  and  $^{40}K$  in Hurchada City

The Frequency distributions of the radionuclides from Hurchada samples were analyzed, and the histograms are given in Figures. (3.17) to (3.19). The graphs of  $^{226}Ra$  and  $^{40}K$  show that the radionuclides are exhibited some degree of multi-modality. This multi-modal feature of the radio-elements demonstrates the complexity of sediments samples but the graphs of  $^{232}Th$  show that these radionuclides demonstrate a normal (bell-shape) distribution

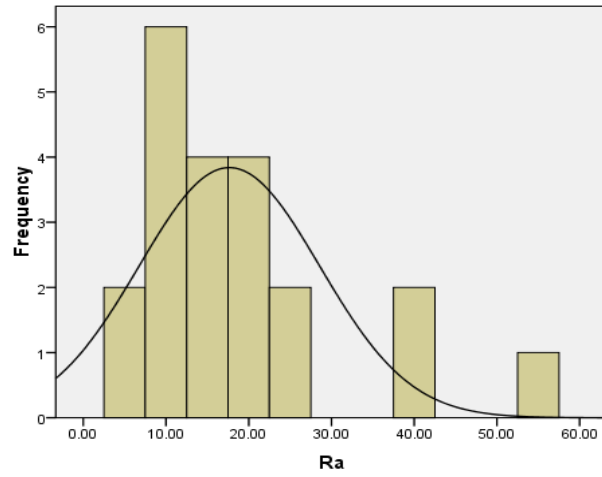


Figure 3.17: The frequency distributions of Ra-226 found in Hurgbada City samples

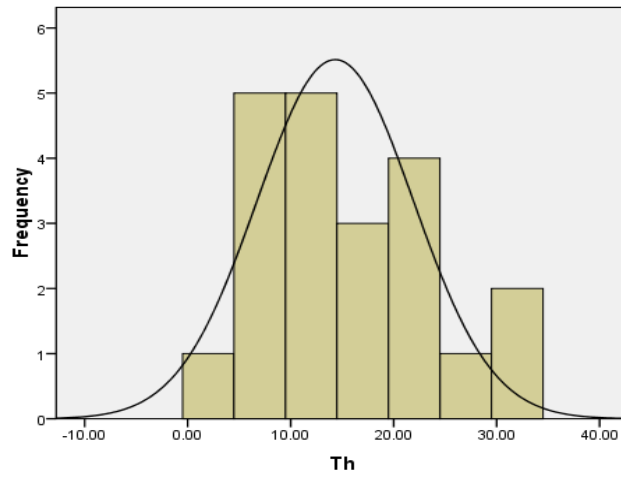


Figure 3.18: The frequency distributions of Th-232 found in Hurgbada City samples

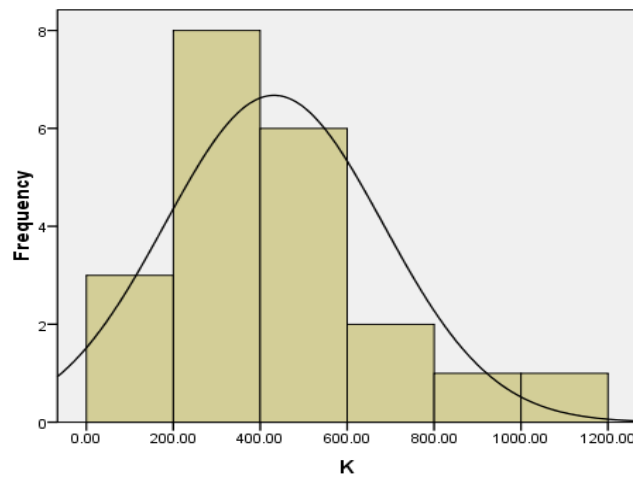


Figure 3.19: Frequency distributions of K-40 found in Hurgbada City samples



Table 3.5 presents the positive skewness in Hurghada samples, which, indicates a distribution with an asymmetric tail extending towards values that are more positive. The activity concentrations of  $^{226}\text{Ra}$ ,  $^{232}\text{Th}$  and  $^{40}\text{K}$  in this Hurghada city are 1.4, 0.5 and 1.1, respectively; small skewness values (Table 3.5), which indicate that the distributions are asymmetric in nature. In Hurghada city, the  $^{226}\text{Ra}$  and  $^{40}\text{K}$  distributions have positive kurtosis value (Table 3.5), indicating peaked distribution, while the  $^{232}\text{Th}$  has negative kurtosis values indicating flat distributions

### 1.3.1 Correlation and Concentration Ratio of Natural Radionuclides in Sediment Samples from Hurghada City

From the activity concentration of  $^{226}\text{Ra}$ ,  $^{232}\text{Th}$  and  $^{40}\text{K}$  given in Table (3.5), the relationships between these radionuclides in sediments samples under investigation were computed and diagrammatically plotted as shown in Table (3.6), and Figure (3.20).

Figure 3. (20-a) shows moderate correlation between  $^{232}\text{Th}$  and  $^{226}\text{Ra}$  with correlation coefficients ( $R=0.589$ ). While the correlation between  $^{232}\text{Th}$  and  $^{40}\text{K}$  is weak and equal ( $R=0.322$ ), as we in figure 3. (20-b). Also we found moderate correlation between  $^{40}\text{K}$  and  $^{226}\text{Ra}$  with correlation coefficient ( $R=0.541$ ) as shown in figure 3. (20-c).

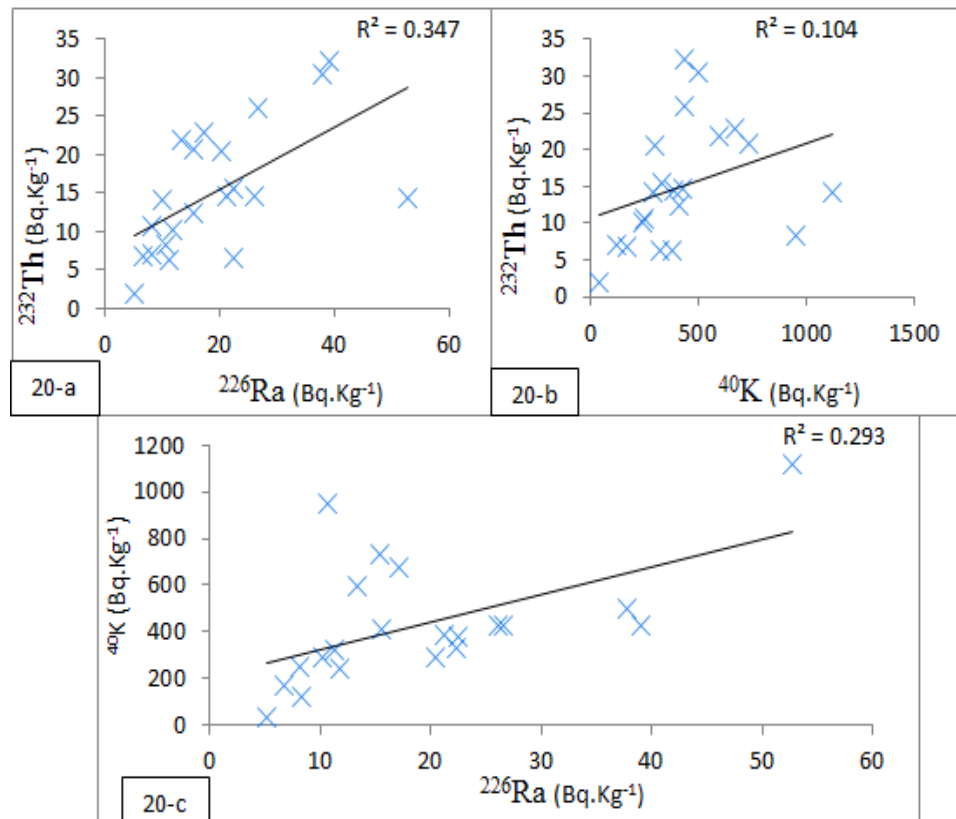


Figure 3.20: Correlation between natural radionuclides in sediment samples from Hurghada city

The mean values of  $^{232}\text{Th}/^{226}\text{Ra}$ ,  $^{232}\text{Th}/^{40}\text{K}$  and  $^{226}\text{Ra}/^{40}\text{K}$  ratios for all samples under investigation are 0.88, 0.04 and 0.05 respectively. Figure 3.21, show  $^{232}\text{Th}/^{226}\text{Ra}$ ,  $^{232}\text{Th}/^{40}\text{K}$  and  $^{226}\text{Ra}/^{40}\text{K}$  activity concentration ratios.

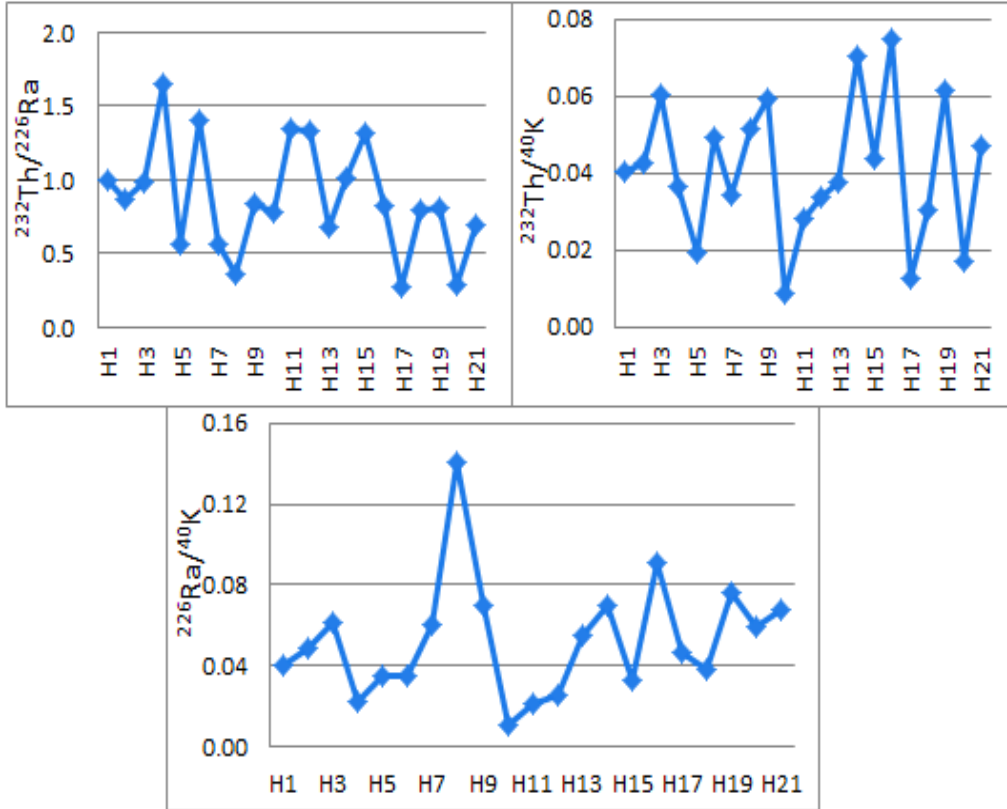


Figure 3.21:  $^{232}\text{Th} / ^{226}\text{Ra}$ ,  $^{232}\text{Th} / ^{40}\text{K}$  and  $^{226}\text{Ra} / ^{40}\text{K}$  ratios in sediment samples from Hurghada, Egypt

Table 3.6: Activity ratios between natural radionuclides in sediment samples from Hurghada city, Egypt

sample	$^{232}\text{Th}/^{226}\text{Ra}$	$^{232}\text{Th}/^{40}\text{K}$	$^{226}\text{Ra}/^{40}\text{K}$
H1	1.004	0.040	0.040
H2	0.870	0.042	0.049
H3	0.979	0.060	0.061
H4	1.646	0.037	0.022
H5	0.561	0.020	0.035
H6	1.405	0.049	0.035
H7	0.563	0.034	0.061
H8	0.366	0.051	0.141
H9	0.844	0.059	0.070

H10	0.778	0.009	0.011
H11	1.346	0.028	0.021
H12	1.329	0.034	0.026
H13	0.687	0.038	0.055
H14	1.010	0.070	0.070
H15	1.324	0.043	0.033
H16	0.827	0.075	0.091
H17	0.270	0.013	0.047
H18	0.799	0.030	0.038
H19	0.807	0.061	0.076
H20	0.286	0.017	0.060
H21	0.695	0.047	0.068
Minimum	0.27	0.01	0.01
Maximum	1.65	0.07	0.14
Average	0.88	0.04	0.05

#### 1.4 Radionuclide Activity Concentrations in Gharib City

The measured activity concentrations of  $^{226}\text{Ra}$ ,  $^{232}\text{Th}$  and  $^{40}\text{K}$  in sediment samples from Gharib City are presented in Table (3.7), that shows the highest values observed for the specific activities of  $^{226}\text{Ra}$ ,  $^{232}\text{Th}$  and  $^{40}\text{K}$  are  $52\pm 4$ ,  $45\pm 5$  and  $1640\pm 93$   $\text{Bqkg}^{-1}$  in (General company of Petroleum), respectively, while the lowest observed values of the specific activities of the same radionuclides are  $6\pm 0.4$  and  $8\pm 2$  (in General Beach) and  $86\pm 5$   $\text{Bqkg}^{-1}$  (in General company of Petroleum), respectively. As shown in Table 3.7, the activity of  $^{226}\text{Ra}$  ranged from 6 to 52  $\text{Bqkg}^{-1}$  with average is 28  $\text{Bqkg}^{-1}$ . The activity concentration of  $^{232}\text{Th}$  varies from 8 to 45  $\text{Bqkg}^{-1}$ , and it is average equal 24  $\text{Bqkg}^{-1}$ . The activity concentration of  $^{40}\text{K}$  varies from 86 to 1640  $\text{Bqkg}^{-1}$ , with average is 381  $\text{Bqkg}^{-1}$ .

Table (3.7) presents the Positive skewness in Gharib samples, which, indicates a distribution with an asymmetric tail extending towards values that are more positive. The activity concentrations of  $^{226}\text{Ra}$ ,  $^{232}\text{Th}$  and  $^{40}\text{K}$  in this Gharib city are 0.2, 0.3 and 2.5, respectively; small skewness values Table (3.7), which indicates that the distributions are asymmetric in nature. In Gharib city, the  $^{226}\text{Ra}$ ,  $^{232}\text{Th}$  and  $^{40}\text{K}$  distributions have positive kurtosis value Table (3.7), indicating peaked distribution.

**Table 3.7:** Activity concentrations of  $^{226}\text{Ra}$ ,  $^{232}\text{Th}$  and  $^{40}\text{K}$  ( $\text{Bqkg}^{-1}$ ) in samples collected from Gharib City.

Samples Location	Sample Name	Activity concentrations( $\text{Bqkg}^{-1}$ )			Total	contribution%		
		$^{226}\text{Ra}$	$^{232}\text{Th}$	$^{40}\text{K}$		Ra	Th	K
south (El-Sakala area )	G1	12±1	12±1	164±9	188	6	6	87
	G2	28±2	23±3	126±7	177	16	13	71
	G3	50±3	27±3	580±32	657	8	4	88
	G4	29±2	21±2	180±10	229	12	9	78
	G5	23±2	18±2	132±8	172	13	10	77
	G6	36±2	32±4	329±18	397	9	8	83
Middle (General Beach)	G7	26±2	29±3	676±38	732	4	4	92
	G8	40±3	38±5	322±18	400	10	10	81
	G9	6±0.4	8±2	592±34	605	1	1	98
	G10	24±2	19±2	131±7	174	14	11	75
	G11	27±2	25±3	450±25	502	5	5	90
	G12	31±2	27±3	463±26	521	6	5	89
North (General company of Petroleum)	G13	37±2	26±3	144±8	207	18	13	70
	G14	27±2	28±3	166±9	222	12	13	75
	G15	27±2	27±3	124±7	177	15	15	70
	G16	20±1	14±2	562±32	597	3	2	94
	G17	52±4	45±5	1640±93	1737	3	3	94
	G18	10±1	11±2	86±5	107	9	10	81
MIN		6	8	86	107	1	1	70
MAX		52	45	1640	1737	18	15	98
AVEG		28	24	381	433	9	8	83
STDEV		12	10	371	382	5	4	9
S.E		3	2	87	90	1	1	2
SKEWNESS		0.2	0.3	2.5	2.5	0.1	0.03	0.01
KURTOSIS		0.2	0.3	7.7	8.0	- 1.1	-1.2	-1.3

The average values are lower than the corresponding worldwide average values, which are 35, 30 and 400  $\text{Bqkg}^{-1}$  for  $^{226}\text{Ra}$ ,  $^{232}\text{Th}$  and  $^{40}\text{K}$  respectively, (UNSCEAR, 2000). Figure 3.22 and 3.23 shows the Activity concentrations and (Mean, Max and Min) Distribution of  $^{226}\text{Ra}$ ,  $^{232}\text{Th}$  and  $^{40}\text{K}$  for the sediment samples in Gharib City.

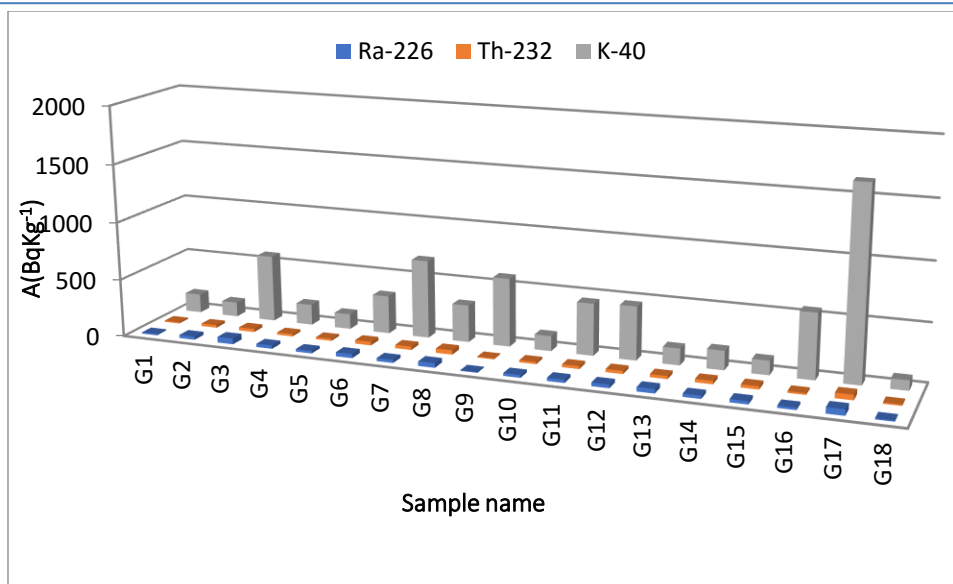


Figure 3.22: Activity concentrations of the radioelements ( $Bqkg^{-1}$ ) found in Gharib City samples

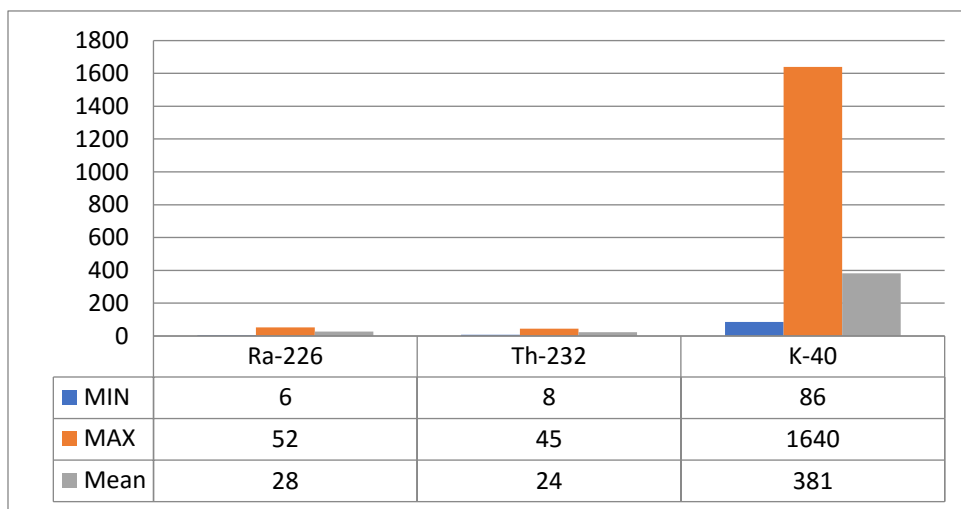


Figure 3.23: Distribution of  $^{226}Ra$ ,  $^{232}Th$  and  $^{40}K$  in Gharib City

The Frequency distributions of the radionuclides from Gharib samples were analyzed, and the histograms are given in Figures. (3.24) to (3.26). The graphs of  $^{226}Ra$  and  $^{232}Th$  show that these radionuclides demonstrate a normal (bell-shape) distribution. While  $^{40}K$  show that this radionuclide exhibited some degree of multi-modality. This multi-modal feature of the radioelements demonstrates the complexity of sediments samples

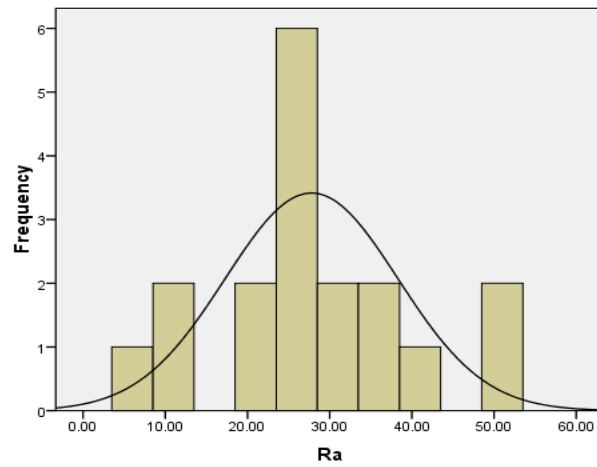


Figure 3.24: The frequency distributions of Ra-226 found in Gharib City samples

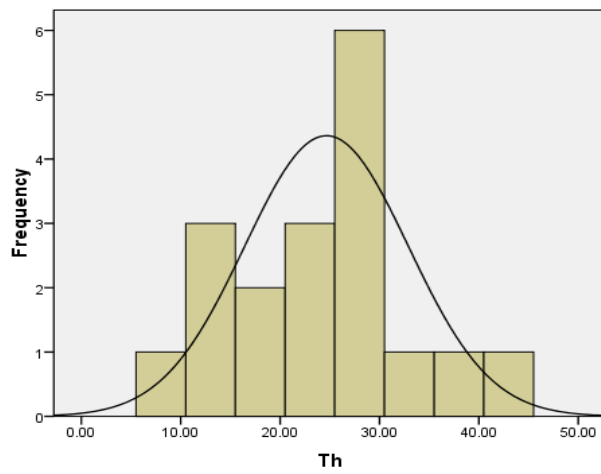


Figure 3.25: The frequency distributions of Th-232 found in Gharib City samples

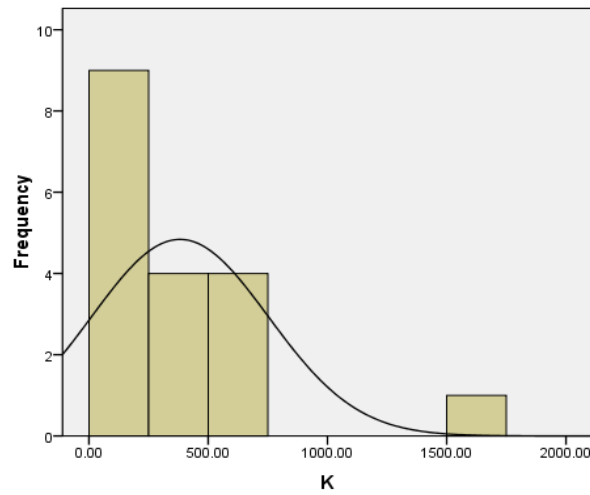


Figure 3. 26: Frequency distributions of K-40 found in Gharib City samples

### 1.4.1 Correlation and Concentration Ratio of Natural Radionuclides in Sediment Samples from Gharib City

From the activity concentration of  $^{226}\text{Ra}$ ,  $^{232}\text{Th}$  and  $^{40}\text{K}$  given in table 3.7, the relationships between these radionuclides in sediments samples under investigation were computed and diagrammatically plotted as shown in Table (3.8), and Figure (3.27).

**Table 3.8:** Activity ratios between natural radionuclides in sediment samples from Gharib city, Egypt

sample	$^{232}\text{Th}/^{226}\text{Ra}$	$^{232}\text{Th}/^{40}\text{K}$	$^{226}\text{Ra}/^{40}\text{K}$
G1	1.036	0.074	0.071
G2	0.820	0.183	0.223
G3	0.541	0.046	0.086
G4	0.728	0.116	0.159
G5	0.780	0.135	0.172
G6	0.887	0.096	0.109
G7	1.104	0.043	0.039
G8	0.958	0.118	0.123
G9	1.335	0.013	0.010
G10	0.768	0.142	0.184
G11	0.906	0.055	0.061
G12	0.875	0.058	0.067
G13	0.698	0.180	0.258
G14	1.029	0.170	0.165
G15	1.012	0.219	0.216
G16	0.721	0.025	0.035
G17	0.866	0.028	0.032
G18	1.062	0.123	0.116
Minimum	0.54	0.01	0.01
Maximum	1.33	0.22	0.26
Average	0.90	0.10	0.12

Figure 3.27 shows strong correlation between  $^{232}\text{Th}$  and  $^{226}\text{Ra}$  while we found moderate correlation between  $^{232}\text{Th}$  and  $^{40}\text{K}$  with correlation coefficients ( $R=0.878$  and  $0.518$ ) respectively. But between  $^{40}\text{K}$  and  $^{226}\text{Ra}$  we found relatively weak correlation with factor ( $R=0.476$ ). The mean values of  $^{232}\text{Th}/^{226}\text{Ra}$ ,  $^{232}\text{Th}/^{40}\text{K}$  and  $^{226}\text{Ra}/^{40}\text{K}$  ratios for all samples under investigation are 0.90, 0.10 and 0.12 respectively. Figure 3.28, show  $^{232}\text{Th}/^{226}\text{Ra}$ ,  $^{232}\text{Th}/^{40}\text{K}$  and  $^{226}\text{Ra}/^{40}\text{K}$  activity concentration ratios.

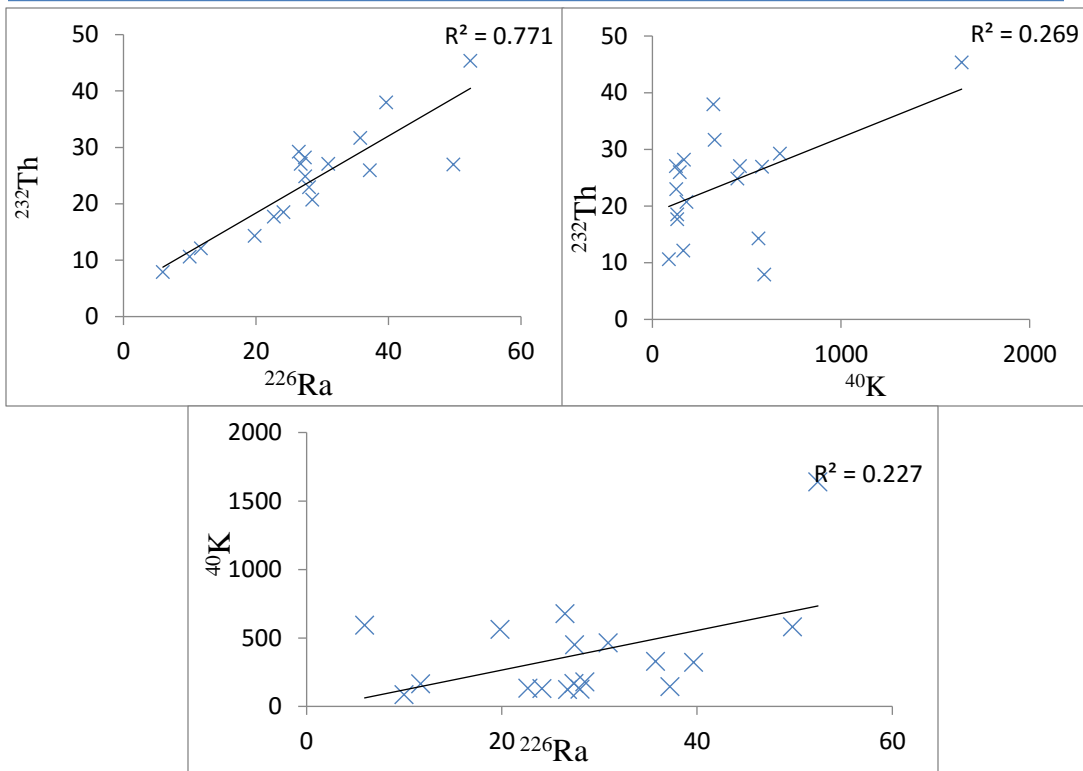


Figure 3.27: Correlation between natural radionuclides in sediment samples from Hurghada city

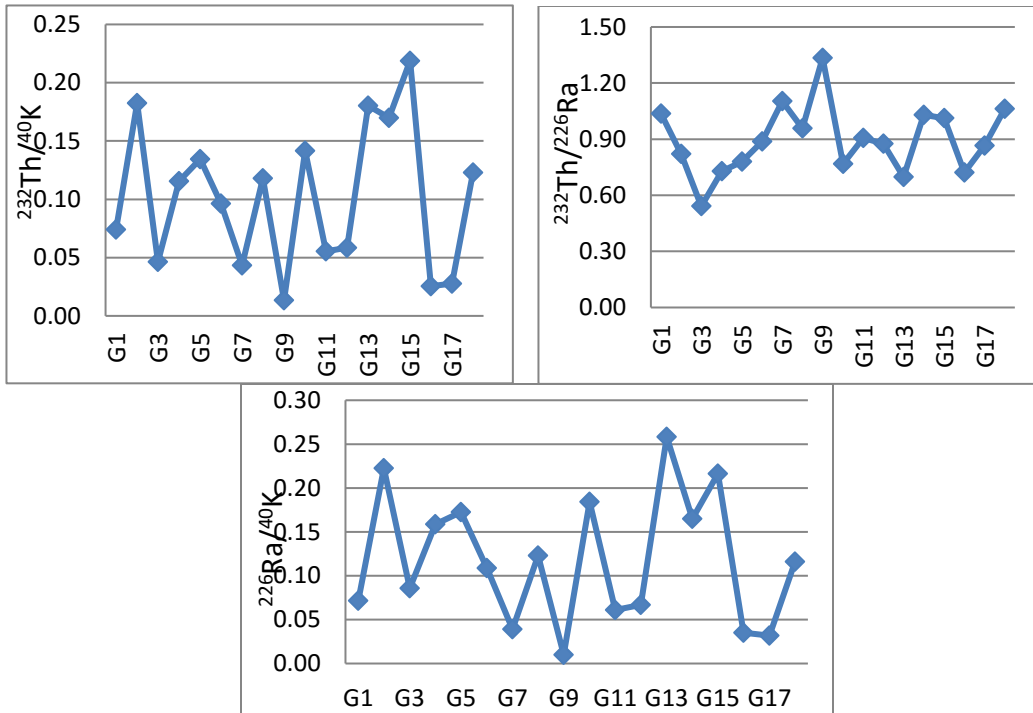


Figure 3.28:  $^{232}\text{Th}/^{226}\text{Ra}$ ,  $^{232}\text{Th}/^{40}\text{K}$  and  $^{226}\text{Ra}/^{40}\text{K}$  ratios in sediment samples from Hurghada, Egypt



From the values of  $^{232}\text{Th}/^{226}\text{Ra}$  we can conclude that there is a good correlation between  $^{232}\text{Th}$  and  $^{226}\text{Ra}$ . On other sides for ratio values of  $^{232}\text{Th}/^{40}\text{K}$  and  $^{226}\text{Ra}/^{40}\text{K}$  indicate that the  $^{40}\text{K}$  concentration always high.

## 2 Radiological hazards indices:

The International Commission on Radiological protection (ICRP) has launched a task group of its Main Commission to address Radiological protection as a part of developing new recommendations. The European Commission has established the Framework for Assessment of Environmental impact (FASSET) project (Larsson 2002). The international Atomic Energy Agency (IAEA) has established a work program to develop safety guidance on the protection of the environment from the effects of ionizing radiation, that will take account of these and other developments (Robinson 2002). IAEA is also holding a series of meetings and symposia on the subject in order to facilitate information exchange and co-operation. Therefore, it is very important to assess the radiological risks of sediments of red sea beaches. Resulting from natural radionuclides in samples under investigation. For this purpose, Radium equivalent activity ( $R_{\text{eq}}$ ), ( $\text{Bqkg}^{-1}$ ), Gamma Dose Rate (D), ( $\text{nGy h}^{-1}$ ), Internal and External Hazard Index ( $H_{\text{in}}$  and  $H_{\text{ex}}$ ) ( $\text{nGy h}^{-1}$ ), Annual Effective Dose Rate, ( $\mu\text{Svy}^{-1}$ ), Excess Lifetime Cancer Risk (ELCR), Gamma activity concentration index ( $I_{\gamma}$ ) and Annual Gonadal Dose Equivalent (AGDE) ( $\text{mSv y}^{-1}$ ). Were computed and represented in Table 3.

### 2.1 Radiological Characterization of Qusier Sediment Samples.

#### 2.1.1 Radium Equivalent Activities ( $R_{\text{eq}}$ )

Radium equivalent activity ( $R_{\text{eq}}$ ) is an index that has been introduced to represent the specific activities of  $^{226}\text{Ra}$ ,  $^{232}\text{Th}$  and  $^{40}\text{K}$  by single quantity, which takes into account the radiation hazards associated with them.  $R_{\text{eq}}$  calculated according equation (25) in chapter 2. This equation is based on the assumption that  $370 \text{ Bqkg}^{-1}$  of  $^{226}\text{Ra}$ ,  $259 \text{ Bqkg}^{-1}$  of  $^{232}\text{Th}$  and  $4810 \text{ Bqkg}^{-1}$  of  $^{40}\text{K}$  produce the same gamma ray dose. The calculated values of  $R_{\text{eq}}$  for Qusier samples under studying are listed in Table 3.9. These values were ranged from 9 to 149 with average value of  $74 \text{ Bqkg}^{-1}$ ; these results indicate that all average values of  $R_{\text{eq}}$  are less than the upper limit  $370 \text{ Bqkg}^{-1}$  (Beretka, and Mathew, 1985) this mean that, those samples are safe, if it use as building materials.

**Table 3.9:** Radium equivalent ( $R_{eq}$ ), the dose rate (D), hazard indices ( $H_{ex}$  and  $H_{in}$ ), annual effective dose rate (AEDE), excess lifetime cancer risk (ELCR), Gamma index ( $I_\gamma$ ) and annual gonadal dose equivalent (AGDE), for Qusier City.

Samples Location	Code no.	$R_{eq}$ Bqkg <sup>-1</sup>	D	$H_{in}$	$H_{ex}$	AED E $\mu$ Sv $y^{-1}$	ELCR ( $10^{-6}$ )	$I_\gamma$	AGDE $\mu$ Sv $y^{-1}$
				nGy h <sup>-1</sup>					
El Edua area	Q1	96	45	0.3	0.3	55	193	0.3	318
	Q2	50	23	0.2	0.1	28	97	0.2	157
	Q3	80	37	0.3	0.2	45	157	0.3	255
	Q4	94	43	0.4	0.3	53	186	0.3	304
	Q5	79	37	0.3	0.2	46	160	0.3	267
	Q6	55	26	0.2	0.1	32	114	0.2	189
	Q7	42	19	0.2	0.1	24	83	0.1	134
Quscir Harbor	Q8	75	36	0.2	0.2	44	153	0.3	256
	Q9	81	38	0.3	0.2	47	163	0.3	271
	Q10	91	42	0.3	0.2	52	182	0.3	300
	Q11	75	35	0.3	0.2	43	152	0.3	251
	Q12	111	53	0.4	0.3	65	228	0.4	384
	Q13	59	28	0.2	0.2	34	120	0.2	200
	Q14	59	27	0.2	0.2	33	116	0.2	188
	Q15	80	37	0.3	0.2	45	157	0.3	256
	Q16	43	20	0.2	0.1	24	85	0.1	139
	Q17	113	51	0.5	0.3	62	218	0.4	349
	Q18	12	6	0.05	0.03	7	24	0.0	38
	Q19	149	70	0.5	0.4	85	299	0.5	497
	Q20	68	33	0.2	0.2	40	141	0.2	240
	Q21	81	38	0.3	0.2	47	163	0.3	271
N. Flaminko Village	Q22	89	40	0.3	0.2	49	172	0.3	278
	Q23	83	37	0.3	0.2	46	160	0.3	259
	Q24	107	48	0.4	0.3	59	205	0.4	328
	Q25	9	4	0.03	0.03	5	19	0.03	31
	Q26	67	30	0.3	0.2	37	130	0.2	211
	Q27	43	20	0.2	0.1	24	84	0.1	137
	MIN	9	4	0.03	0.03	5	19	0.03	31
	MAX	149	70	0.5	0.4	85	299	0.5	497
	AVEG	74	34	0.3	0.2	42	147	0.2	241
	Range	9-149	4-70	0.03-0.5	0.03-0.4	5-85	19-299	0.03-0.5	31-497

Figure 3.29; show the relative contribution to  $Ra_{eq}$  owing to  $^{226}Ra$ ,  $^{232}Th$  and  $^{40}K$ . for sediment samples under investigation in Qusier city It's noticed that the contribution owing of  $^{226}Ra$ ,  $^{232}Th$  and  $^{40}K$  were in range between (14% and 51%), ( 25% to 59%) and ( 6% to 51%) respectively.

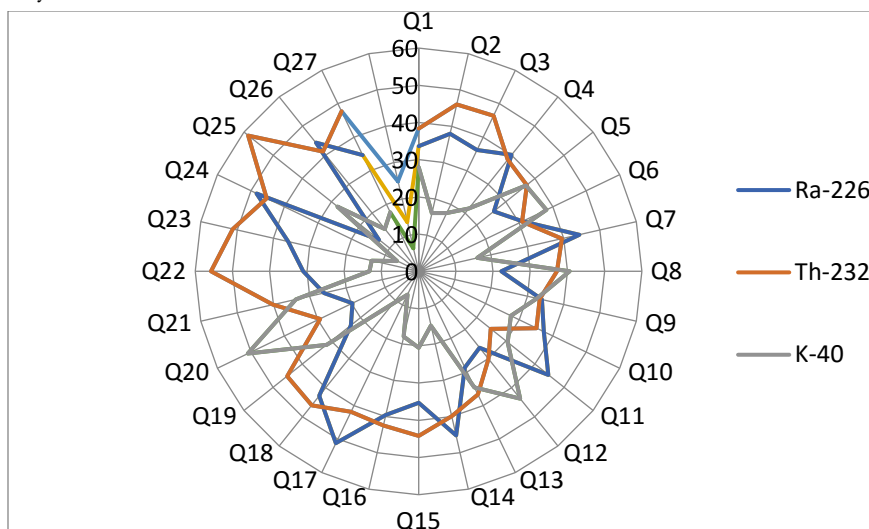


**Figure 3. 29:** The relative contribution (%) of  $^{226}Ra$ ,  $^{232}Th$  and  $^{40}K$  to Radium equivalent in every sample from Qusier City.

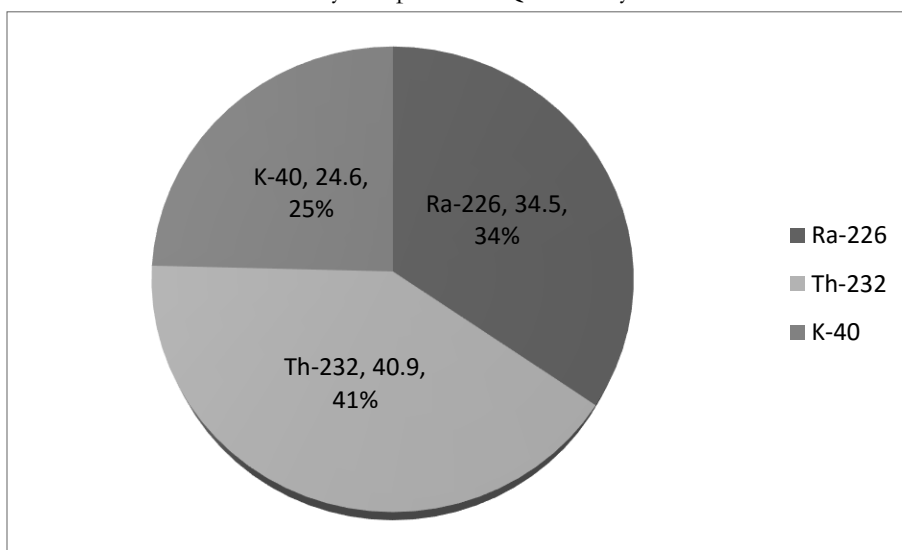


**Figure 3.30:** The average relative contribution to Radium equivalent activity ( $Ra_{eq}$ ) due to  $^{226}Ra$ ,  $^{232}Th$  and  $^{40}K$  in sediment samples from Qusier city  
 Figure 3.30, shows the average relative contribution of  $^{226}Ra$ ,  $^{232}Th$  and  $^{40}K$  contents of  $Ra_{eq}$  for samples under consideration, the average relative contribution to  $Ra_{eq}$  owing to  $^{226}Ra$ ,  $^{232}Th$  and  $^{40}K$  are 34%, 41% and 25%, respectively. It is evident that the contribution from  $^{232}Th$  is the highest where the contribution from  $^{40}K$  is the smallest.

**2.1.2 Absorbed Gamma Dose Rate (D)**

From Table 3.9, values of absorbed dose (D) were ranged from 4 to 70 with average value of 34 nGy h<sup>-1</sup>, these average value is less than the world average value (57 nGy.h<sup>-1</sup>) (UNSCEAR, 2000).

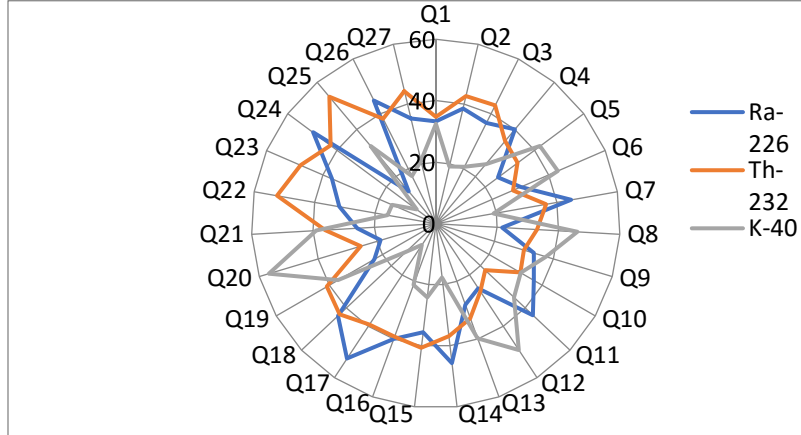


**Figure 3.31:** The relative contribution (%) of <sup>226</sup>Ra, <sup>232</sup>Th and <sup>40</sup>K to absorbed dose rate in every sample from Qusier City.

The relative contribution (%) of <sup>226</sup>Ra, <sup>232</sup>Th and <sup>40</sup>K to absorbed dose rate in every sample from Qusier City can be seen in Figure 3.31. From it, one can notice that the contribution absorbed dose rate (D) owing to <sup>226</sup>Ra, <sup>232</sup>Th and <sup>40</sup>K in sediment samples under investigation were ranged between (14% to 53%), (22% to 54%) and (8% to 57%) respectively Figure 3.32, shows the average relative contribution to (D) in for all samples from total investigated area owing to <sup>226</sup>Ra, <sup>232</sup>Th and <sup>40</sup>K are 35%, 37% and 28%, respectively. It is evident that the contribution from <sup>232</sup>Th is the highest one where the contribution from <sup>40</sup>K is the smallest; these indicate that the contribution to (D) is owing to <sup>232</sup>Th followed by <sup>226</sup>Ra followed by <sup>40</sup>K.

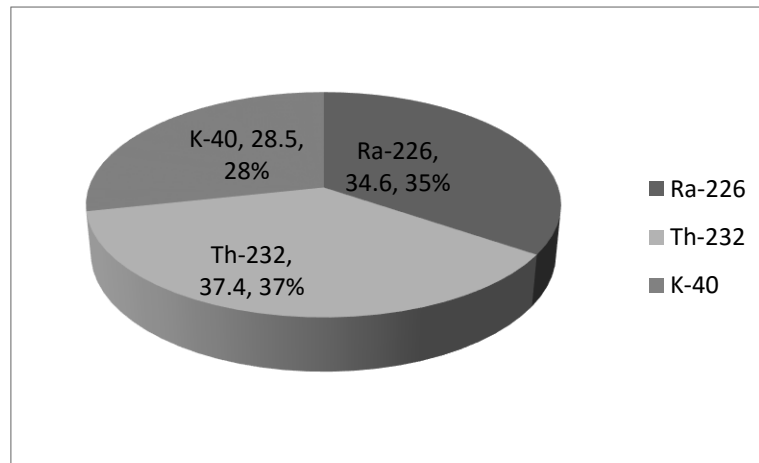


**Figure 3.32:** The average relative contribution to absorbed dose rate (D) due to <sup>226</sup>Ra, <sup>232</sup>Th and <sup>40</sup>K in investigated area-Qusier city

### 2.1.3 Internal Radiation Hazard ( $H_{in}$ )

Radon and its short-lived progeny are hazardous to the respiratory organ. Internal exposure of  $^{222}\text{Rn}$  and its radioactive progeny is controlled by the internal hazard index ( $H_{in}$ ). Values of internal hazard index ( $H_{in}$ ), ranged from 0.03 to 0.5 with average value 0.3 as given in Table 3.9, for Qusier samples under investigation, which were lower than the unity, acceptable level (Beretka, and Mathew, 1985). Figure 3.33, shows the relative contribution of  $H_{in}$  owing to  $^{226}\text{Ra}$ ,  $^{232}\text{Th}$  and  $^{40}\text{K}$  in all measured samples, the contribution to  $H_{in}$  owing to  $^{226}\text{Ra}$ ,  $^{232}\text{Th}$  and  $^{40}\text{K}$  ranged from (24% to 68%), from (17% to 52%) and from (4% to 43%) for Qusier sediment samples under investigation respectively. Figure 3.34, shows the average relative contribution to ( $H_{in}$ ) owing to  $^{226}\text{Ra}$ ,  $^{232}\text{Th}$  and  $^{40}\text{K}$  are 51%, 30% and 19%, respectively. It is evident that the contribution from  $^{226}\text{Ra}$  is the highest one where the contribution from  $^{40}\text{K}$  is the smallest; these indicate that the contribution to ( $H_{in}$ ) is owing to  $^{226}\text{Ra}$  followed by  $^{232}\text{Th}$  followed by  $^{40}\text{K}$ .

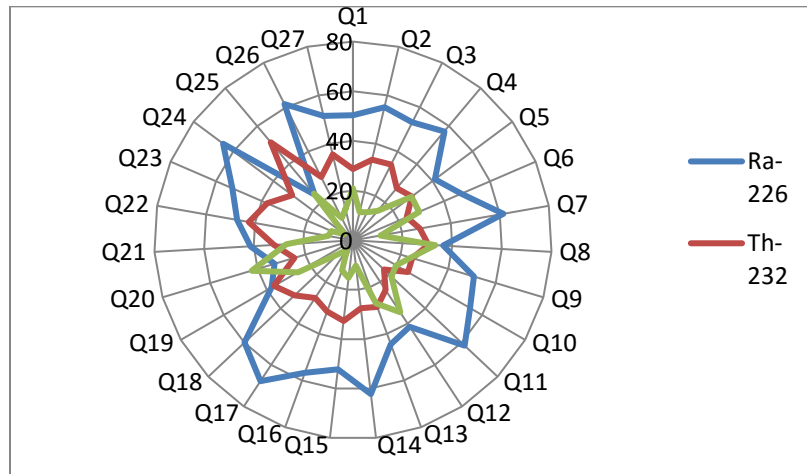
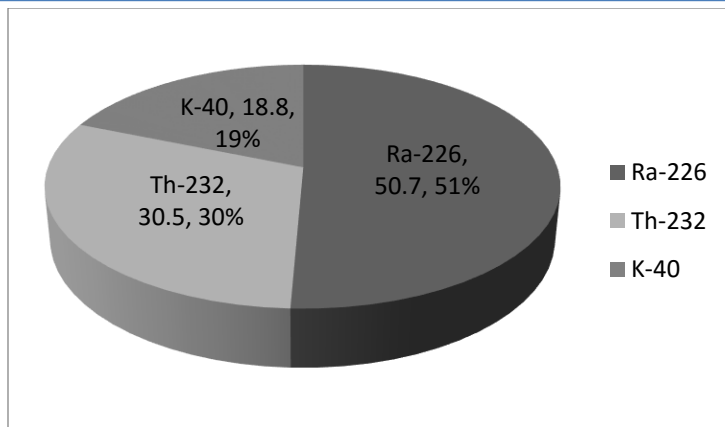


Figure 3.33: The relative contribution (%) of  $^{226}\text{Ra}$ ,  $^{232}\text{Th}$  and  $^{40}\text{K}$  to internal hazard index ( $H_{in}$ ) in every sample from Qusier City.

### 2.1.4 External Radiation Hazard ( $H_{ex}$ )

The External hazard index ( $H_{ex}$ ), values ranged from 0.03 to 0.4 with average value 0.2 as given in table 3.9, for Qusier samples under investigation, which were lower than the unity, acceptable level (Beretka, and Mathew, 1985).

Figure 3.35, shows the relative contribution of  $H_{ex}$  owing to  $^{226}\text{Ra}$ ,  $^{232}\text{Th}$  and  $^{40}\text{K}$  in all measured samples. The contribution to  $H_{in}$  owing to  $^{226}\text{Ra}$ ,  $^{232}\text{Th}$  and  $^{40}\text{K}$  ranged from (14% to 51%), (25% to 59%) and from (6% to 51%) for Qusier sediment samples under investigation respectively. Figure 3.36, shows the average relative contribution to ( $H_{ex}$ ) owing to  $^{226}\text{Ra}$ ,  $^{232}\text{Th}$  and  $^{40}\text{K}$  are 34%, 41% and 25%, respectively. It is evident that the contribution from  $^{232}\text{Th}$  is the highest one where the contribution from  $^{40}\text{K}$  is the smallest; these indicate that the contribution to ( $H_{ex}$ ) is owing to  $^{232}\text{Th}$  followed by  $^{226}\text{Ra}$  followed by  $^{40}\text{K}$ .



**Figure 3.34:** The average relative contribution to internal hazard index ( $H_{in}$ ) due to  $^{226}\text{Ra}$ ,  $^{232}\text{Th}$  and  $^{40}\text{K}$  in sediment samples from Qusier city

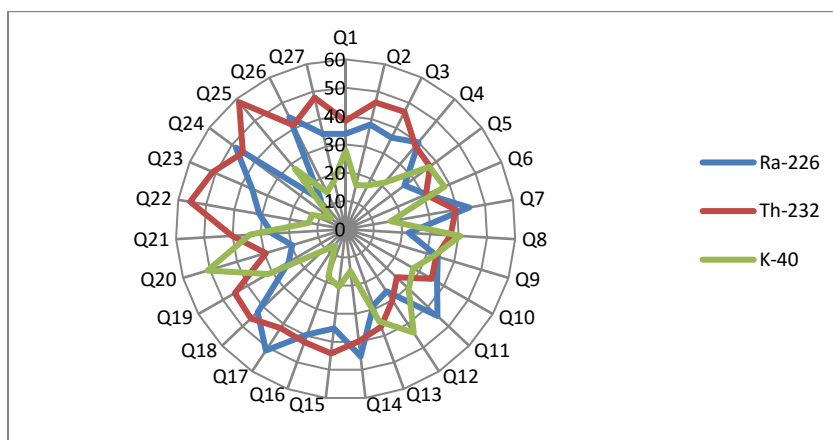


**Figure 3.35:** The relative contribution (%) of  $^{226}\text{Ra}$ ,  $^{232}\text{Th}$  and  $^{40}\text{K}$  to External hazard index ( $H_{ex}$ ) in every sample from Qusier City.

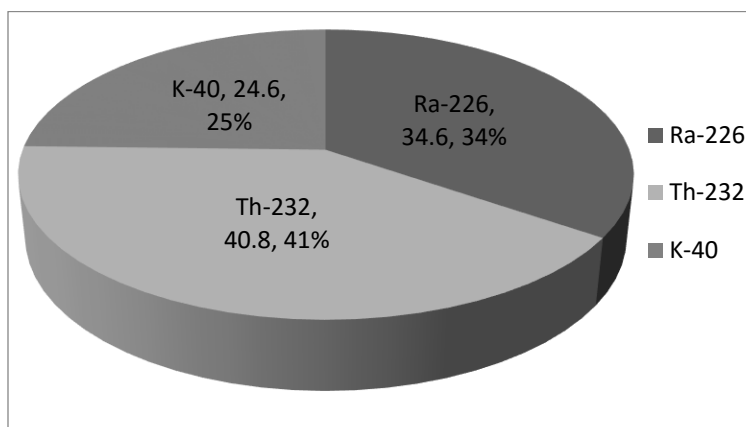


**Figure 3.36:** The average relative contribution to External hazard index ( $H_{ex}$ ) due to  $^{226}\text{Ra}$ ,  $^{232}\text{Th}$  and  $^{40}\text{K}$  in sediment samples from Qusier city

**2.1.5 Annual effective dose**

Table 3.9, shows the annual effective doses outdoors from measured sediment samples. It can see that the annual outdoor effective dose of samples under investigation from Qusier city varied from 5 to 85  $\mu\text{Svy}^{-1}$ , with average value of 42  $\mu\text{Svy}^{-1}$ . It evident that the obtained average annual effective doses for outdoor in this study are smaller than the world average 70  $\mu\text{Svy}^{-1}$  reported in UNSCEAR (2000). The distribution patterns of (AEDE) at Qusier city are three patterns as it appears in (Figure3.37).

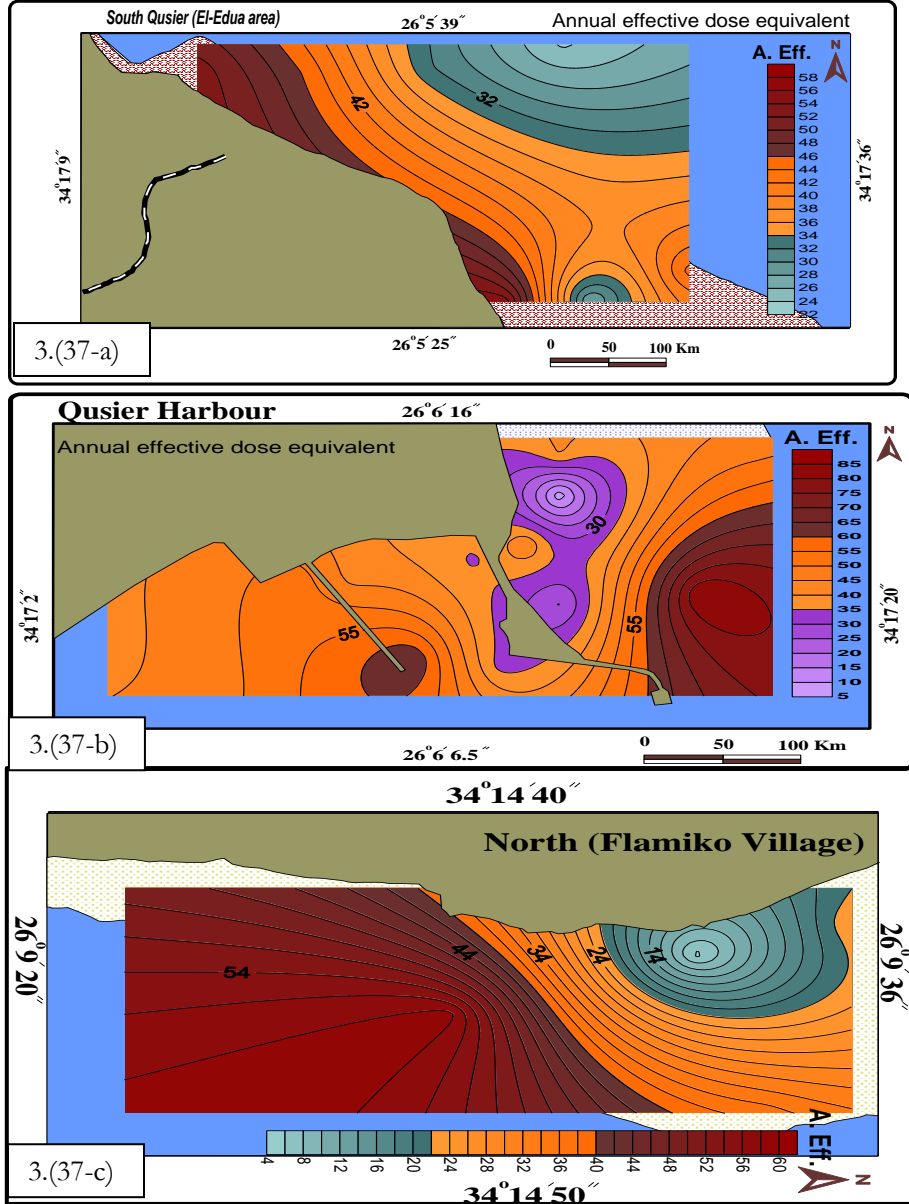


**Figure 3.37:** The distribution patterns of AEDE at Qusier city.

The first is for, El Edua area, figure 3.(37-a) ,we can note that the (AEDE) increase near the coast that may attribute by long dead reef flat considered to be contains the amount of radioactive waste generated by human activity like sewage. Also, the levels of natural radioactivity in this co-produced water depend on the source rocks and the associated brine water. But when we look in figure 3. (37-b) we can see the highest values of (AEDE) recorded at marine area were concentrated inside the shipping zone and decreasing abruptly seaward and southward. While the recorded concentrations of  $^{232}\text{Th}$  series and  $^{40}\text{K}$  in phosphate rocks of all types are similar to those observed normally in soil (El-TaHER & Madkour, 2011) documented that the concentration of  $^{238}\text{U}$  and its decay products tend to be elevated in phosphate deposits of sedimentary origin. A typical concentration of  $^{238}\text{U}$  series in sedimentary phosphate deposits is  $121 \text{ mgkg}^{-1}$  ( $1500 \text{ Bqkg}^{-1}$ ) with a range of  $372\text{--}3224 \text{ Bqkg}^{-1}$  (UNSCEAR, 1993). While the in Flaminko village figure 3.(37-c), the AEDE increase in area which have small-branched colonies of *Acropora sp.*, *Stylophora sp.* at a depth of 45cm. maybe this species stopping water motion.

#### 2.1.6 Gamma index ( $I_\gamma$ )

Gamma index ( $I_\gamma$ ) was estimated for sediments under test and the derived values are presented in Table 3.9. It can be seen that, gamma activity index values were ranged from 0.03 to 0.5 with average value of 0.2. It is observed that, all samples have gamma index  $I_\gamma < 2$  which indicates gamma dose contribution from these sediment samples was not exceed  $0.3 \text{ mSv.y}^{-1}$  (European Commission in 2000). Figure (3. 38), shows the relative contribution to gamma index  $I_\gamma$  owing to  $^{226}\text{Ra}$ ,  $^{232}\text{Th}$  and  $^{40}\text{K}$ , where they ranged from (13% to 50%), (26% to 60%) and (6% to 50%) for Qusier sediment samples under investigation respectively.



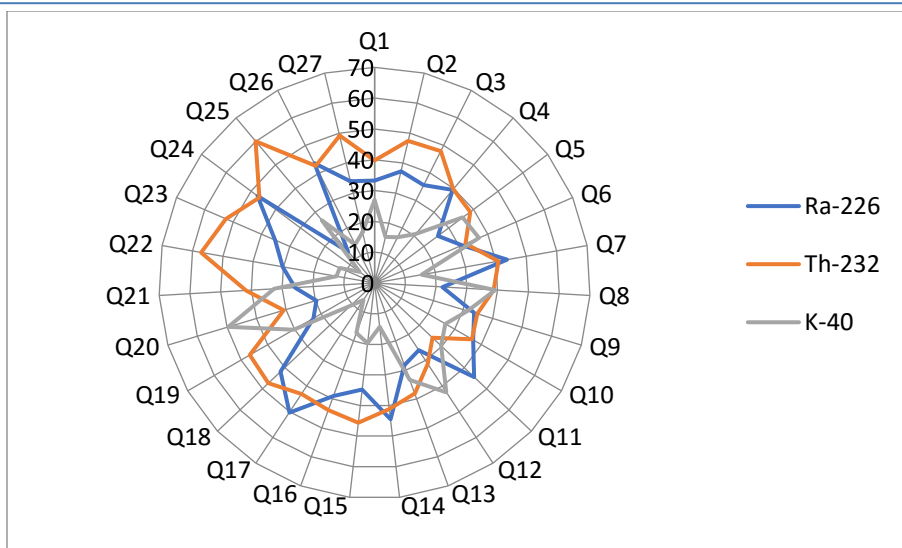


**Figure 3.38:** The relative contribution (%) of  $^{226}\text{Ra}$ ,  $^{232}\text{Th}$  and  $^{40}\text{K}$  to Gamma activity index ( $I_\gamma$ ) in every sample from Qusier City.

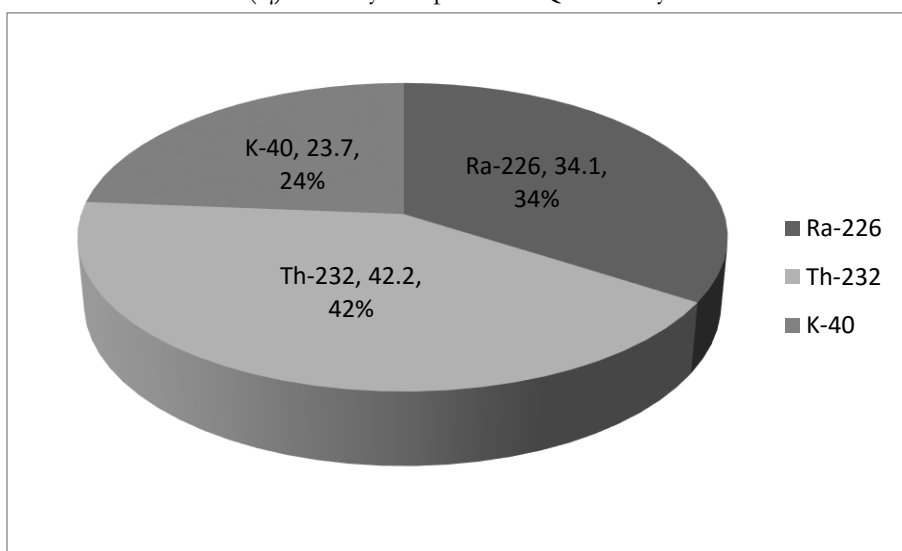


**Figure 3. 39:** The average relative contribution to Gamma activity index ( $I_\gamma$ ) due to  $^{226}\text{Ra}$ ,  $^{232}\text{Th}$  and  $^{40}\text{K}$  in sediment samples from Qusier city

Figure 3.39, shows the average relative contribution to  $I_\gamma$  owing to  $^{226}\text{Ra}$ ,  $^{232}\text{Th}$  and  $^{40}\text{K}$  are 34%, 42% and 24%, respectively. It is evident that the contribution from  $^{232}\text{Th}$  is the highest one where the contribution from  $^{40}\text{K}$  is the smallest; these indicate that the contribution to  $I_\gamma$  is owing to  $^{232}\text{Th}$  followed by  $^{226}\text{Ra}$  followed by  $^{40}\text{K}$ .

### 2.1.7 Excess Lifetime Cancer Risk (ELCR)

The obtained values of (ELCR) for the studied samples are summarized in Table 3.9. As we shown in Table 3.9, (ELCR) values ranged from  $19 \times 10^{-6}$  to  $299 \times 10^{-6}$  with average value of  $147 \times 10^{-6}$ , the average ELCR. It evident that the obtained average ELCR in this study are smaller than the world average  $2900 \times 10^{-6}$  reported in UNSCEAR (2000). The distribution patterns of (ELCR) at Qusier city show three patterns (Figure3.40- a,b and c). The first is for, El Edua area we can see that the (ELCR) increase near the coast as shown in Figure3. (40-a) while we see increasing of (ELCR) inside the shipping zone, figure 3. (40-b). Finally in Flaminko village the increasing of (ELCR) toward the coral area as it appears in figure 3. (40-c).

### 2.1.8 Annual Gonadal Dose Equivalent (AGDE)

The obtained values of (AGDE) for the studied samples are summarized in Table 3.9. As we shown in Table 3.9, AGDE values ranged from 0.031 to 0.497 with average value of 0.241  $\text{mSvy}^{-1}$ , the average AGDE value is closed to the world average values for soil 0.298  $\text{mSvy}^{-1}$  (Zaidi et al., 1999). The annual gonadal dose equivalent results do not exceed the permissible recommended limits, indicating that the hazardous effects of the radiation are negligible.

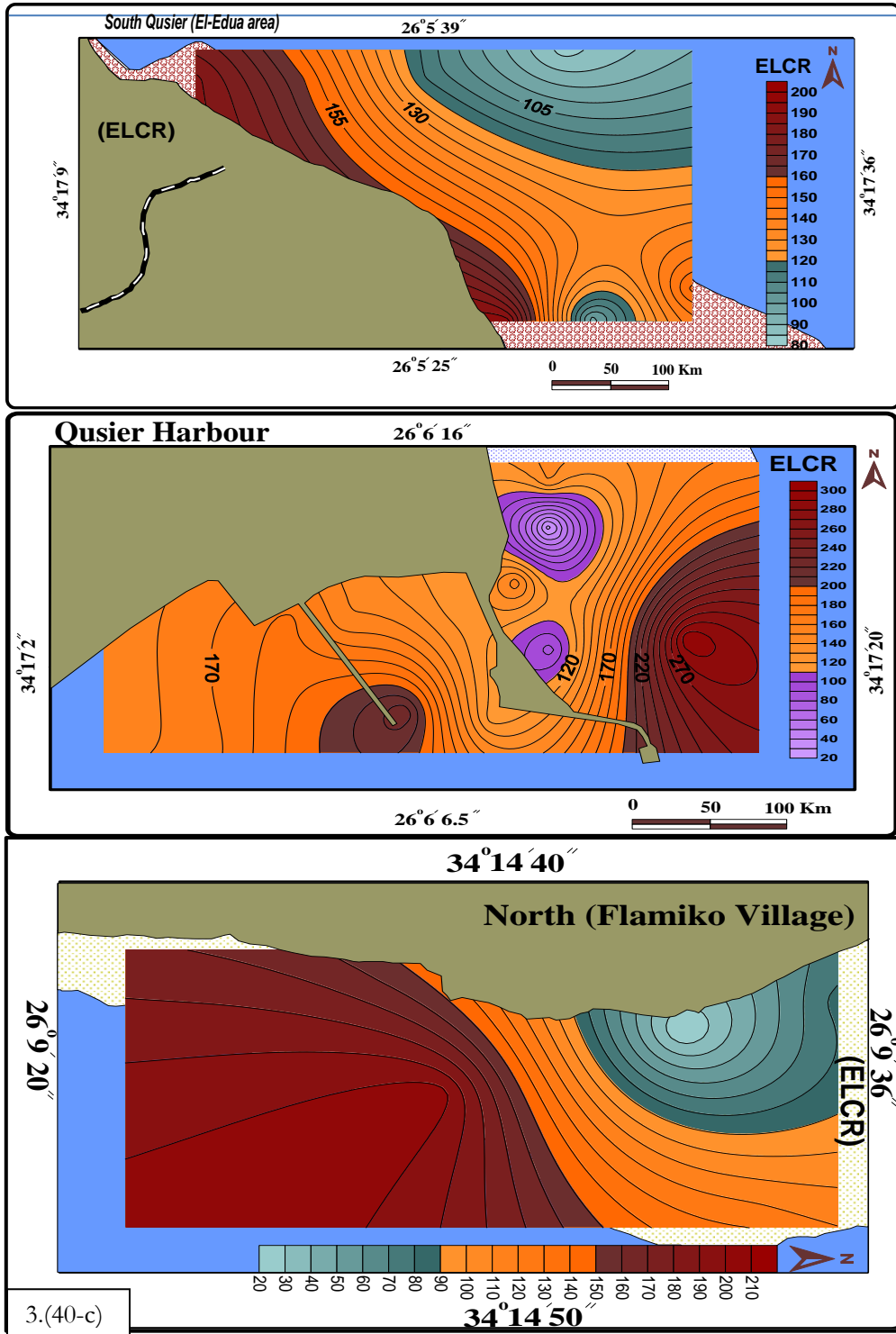


Figure3.40: The distribution patterns of ELCR at Qusier city

## 2.2 Radiological Characterization of Safaga Sediment Samples

### 2.2.1 Radium Equivalent Activities ( $Ra_{eq}$ )

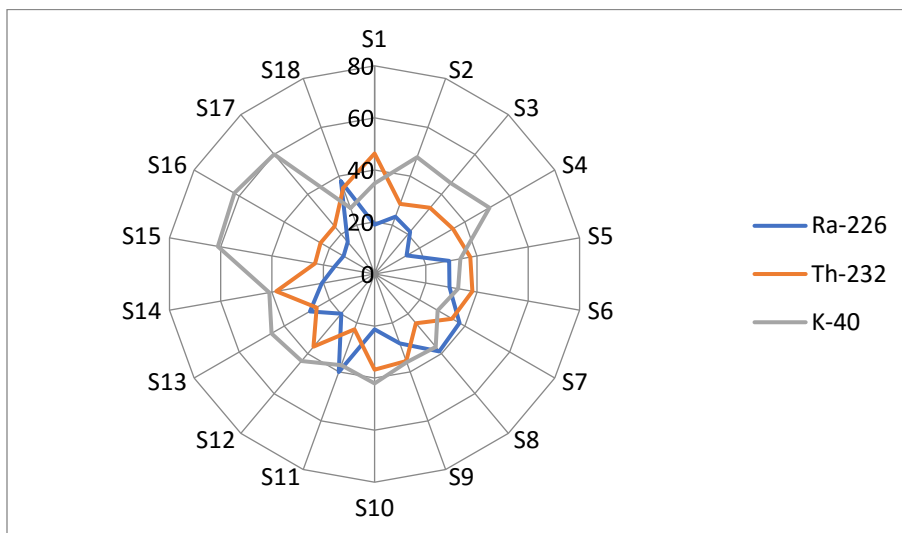
The calculated values of  $Ra_{eq}$  for Safaga samples under study are given in Table 3.10. These values were ranged from 32 to 141 with average value of  $86 \text{ Bqkg}^{-1}$ ; these results indicate all average values of  $Ra_{eq}$  are less than the upper limit  $370 \text{ Bqkg}^{-1}$  (Beretka, and Mathew, 1985) this mean that, it is safe, if it use as building materials

**Table 3.10:** Radium equivalent ( $Ra_{eq}$ ), the dose rate (D), hazard indices ( $H_{ex}$  and  $H_{in}$ ), annual effective dose rate (AEDE), excess lifetime cancer risk (ELCR), Gamma index ( $I_\gamma$ ) and annual gonadal dose equivalent (AGDE) for Safaga City

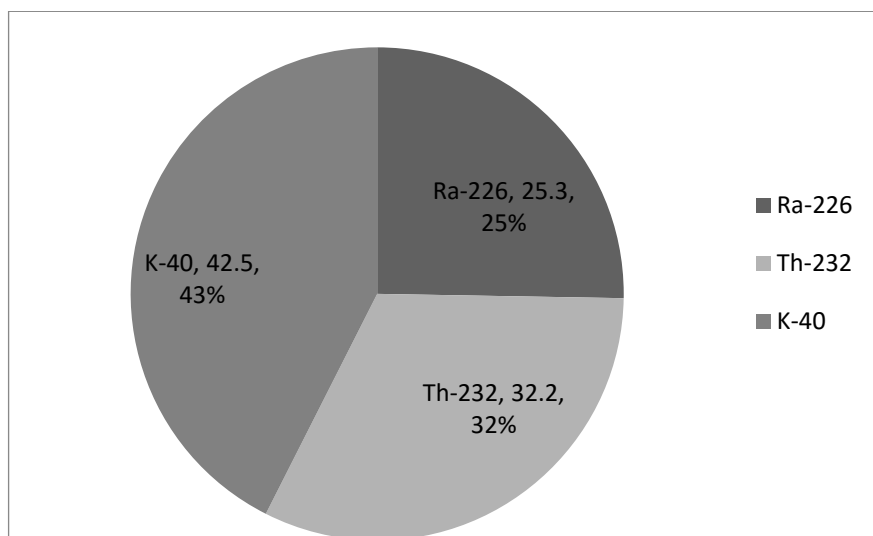
Samples Location	Code no	$Ra_{eq}$ $\text{Bqkg}^{-1}$	D	$H_{in}$	$H_{ex}$	AEDE $\mu\text{Svy}^{-1}$	ELCR ( $10^{-6}$ )	$I_\gamma$	AGDE $\mu\text{Svy}^{-1}$
			nGyh <sup>-1</sup>						
Km 17 Mangrove area	S1	75	35	0.2	0.2	43	151	0.3	252
	S2	32	15	0.1	0.1	19	66	0.1	111
	S3	81	39	0.3	0.2	48	168	0.3	283
	S4	91	44	0.3	0.2	54	190	0.3	323
	S5	66	31	0.2	0.2	38	134	0.2	222
	S6	49	23	0.2	0.1	28	99	0.16	164
Abu Tartour Harbor	S7	141	66	0.5	0.4	81	283	0.5	466
	S8	81	39	0.3	0.2	48	167	0.3	278
	S9	85	40	0.3	0.2	49	173	0.3	288
	S10	69	33	0.2	0.2	40	142	0.2	238
	S11	106	51	0.4	0.3	63	219	0.4	364
	S12	69	33	0.2	0.2	40	142	0.2	239
Touristic Harbor	S13	109	53	0.4	0.3	64	226	0.4	380
	S14	119	57	0.4	0.3	69	243	0.4	409
	S15	93	46	0.3	0.3	56	197	0.3	339
	S16	102	50	0.3	0.3	62	217	0.3	372
	S17	95	47	0.3	0.3	58	202	0.3	346
	S18	93	44	0.4	0.25	54	187	0.3	308
	MIN	32	15	0.1	0.1	19	66	0.1	111
	MAX	141	66	0.5	0.4	81	283	0.5	466
	AVEG	86	41	0.3	0.2	51	178	0.3	299
	RANGE	32-141	15-66	0.1-0.4	0.1-0.4	19-81	66-283	0.1-0.5	111-466

Figure 3.41; show the relative contribution to  $Ra_{eq}$  owing to  $^{226}\text{Ra}$ ,  $^{232}\text{Th}$  and  $^{40}\text{K}$  for sediment samples under investigation in Safaga city. It's noticed that the contribution owing to  $^{226}\text{Ra}$ ,

$^{232}\text{Th}$  and  $^{40}\text{K}$  were ranged between (14% to 40%), (23% to 46%) and (27% to 62%) for sediment samples under investigation respectively. Figure 3.42, shows the average relative contribution of  $^{226}\text{Ra}$ ,  $^{232}\text{Th}$  and  $^{40}\text{K}$  contents of  $\text{Ra}_{\text{eq}}$  for samples under consideration, the average relative contribution to  $\text{Ra}_{\text{eq}}$  owing to  $^{226}\text{Ra}$ ,  $^{232}\text{Th}$  and  $^{40}\text{K}$  are 25%, 32% and 43%, respectively. It is evident that the contribution from  $^{40}\text{K}$  is the highest one where the contribution from  $^{226}\text{Ra}$  is the smallest.



**Figure 3.41:** The relative contribution (%) of  $^{226}\text{Ra}$ ,  $^{232}\text{Th}$  and  $^{40}\text{K}$  to Radium equivalent in ( $\text{H}_{\text{ex}}$ ) in every sample from Safaga City.



**Figure 3.42:** The average relative contribution to Radium equivalent activity ( $\text{Ra}_{\text{eq}}$ ) due to  $^{226}\text{Ra}$ ,  $^{232}\text{Th}$  and  $^{40}\text{K}$  in sediment samples from Safaga city

**2.2.2 Absorbed Gamma Dose Rate (D)**

From Table 3.10, values of absorbed dose (D) were ranged from 15 to 66 with average value of 41 nGyh<sup>-1</sup>, this average value is less than the world average value of (D) is 57 nGyh<sup>-1</sup> (UNSCEAR, 2000).

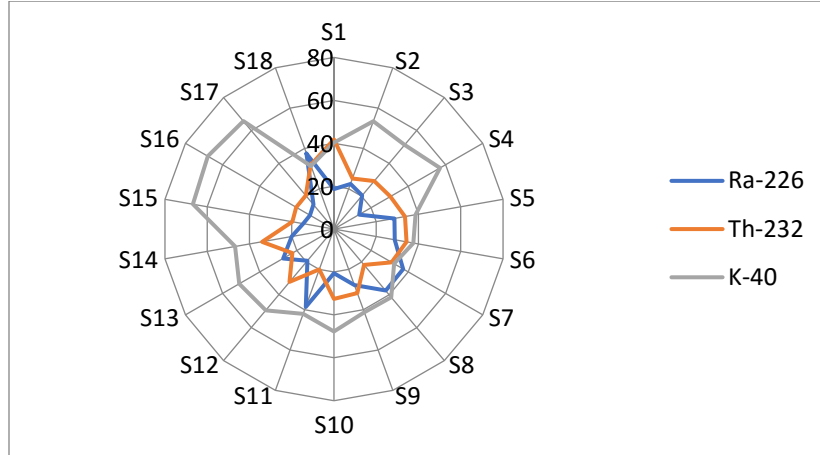


**Figure 3.43:** The relative contribution (%) of <sup>226</sup>Ra, <sup>232</sup>Th and <sup>40</sup>K to absorbed dose rate in every sample from Safaga City.

Figure 3.43; show the relative contribution to absorbed Dose rate owing to <sup>226</sup>Ra, <sup>232</sup>Th and <sup>40</sup>K. it's noticed that the contribution owing to <sup>226</sup>Ra, <sup>232</sup>Th and <sup>40</sup>K were ranged between (13% to 39%), (20% to 42%) and (31% to 68%) for sediment samples in Safaga city-under investigation respectively. Figure 3.44, shows the average relative contribution to (D) owing to <sup>226</sup>Ra, <sup>232</sup>Th and <sup>40</sup>K are 24%, 28% and 48%, respectively. It is evident that the contribution from <sup>40</sup>K is the highest one where the contribution from <sup>226</sup>Ra is the smallest; these indicate that the contribution to (D) is owing to <sup>40</sup>K followed by <sup>232</sup>Th followed by <sup>226</sup>Ra.

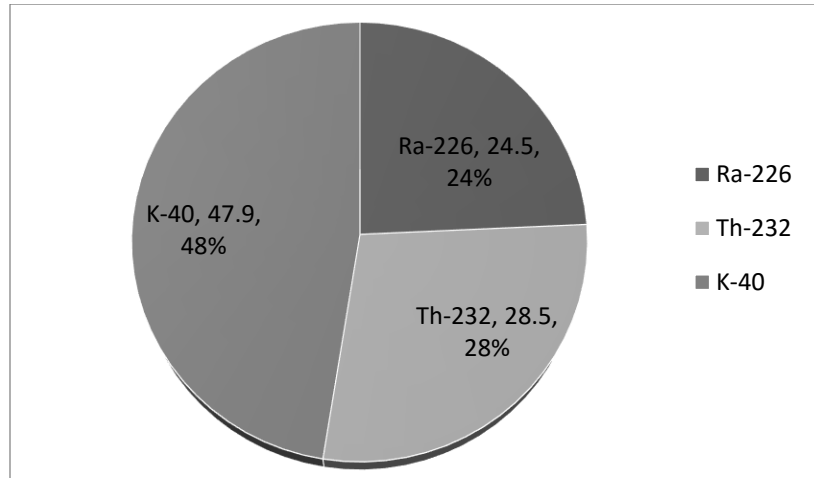


**Figure 3.44:** The average relative contribution to absorbed dose rate (D) due to <sup>226</sup>Ra, <sup>232</sup>Th and <sup>40</sup>K in sediment samples from Safaga city.

**2.2.3 Internal Radiation Hazard ( $H_{in}$ )**

Values of internal hazard index ( $H_{in}$ ), ranged from 0.01 to 0.4 with average value 0.3 as given in Table 3.10, for samples under investigation, which were lower than the unity, acceptable level (Beretka, and Mathew, 1985). Figure 3.45, shows the relative contribution of  $H_{in}$  owing to  $^{226}\text{Ra}$ ,  $^{232}\text{Th}$  and  $^{40}\text{K}$  in all measured samples. The contribution to  $H_{in}$  owing to  $^{226}\text{Ra}$ ,  $^{232}\text{Th}$  and  $^{40}\text{K}$  ranged from 24% to 57%, from 16% to 39% and from 20% to 55% for sediment samples under investigation respectively. Figure 3.46, shows the average relative contribution to ( $H_{in}$ ) owing to  $^{226}\text{Ra}$ ,  $^{232}\text{Th}$  and  $^{40}\text{K}$  are 40%, 26% and 34%, respectively. It is evident that the contribution from  $^{226}\text{Ra}$  is the highest one where the contribution from  $^{232}\text{Th}$  is the smallest; these indicate that the contribution to ( $H_{in}$ ) is owing to  $^{226}\text{Ra}$  followed by  $^{40}\text{K}$  followed by  $^{232}\text{Th}$ .

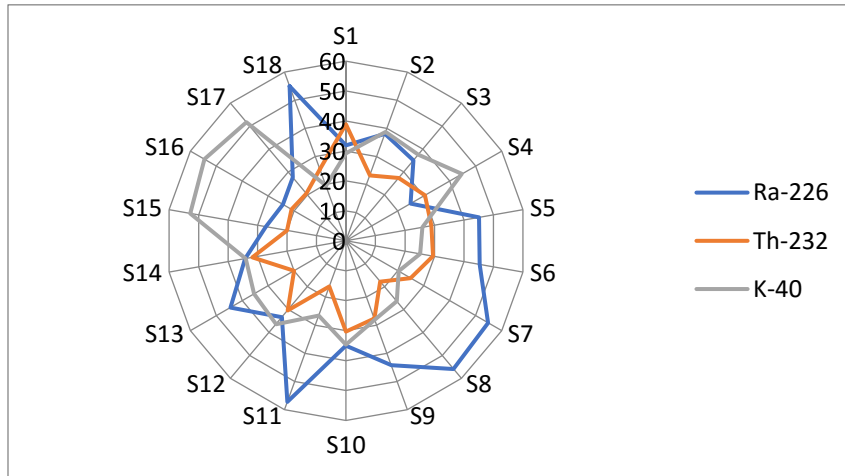


**Figure 3.45:** The relative contribution (%) of  $^{226}\text{Ra}$ ,  $^{232}\text{Th}$  and  $^{40}\text{K}$  to internal hazard index ( $H_{in}$ ) in every sample from Safaga City.

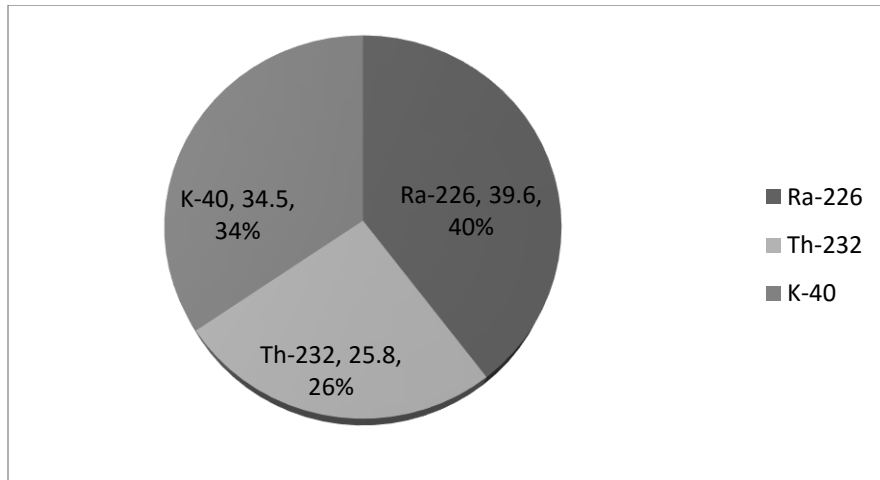


**Figure 3.46:** The average relative contribution to internal hazard index ( $H_{in}$ ) due to  $^{226}\text{Ra}$ ,  $^{232}\text{Th}$  and  $^{40}\text{K}$  in sediment samples from Safaga city.

**2.2.4 External Radiation Hazard ( $H_{ex}$ )**

The External hazard index ( $H_{ex}$ ), values ranged from 0.1 to 0.4 with average value 0.2 as given in Table 3.10, for samples under investigation, which were lower than the unity, acceptable level (Beretka, and Mathew, 1985). Figure (3.47), shows the relative contribution of  $H_{ex}$  owing to  $^{226}\text{Ra}$ ,  $^{232}\text{Th}$  and  $^{40}\text{K}$  in all measured samples. the contribution to  $H_{in}$  owing to  $^{226}\text{Ra}$ ,  $^{232}\text{Th}$  and  $^{40}\text{K}$  range between (14% to 40%), (23% to 46%) and (27% to 62%) for sediment samples under investigation respectively. Figure (3.48), shows the average relative contribution to ( $H_{ex}$ ) owing to  $^{226}\text{Ra}$ ,  $^{232}\text{Th}$  and  $^{40}\text{K}$  are 25%, 32% and 43%, respectively. It is evident that the contribution from  $^{40}\text{K}$  is the highest one where the contribution from  $^{226}\text{Ra}$  is the smallest; these indicate that the contribution to ( $H_{ex}$ ) is owing to  $^{40}\text{K}$  followed by  $^{232}\text{Th}$  followed by  $^{226}\text{Ra}$

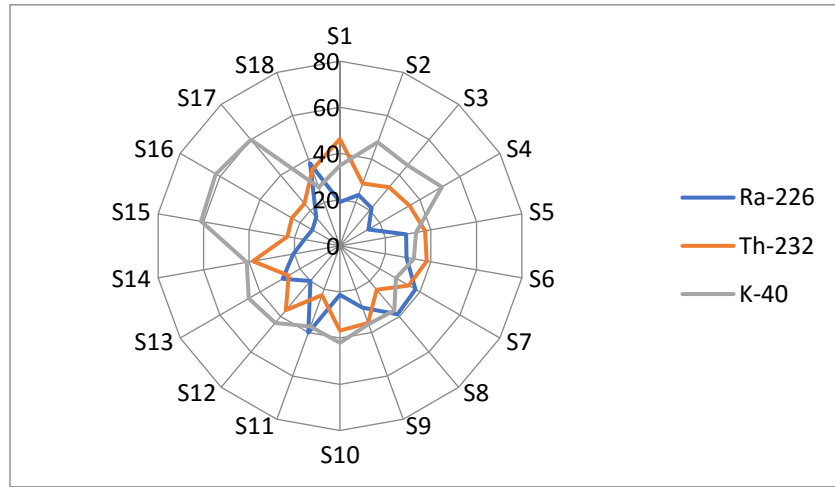


**Figure 3.47:** The relative contribution (%) of  $^{226}\text{Ra}$ ,  $^{232}\text{Th}$  and  $^{40}\text{K}$  to External hazard index ( $H_{ex}$ ) in every sample from Safaga City.

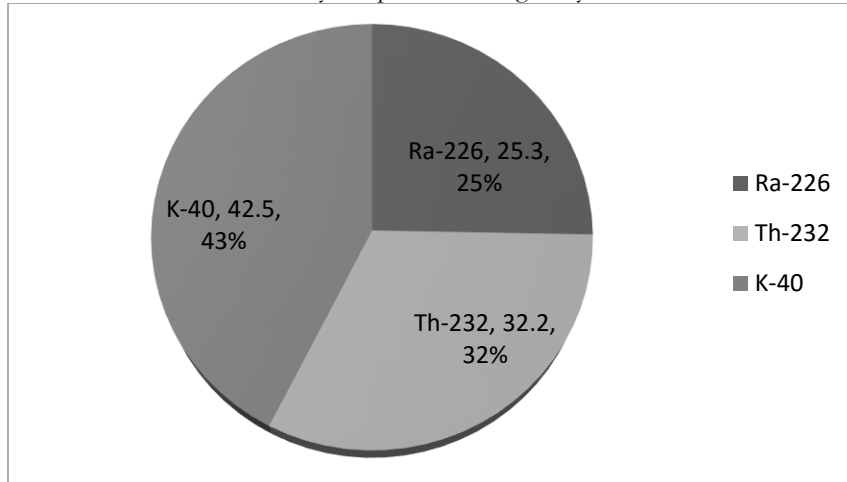


**Figure 3.48:** The average relative contribution to External hazard index ( $H_{ex}$ ) due to  $^{226}\text{Ra}$ ,  $^{232}\text{Th}$  and  $^{40}\text{K}$  in sediment samples from Safaga city



### 2.2.5 Annual Effective Dose

Table 3.10, shows the annual effective doses outdoors from measured sediment samples. It can be seen that the annual outdoor effective dose of samples under investigation from Safaga city varied from 19 to 81  $\mu\text{Sv}\cdot\text{y}^{-1}$ , with average value of 51  $\mu\text{Sv}\cdot\text{y}^{-1}$ . It is evident that the obtained average annual effective doses for outdoor in this study are smaller than the world average 70  $\mu\text{Sv}\cdot\text{y}^{-1}$  reported in UNSCEAR (2000).

The distribution patterns of (AEDE) at Safaga city show three patterns Figure 3. (49-a,b and c). The first one for, Mangrove area (k 17) we can see that the (AEDE) increase inside the zone which is concentrated by mangrove trees (*Avicennia marina*) may be because mangrove trees make stagnant water movement and tidal zone reach by sand, mud and small rocks as shown in Figure 3.49-a) while we find increasing of (AEDE) near the coast inside the shipping zone. The activities like exporting of the Egyptian phosphate, packed cement and crude oil may be the reason for this increasing of (AEDE) figure 3.(49-b). Also the increasing of (AEDE) in Touristic Harbour figure 3.49-c). May be due to landfilling and dredging on beach and intertidal zone during construction of this marina. The fill operation has been used sediments transported from the natural land of this site, and mountain area, there are many solid wastes and disposal of garbage from the boats in addition to, sunken boats at the area. Patch reefs and fringing reefs characterize the area in front of Tourist Harbour. The coral species in this area are *Acropora* sp., and *Stylophora pistillata*. Along the intertidal zone, there are some patches of seagrass. Dense algal species and coralline algae are incorporated with the reefs.

### 2.2.6 Gamma Index ( $I_\gamma$ )

Gamma index ( $I_\gamma$ ) was estimated for sediments under test and the derived values are presented in Table 3.10. It can be seen that, gamma activity index values were ranged from 0.1 to 0.5 with average value of 0.3. It is observed that, all samples have gamma index  $I_\gamma < 2$  which indicates gamma dose contribution from these sediment samples was not exceed 0.3  $\text{mSv}\cdot\text{y}^{-1}$ . Figure 3.50, shows the relative contribution to gamma index  $I_\gamma$  owing to  $^{226}\text{Ra}$ ,  $^{232}\text{Th}$  and  $^{40}\text{K}$ , where they ranged between (14% to 40%), (24% to 48%) and (26% to 61%) for sediment samples under investigation respectively.

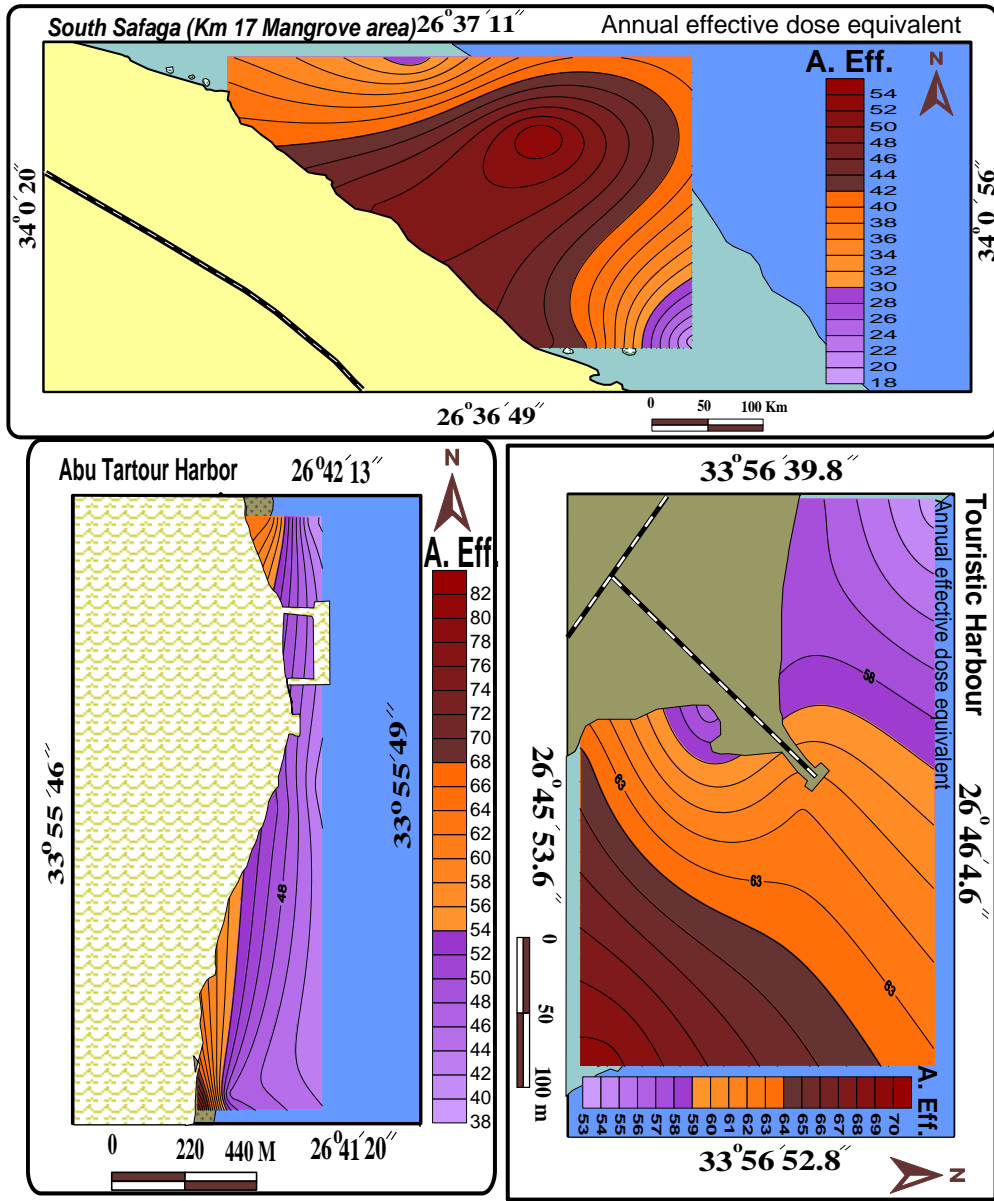
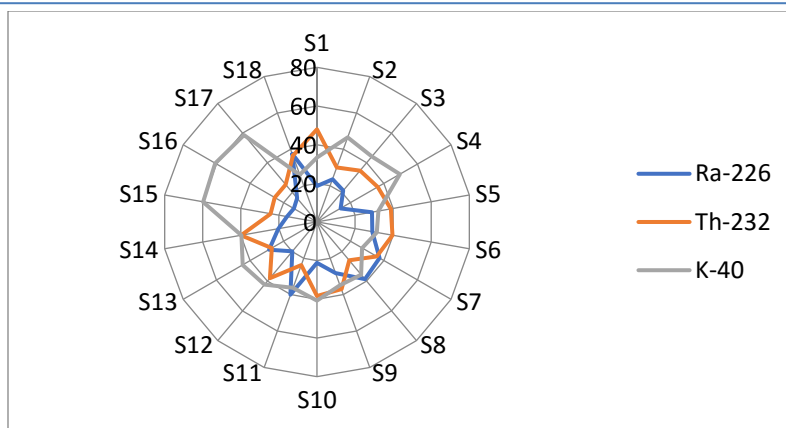
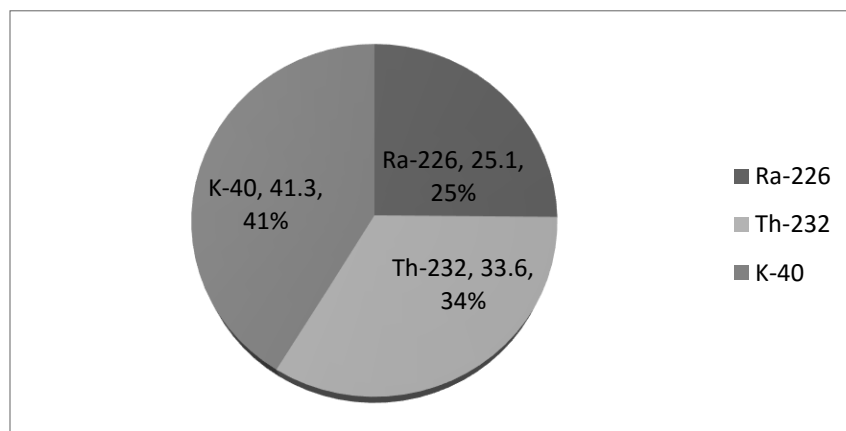


Figure3.49: The distribution patterns of AEDE at Safaga city.



**Figure 3.50:** The relative contribution (%) of  $^{226}\text{Ra}$ ,  $^{232}\text{Th}$  and  $^{40}\text{K}$  to Gamma activity index ( $I_\gamma$ ) in every sample from Safaga City.



**Figure 3.51:** The average relative contribution to Gamma activity index ( $I_\gamma$ ) due to  $^{226}\text{Ra}$ ,  $^{232}\text{Th}$  and  $^{40}\text{K}$  in sediment samples from Safaga city

Figure 3.51, shows the average relative contribution to  $I_\gamma$  owing to  $^{226}\text{Ra}$ ,  $^{232}\text{Th}$  and  $^{40}\text{K}$  are 25%, 34% and 41%, respectively. It is evident that the contribution from  $^{40}\text{K}$  is the highest one where the contribution from  $^{226}\text{Ra}$  is the smallest; these indicate that the contribution to  $I_\gamma$  is owing to  $^{40}\text{K}$  followed by  $^{232}\text{Th}$  followed by  $^{226}\text{Ra}$ .

### 2.2.7 Excess lifetime cancer risk (ELCR)

The obtained values of ELCR for the studied samples are summarized in Table 3.10. As we shown in Table 3.10, ELCR values ranged from  $66 \times 10^{-6}$  to  $283 \times 10^{-6}$  with average value of  $178 \times 10^{-6}$ . It evident that the obtained average ELCR in this study are smaller than the world average  $2900 \times 10^{-6}$  reported in UNSCEAR (2000). The distribution patterns of (ELCR) at Safaga city show three patterns (Figure3.52-a,b and c). The first one for, Mangrove area (k 17) we can see that the (ELCR) increase area as shown in (Figure3.52-a)

While we see increasing and decreasing area of (ELCR) in Abu-Tartour harbour in figure 3.52-b). Finally in Touristic Harbour the increasing of (ELCR) shown in figure 3.52-c), as we have explained the reasons previously.

2.2.8 Annual gonadal dose equivalent (AGDE)

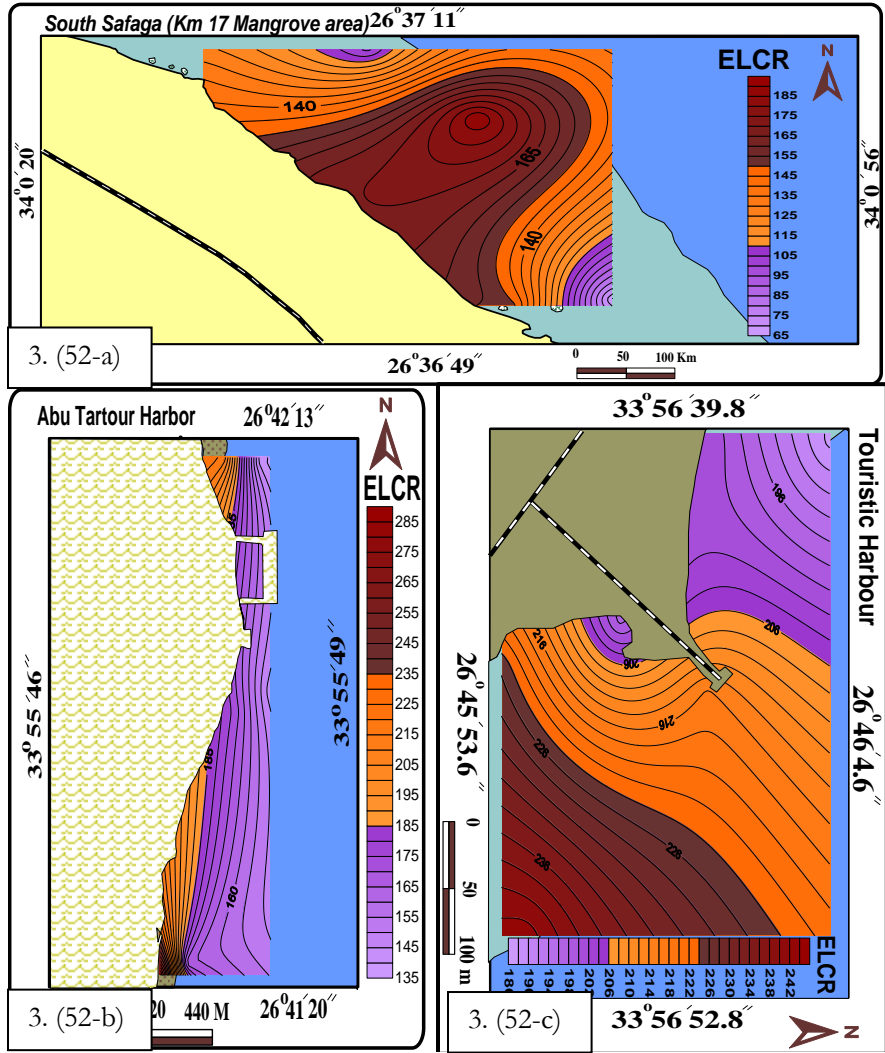


Figure 3.52: The distribution patterns of ELCR at Safaga city

The obtained values of AGDE for the studied samples are summarized in Table 3.10. As we shown in Table 3.10, AGDE values ranged from 111 to 466 with average value of 299  $\mu\text{Sv y}^{-1}$ , the average AGDE value is higher than the world average values for soil 0.298  $\text{mSv y}^{-1}$  (Zaidi et al., 1999). The annual gonadal dose equivalent results exceed the permissible recommended limits, indicating that the hazardous effects of the radiation are serious.

## 2.3 Radiological Characterization of Hurghada Sediment Samples.

### 2.3.1 Radium Equivalent Activities ( $Ra_{eq}$ )

The calculated values of  $Ra_{eq}$  for Hurghada samples under study are given in Table 3.11. These values were ranged from 11 to 159 with average value of  $74 \text{ Bqkg}^{-1}$ ; these results indicate all average values of  $Ra_{eq}$  are less than the upper limit  $370 \text{ Bqkg}^{-1}$  (Beretka, and Mathew, 1985) this mean that, it is safe, if it use as building materials.

Figure 3.53; show the relative contribution to  $Ra_{eq}$  owing to  $^{226}\text{Ra}$ ,  $^{232}\text{Th}$  and  $^{40}\text{K}$ . for sediment samples under investigation in Hurghada city It's noticed that the contribution owing to  $^{226}\text{Ra}$ ,  $^{232}\text{Th}$  and  $^{40}\text{K}$  were ranged between (11% to 48%), (12% to 41%) and (26% to 77%) for sediment samples under investigation respectively. Figure 3.54, shows the average relative contribution of  $^{226}\text{Ra}$ ,  $^{232}\text{Th}$  and  $^{40}\text{K}$  contents of  $Ra_{eq}$  for samples under consideration,

**Table 3.11.** Radium equivalent ( $Ra_{eq}$ ), the dose rate ( $D$ ), hazard indices ( $H_{ex}$  and  $H_{in}$ ), annual effective dose rate (AEDE), excess lifetime cancer risk (ELCR), Gamma index ( $I_\gamma$ ) and annual gonadal dose equivalent (AGDE) for Hurghada City

Sample Location	Code no.	$Ra_{eq}$ $\text{Bqkg}^{-1}$	D	$H_{in}$	$H_{ex}$	AEDE $\mu\text{Svy}^{-1}$	ELCR $10^{-6}$	$I_\gamma$	AGDE $\mu\text{Svy}^{-1}$
				nGy $\text{h}^{-1}$					
North Safer Hotel	H1	29	14	0.1	0.1	17	60	0.1	101
	H2	45	21	0.2	0.1	26	92	0.1	154
	H3	97	46	0.3	0.3	56	196	0.3	326
	H4	91	44	0.3	0.2	54	189	0.3	321
	H5	45	22	0.2	0.1	27	96	0.2	163
	H6	53	25	0.2	0.1	31	107	0.2	181
Hurghada Harbor	H7	80	38	0.3	0.2	47	165	0.3	277
	H8	11	5	0.0	0.0	6	21	0.0	35
	H9	27	13	0.1	0.1	16	55	0.1	92
	H10	96	49	0.3	0.3	60	210	0.3	366
	H11	101	50	0.3	0.3	61	213	0.3	364
	H12	102	49	0.3	0.3	60	212	0.3	360
NIOF area	H13	71	34	0.3	0.2	42	147	0.2	246
	H14	72	34	0.3	0.2	42	145	0.2	241
	H15	42	20	0.1	0.1	25	87	0.1	148
	H16	118	55	0.4	0.3	68	237	0.4	390
	H17	159	79	0.6	0.4	97	339	0.5	574
	H18	65	31	0.2	0.2	39	135	0.2	228
	H19	120	56	0.4	0.3	69	241	0.4	400
	H20	61	30	0.2	0.2	36	127	0.2	214
	H21	70	33	0.2	0.2	41	143	0.2	237
	MIN	11	5	0.0	0.0	6	21	0.0	35
	MAX	159	79	0.6	0.4	97	339	0.5	574
	AVEG	74	36	0.3	0.2	44	153	0.2	258
	RANGE	11-159	5-79	0.0- 0.3	0.0- 0.4	6-97	21- 339	0.0- 0.5	35- 574

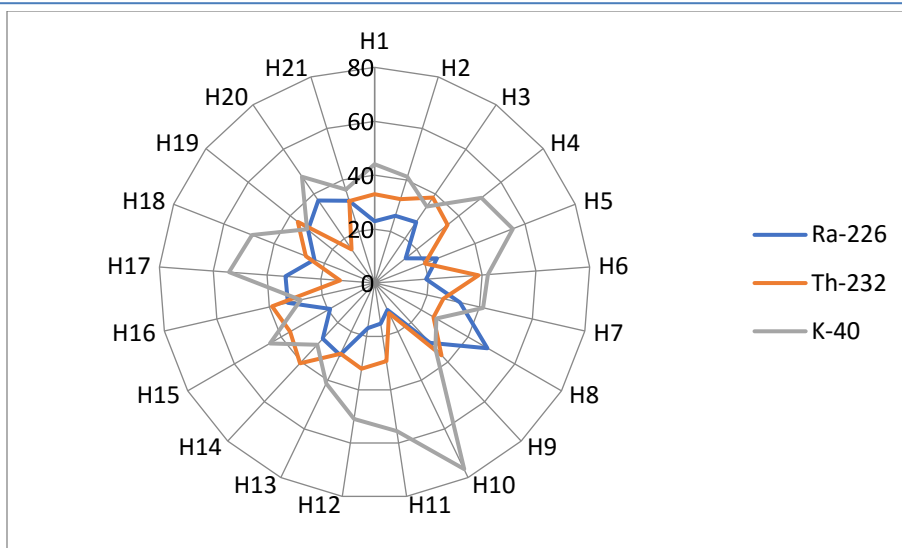


**Figure 3.53:** The relative contribution (%) of  $^{226}\text{Ra}$ ,  $^{232}\text{Th}$  and  $^{40}\text{K}$  to Radium equivalent in ( $H_{ex}$ ) in every sample from Hurghada City.

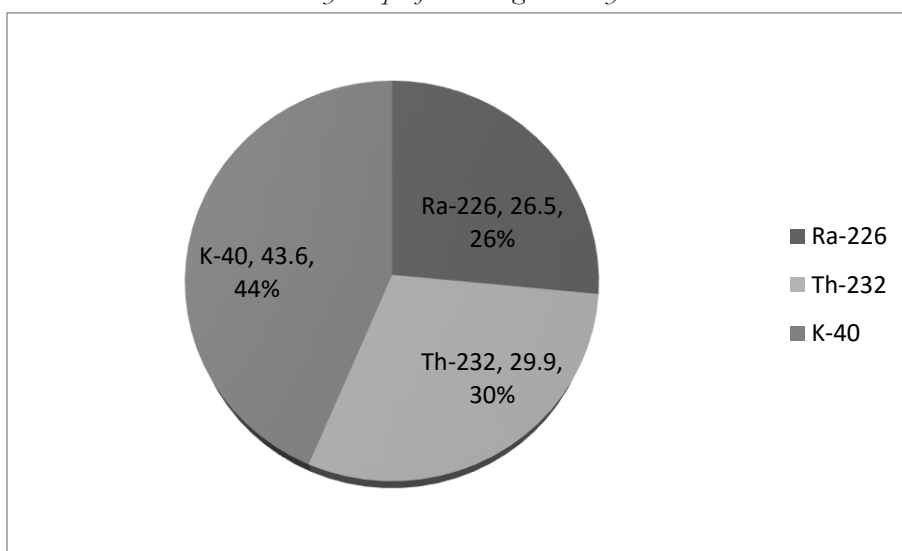


**Figure 3.54:** The average relative contribution to Radium equivalent activity ( $Ra_{eq}$ ) due to  $^{226}\text{Ra}$ ,  $^{232}\text{Th}$  and  $^{40}\text{K}$  in sediment samples from Hurghada city

The average relative contribution to  $Ra_{eq}$  owing to  $^{226}\text{Ra}$ ,  $^{232}\text{Th}$  and  $^{40}\text{K}$  are 26%, 30% and 44%, respectively. It is evident that the contribution from  $^{40}\text{K}$  is the highest one where the contribution from  $^{226}\text{Ra}$  is the smallest; these indicate that the contribution to  $Ra_{eq}$  is owing to  $^{40}\text{K}$  followed by  $^{232}\text{Th}$  followed by  $^{226}\text{Ra}$ .

### 2.3.2 Absorbed gamma dose rate (D)

From Table (3.11), values of absorbed dose (D) were ranged from 5 to 79 with average value of 36 nGyh<sup>-1</sup>, which is less than the world average value 57 nGyh<sup>-1</sup> (UNSCEAR, 2000).

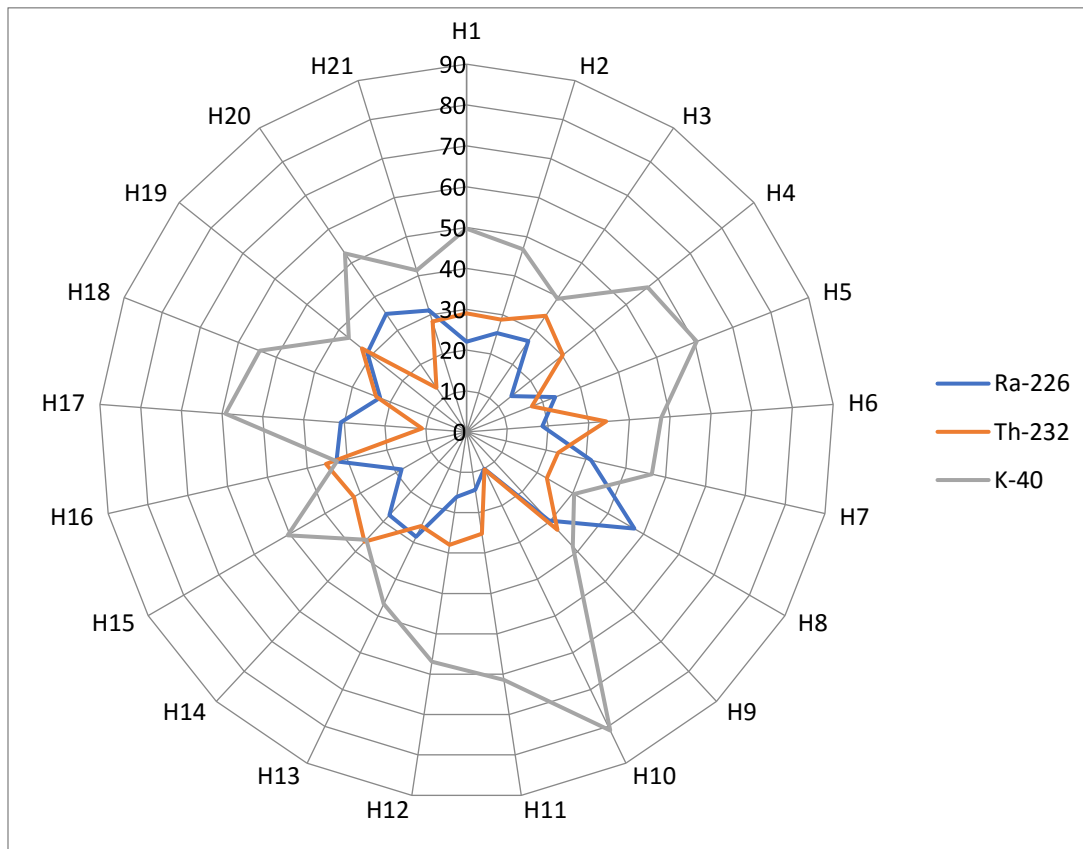


**Figure 3.55:** The relative contribution (%) of <sup>226</sup>Ra, <sup>232</sup>Th and <sup>40</sup>K to absorbed dose rate in every sample from Hurgbada City.

Figure 3.55; show the relative contribution to absorbed Dose rate owing to <sup>226</sup>Ra, <sup>232</sup>Th and <sup>40</sup>K. It's noticed that the contribution owing to <sup>226</sup>Ra, <sup>232</sup>Th and <sup>40</sup>K were ranged from 10% to 47%, from 10% to 37% and from 30% to 81% for sediment samples under investigation respectively. Figure 3.56, shows the average relative contribution to **D** owing to <sup>226</sup>Ra, <sup>232</sup>Th and <sup>40</sup>K are 25%, 26% and 49%, respectively. It is evident that the contribution from <sup>40</sup>K is the highest one where the contribution from <sup>226</sup>Ra is the smallest; these indicate that the contribution to **D** is owing to <sup>40</sup>K followed by <sup>232</sup>Th followed by <sup>226</sup>Ra.

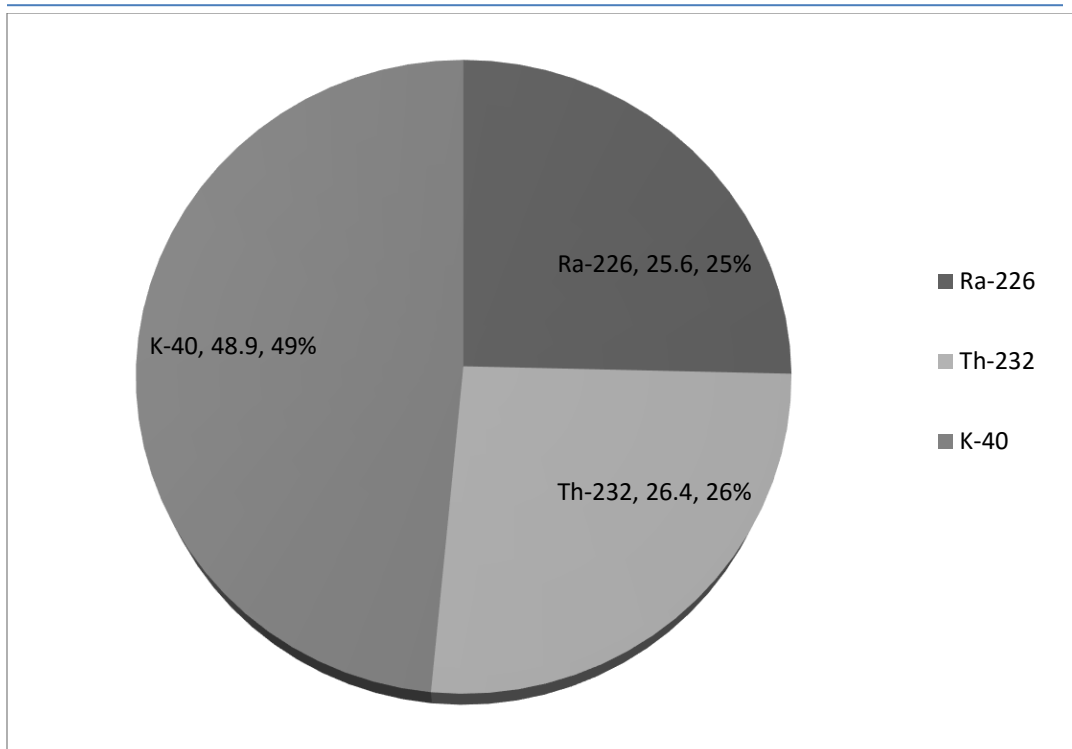


**Figure 3.56:** The average relative contribution to absorbed dose rate ( $D$ ) due to  $^{226}\text{Ra}$ ,  $^{232}\text{Th}$  and  $^{40}\text{K}$  in sediment samples from Hurghada city.

### 2.3.3 Internal radiation hazard ( $H_{in}$ )

Values of internal hazard index ( $H_{in}$ ), ranged from 0.04 to 0.6 with average value 0.3 as given in Table 3.11, for samples under investigation, which were lower than the unity, acceptable level (Beretka, and Mathew, 1985). Figure (3.57), shows the relative contribution of ( $H_{in}$ ) owing to  $^{226}\text{Ra}$ ,  $^{232}\text{Th}$  and  $^{40}\text{K}$  in all measured samples. The contribution to ( $H_{in}$ ) owing to  $^{226}\text{Ra}$ ,  $^{232}\text{Th}$  and  $^{40}\text{K}$  ranged between (20% to 65%), (10% to 32%) and (18% to 69%) for sediment samples under investigation respectively. Figure 3.58, shows the average relative contribution to ( $H_{in}$ ) owing to  $^{226}\text{Ra}$ ,  $^{232}\text{Th}$  and  $^{40}\text{K}$  are 41%, 24% and 35%, respectively. It is evident that the contribution from  $^{226}\text{Ra}$  is the highest one where the contribution from  $^{232}\text{Th}$  is the smallest; these indicate that the contribution to ( $H_{in}$ ) is owing to  $^{226}\text{Ra}$  followed by  $^{40}\text{K}$  followed by  $^{232}\text{Th}$ .



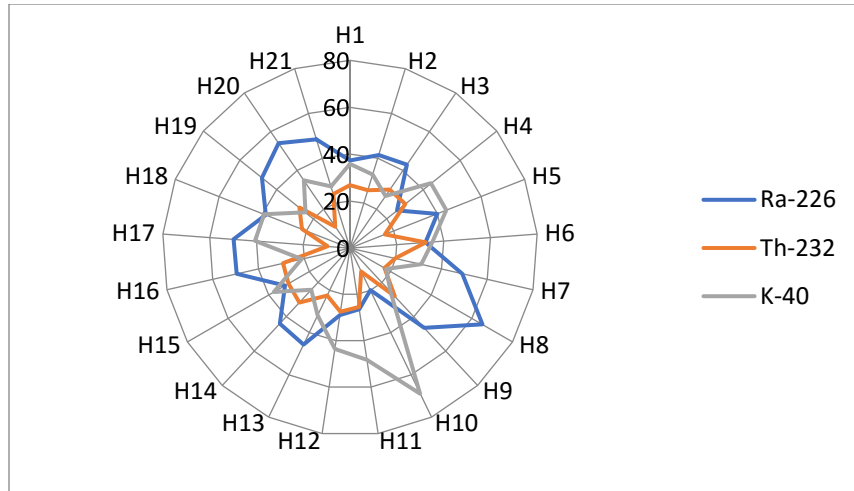


**Figure 3.57:** The relative contribution (%) of  $^{226}\text{Ra}$ ,  $^{232}\text{Th}$  and  $^{40}\text{K}$  to internal hazard index ( $H_{in}$ ) in every sample from Hurgada City.

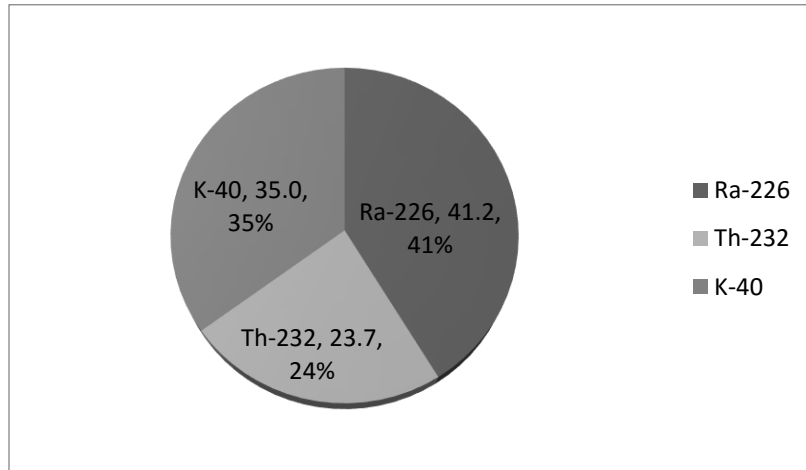


**Figure 3.58:** The average relative contribution to internal hazard index ( $H_{in}$ ) due to  $^{226}\text{Ra}$ ,  $^{232}\text{Th}$  and  $^{40}\text{K}$  in sediment samples from Hurgada city.

### 2.3.4 External radiation hazard ( $H_{ex}$ )

The External hazard index ( $H_{ex}$ ), values ranged from 0.03 to 0.4 with average value 0.2 as given in Table 3.11, for samples under investigation, which were lower than the unity, acceptable level (Beretka, and Mathew, 1985). Figure 3.59, shows the relative contribution of ( $H_{ex}$ ) owing to  $^{226}\text{Ra}$ ,  $^{232}\text{Th}$  and  $^{40}\text{K}$  in all measured samples. the contribution to ( $H_{in}$ ) owing to  $^{226}\text{Ra}$ ,  $^{232}\text{Th}$  and  $^{40}\text{K}$  ranged between (11% to 48%), (12% to 41%) and (26% to 77%) for sediment samples under investigation respectively.

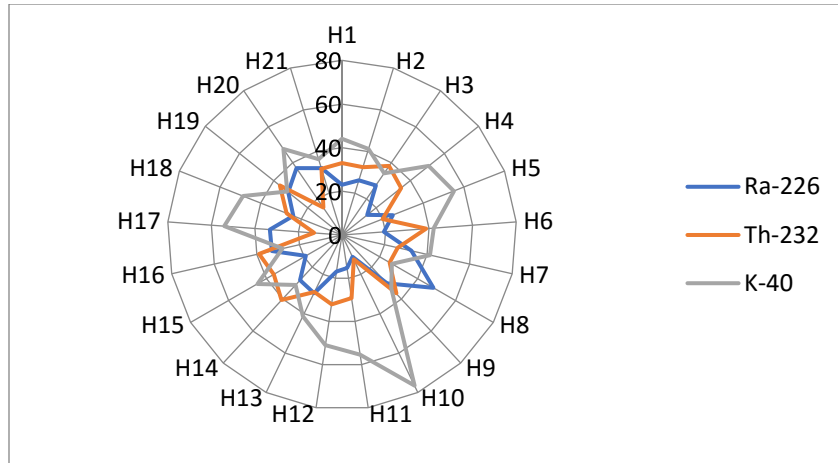


**Figure 3.59:** The relative contribution (%) of  $^{226}\text{Ra}$ ,  $^{232}\text{Th}$  and  $^{40}\text{K}$  to External hazard index ( $H_{\text{ex}}$ ) in every sample from Hurghada City.

Figure 3.60, shows the average relative contribution to ( $H_{\text{ex}}$ ) owing to  $^{226}\text{Ra}$ ,  $^{232}\text{Th}$  and  $^{40}\text{K}$  are 26%, 30% and 44%, respectively. It is evident that the contribution from  $^{40}\text{K}$  is the highest one where the contribution from  $^{226}\text{Ra}$  is the smallest; these indicate that the contribution to ( $H_{\text{ex}}$ ) is owing to  $^{40}\text{K}$  followed by  $^{232}\text{Th}$  followed by  $^{226}\text{Ra}$

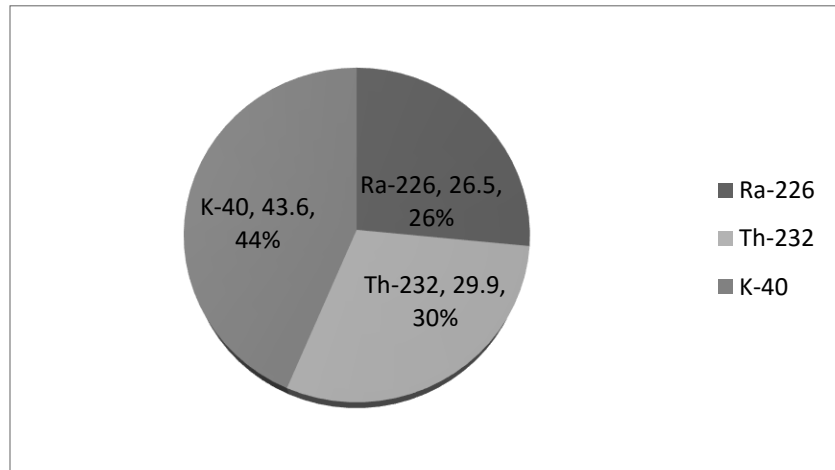


**Figure 3.60:** The average relative contribution to External hazard index ( $H_{\text{ex}}$ ) due to  $^{226}\text{Ra}$ ,  $^{232}\text{Th}$  and  $^{40}\text{K}$  in sediment samples from Hurghada city

### 2.3.5 Annual effective dose.

Table 3.11, shows the annual effective doses outdoors from measured sediment samples. It can be seen that the annual outdoor effective dose of samples under investigation from Hurghada city varied from 6 to 97  $\mu\text{Svy}^{-1}$ , with an average value of 44  $\mu\text{Svy}^{-1}$ . It is evident that the obtained average annual effective doses for outdoor in this study are smaller than the world average 70  $\mu\text{Svy}^{-1}$  reported in UNSCEAR (2000).

The distribution patterns of (AEDE) at Hurghada city show three patterns (Figure 3.61-a,b and c). The first one for, Safier Hotel area we can see that the (AEDE) increase in the middle of area under investigation this area called lagoon so may be this increasing as a result of landfilling dredging and reclamation of intertidal zone where the original coastline of this area has been completely altered by dredging and landfilling operations.as shown in (Figure3.61-a) while in Hurghada Harbour we can see increasing of (AEDE) in the northern part, may be this result due to this site was used to repair, maintain and construct fishing ships which lead to increasing of (AEDE) figure 3. (61-b). Also the increasing of (AEDE) in National Institute of Oceanography and Fisheries (NIOF) around the marine figure 3. (61-c). May be due to activity of researcher focused in this area which like lagoon also the source rock at (NIOF) is composed of limestone and raised reefs and this area is characterized by seagrasses and algae in intertidal and subtidal area in addition to coral

### 2.3.6 Gamma index ( $I_\gamma$ )

$I_\gamma$  was estimated for sediments under test and the derived values are presented in Table 3.11. It can be seen that, gamma activity index values were ranged from 0.04 to 0.5 with average value of 0.2. It is observed that, all samples have gamma index  $I_\gamma < 2$  which indicates gamma dose contribution from these sediment samples was not exceed  $0.3 \text{ mSv.y}^{-1}$

Figure 3.62, shows the relative contribution to gamma index  $I_\gamma$  owing to  $^{226}\text{Ra}$ ,  $^{232}\text{Th}$  and  $^{40}\text{K}$ , where they ranged between (11% to 48%), (13% to 42%) and (26% to 76%) for sediment samples under investigation respectively. Figure 3.63, shows the average relative contribution to  $I_\gamma$  owing to  $^{226}\text{Ra}$ ,  $^{232}\text{Th}$  and  $^{40}\text{K}$  are 27%, 31% and 42%, respectively. It is evident that the contribution from  $^{40}\text{K}$  is the highest one where the contribution from  $^{226}\text{Ra}$  is the smallest; these indicate that the contribution to  $I_\gamma$  is owing to  $^{40}\text{K}$  followed by  $^{232}\text{Th}$  followed by  $^{226}\text{Ra}$ .

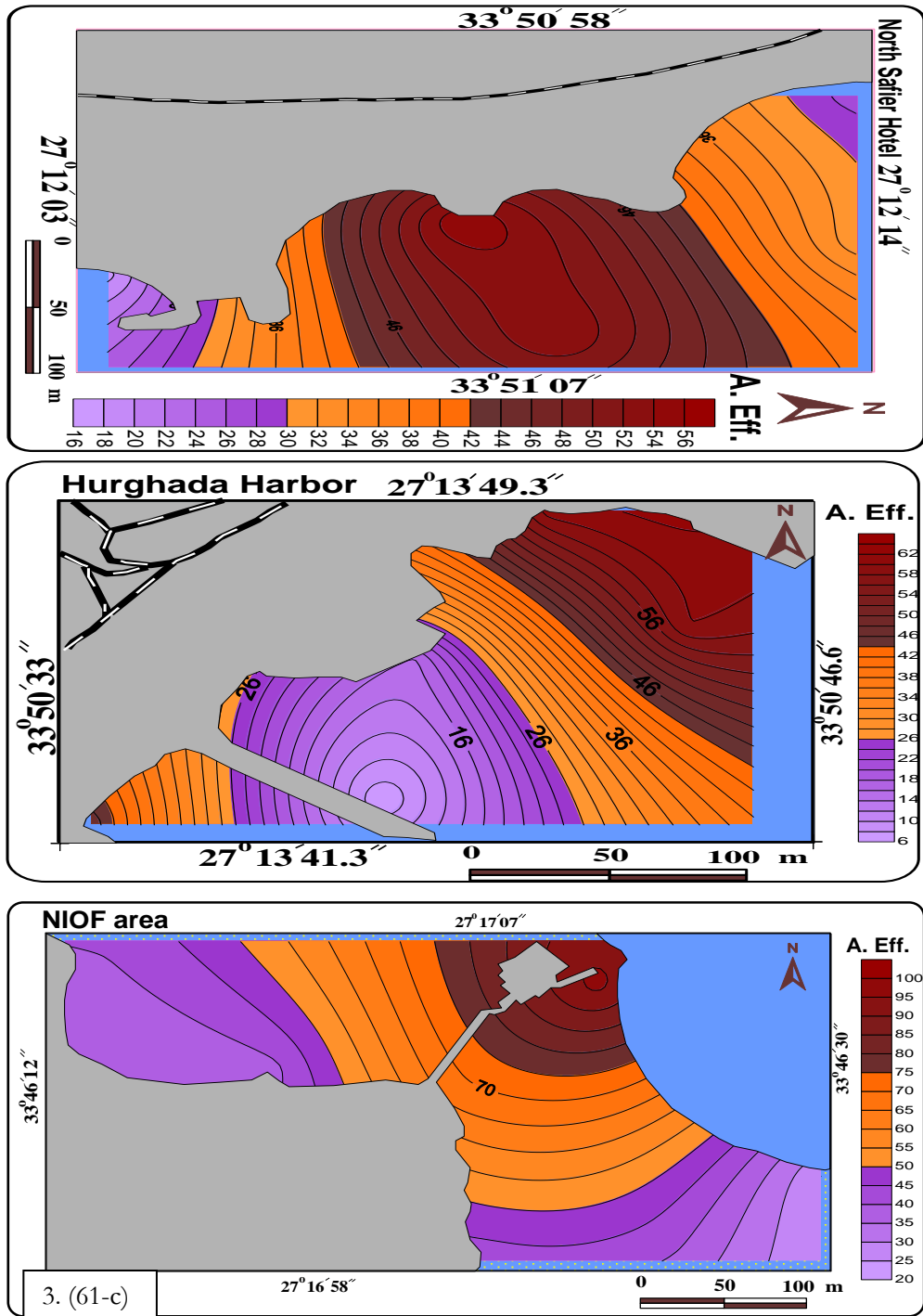
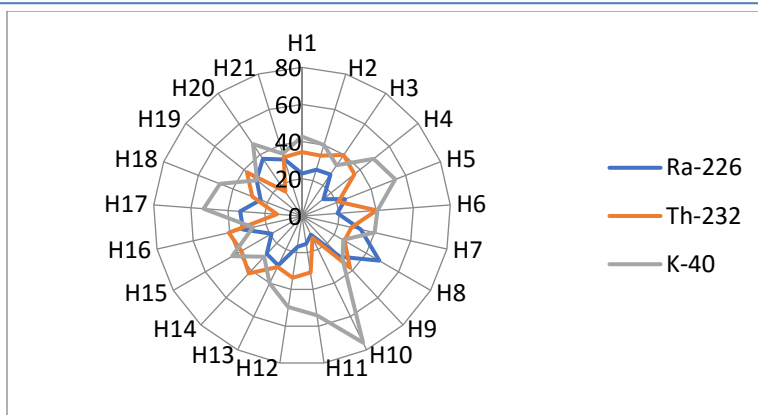
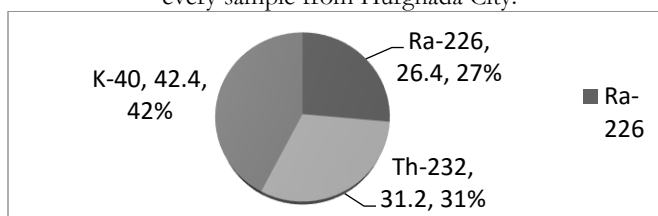


Figure 3.61: The distribution patterns of AEDE at Hurghada city



**Figure 3.62:** The relative contribution (%) of  $^{226}\text{Ra}$ ,  $^{232}\text{Th}$  and  $^{40}\text{K}$  to Gamma activity index ( $I_\gamma$ ) in every sample from Hurghada City.



**Figure 3.63:** The average relative contribution to Gamma activity index ( $I_\gamma$ ) due to  $^{226}\text{Ra}$ ,  $^{232}\text{Th}$  and  $^{40}\text{K}$  in sediment samples from Hurghada city

### 2.3.7 Excess lifetime cancer risk (ELCR)

The obtained values of ELCR for the studied samples are summarized in Table 3.11. As we shown in Table 3.11, ELCR values ranged from  $21 \times 10^{-6}$  to  $339 \times 10^{-6}$  with average value of  $153 \times 10^{-6}$ . It evident that the obtained average ELCR in this study are smaller than the world average  $2900 \times 10^{-6}$  reported in UNSCEAR (2000).

The distribution patterns of (ELCR) at Hurghada city show three patterns (Figure 3.64-a, b and c). The first one for, Safier Hotel area we can see that the (ELCR) increasing at the center and decreases on both sides as shown in (Figure 3.64-a), while (ELCR) in Hurghada Harbour Increase at the northern region and decreases in the direction of the south as illustrated in (figure 3.64-b). In NIOF area the increasing of (ELCR) surrounded the marine as shown in (figure 3.64-c). The reasons for this are the same as we have explained previously in (AEDE). It evident that the obtained average ELCR in this study are smaller than the world average  $2900 \times 10^{-6}$  reported in UNSCEAR (2000). It evident that the obtained average ELCR in this study are smaller than the world average  $2900 \times 10^{-6}$  reported in UNSCEAR (2000).

### 2.3.8 Annual gonadal dose equivalent (AGDE)

The obtained values of AGDE for the studied samples are summarized in Table 3.11. As we shown in Table 3.11, AGDE values ranged from 35 to 574 with average value of  $258 \mu\text{Sv y}^{-1}$ , the average AGDE value is closed to the world average values for soil  $0.298 \text{ mSv y}^{-1}$  (Zaidi et

al., 1999). The annual gonadal dose equivalent results do not exceed the permissible recommended limits, indicating that the hazardous effects of the radiation are negligible.

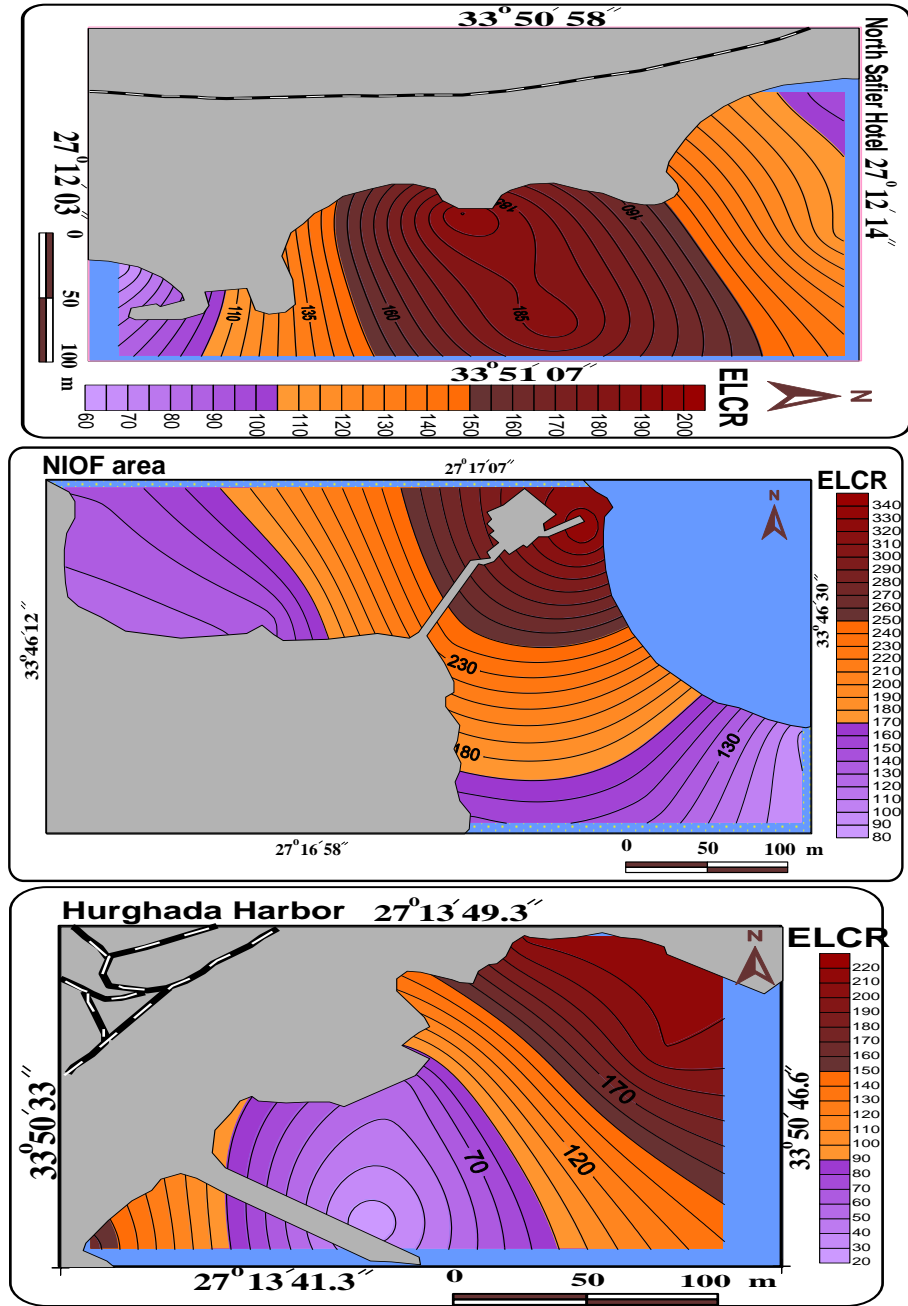


Figure 3.64: The distribution patterns of ELCR at Hurghada city

## 2.4 Radiological Characterization of Ras Gharib Sediment Samples.

### 2.4.1 Radium Equivalent Activities ( $Ra_{eq}$ )

The calculated values of  $Ra_{eq}$  for Gharib samples under study are given in Table 3.12. These values were ranged from 32 to 244 with average value of 92 Bqkg<sup>-1</sup>; these results indicate all average values of  $Ra_{eq}$  are less than the upper limit 370 Bqkg<sup>-1</sup> (Beretka, and Mathew, 1985) this mean that, it is safe, if it use as building materials.

Figure (3.65); show the relative contribution to  $Ra_{eq}$  owing to <sup>226</sup>Ra, <sup>232</sup>Th and <sup>40</sup>K. for sediment samples under investigation in Gharib city. It's noticed that the contribution owing to <sup>226</sup>Ra, <sup>232</sup>Th and <sup>40</sup>K were ranged between (9% to 44%), (18% to 52%) and (13% to 72%) for sediment samples under investigation respectively. Figure 3.66, shows the average relative contribution of <sup>226</sup>Ra, <sup>232</sup>Th and <sup>40</sup>K contents of  $Ra_{eq}$  for samples under consideration, the average relative contribution to  $Ra_{eq}$  owing to <sup>226</sup>Ra, <sup>232</sup>Th and <sup>40</sup>K are 32%, 39% and 29%, respectively. It is evident that the contribution from <sup>232</sup>Th is the highest one where the contribution from <sup>40</sup>K is the smallest.

**Table 3.12:** Radium equivalent ( $Ra_{eq}$ ), the dose rate (D), hazard indices ( $H_{ex}$  and  $H_{in}$ ), annual effective dose rate (AEDE), excess lifetime cancer risk (ELCR), Gamma index ( $I_\gamma$ ) and annual gonadal dose equivalent (AGDE) for Gharib city.

Sample Location	Code no.	$Ra_{eq}$ Bqkg <sup>-1</sup>	D	$H_{in}$	$H_{ex}$	AEDE $\mu$ Svy <sup>-1</sup>	ELCR (10 <sup>-6</sup> )	$(I_\gamma)$	AGDE $\mu$ Sv y <sup>-1</sup>
				nGy h <sup>-1</sup>					
south (El-Sakala area)	G1	42	19	0.1	0.1	24	83	0.1	138
	G2	71	32	0.3	0.2	39	137	0.2	222
	G3	133	63	0.5	0.4	77	271	0.4	449
	G4	72	33	0.3	0.2	41	142	0.2	231
	G5	58	27	0.2	0.2	33	114	0.2	185
	G6	106	49	0.4	0.3	60	211	0.4	346
middle (General Beach)	G7	120	58	0.4	0.3	71	247	0.4	416
	G8	119	54	0.4	0.3	67	234	0.4	382
	G9	63	32	0.2	0.2	39	136	0.2	237
	G10	61	28	0.2	0.2	34	119	0.2	193
	G11	98	46	0.3	0.3	57	198	0.3	330
	G12	105	50	0.4	0.3	61	213	0.4	354
north (General Company of petroleum)	G13	85	39	0.3	0.2	48	166	0.3	269
	G14	81	37	0.3	0.2	45	157	0.3	255
	G15	75	34	0.3	0.2	41	145	0.3	235
	G16	84	41	0.3	0.2	50	175	0.3	298
	G17	244	119	0.8	0.7	146	510	0.8	866
	G18	32	15	0.1	0.1	18	63	0.1	102
	MIN	32	15	0.1	0.1	18	63	0.1	102
	MAX	244	119	0.8	0.7	146	510	0.8	866
	AVEG	92	43	0.3	0.2	53	185	0.3	306
	RANGE	32-244	15-119	0.1-0.5	0.1-0.7	18-146	63-510	0.1-0.8	102-866

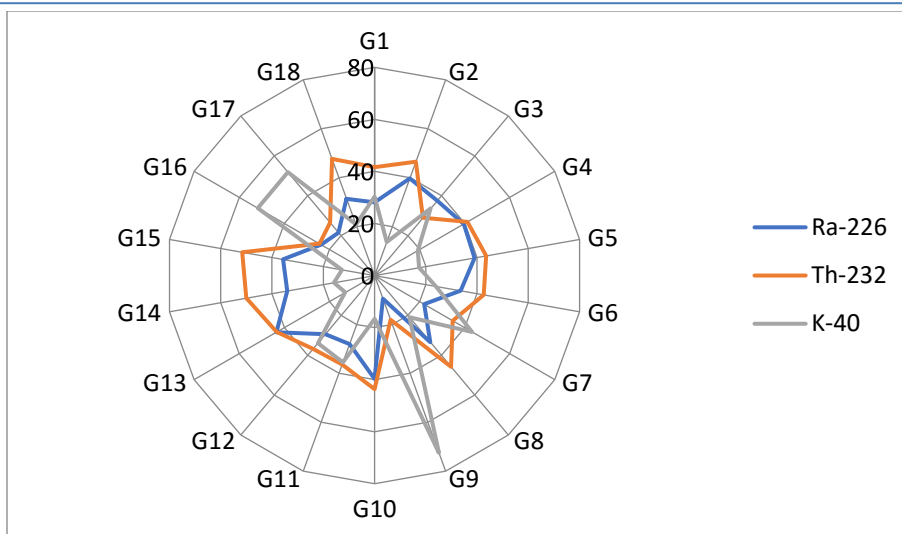


**Figure 3.65:** The relative contribution (%) of  $^{226}\text{Ra}$ ,  $^{232}\text{Th}$  and  $^{40}\text{K}$  to Radium equivalent in ( $H_{ex}$ ) in every sample from Gharib City.

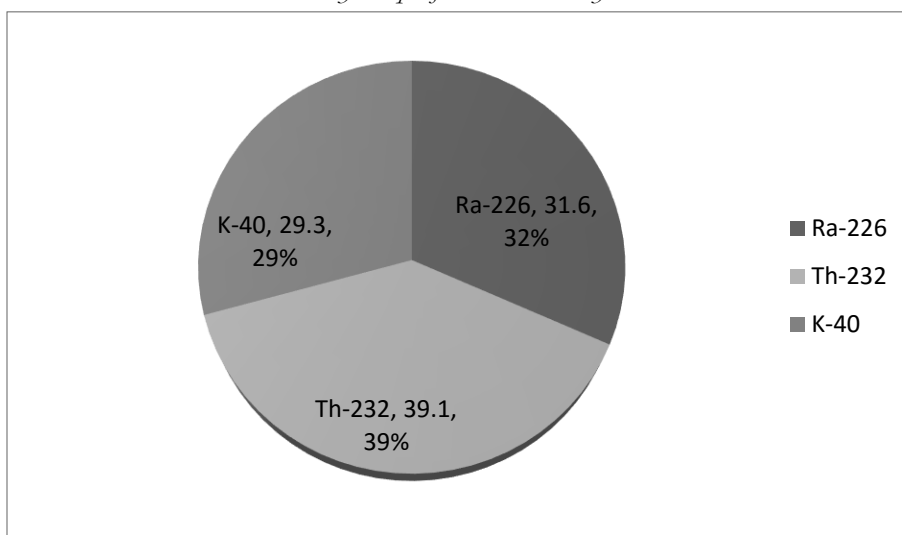


**Figure 3.66:** The average relative contribution to Radium equivalent activity ( $Ra_{eq}$ ) due to  $^{226}\text{Ra}$ ,  $^{232}\text{Th}$  and  $^{40}\text{K}$  in sediment samples from Gharib city

#### 2.4.2 Absorbed gamma dose rate (D)

From Table (3.12), values of absorbed dose (D) were ranged from 15 to 119 with average value of  $43 \text{ nGy h}^{-1}$ , these average value is less than the world average value of D is  $57 \text{ nGy.h}^{-1}$  (UNSCEAR, 2000). The relative contribution (%) of  $^{226}\text{Ra}$ ,  $^{232}\text{Th}$  and  $^{40}\text{K}$  to absorbed dose rate in every sample from Gharib City can be seen in Figure (3.67). From it, one can notice that the contribution absorbed dose rate (D) owing to  $^{226}\text{Ra}$ ,  $^{232}\text{Th}$  and  $^{40}\text{K}$  in sediment samples



under investigation were ranged between (9% to 44%), (15% to 48%) and (15% to 78%) for sediment samples under investigation respectively.

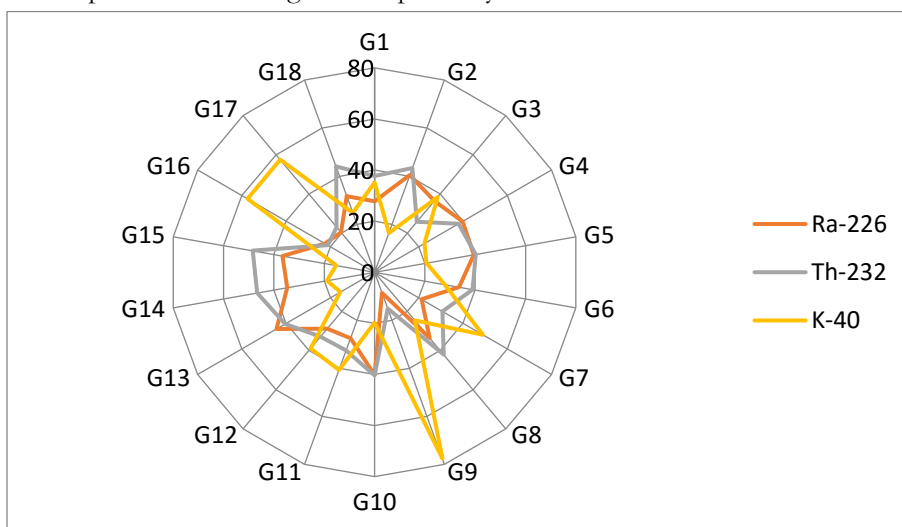


**Figure 3.67:** The relative contribution (%) of  $^{226}\text{Ra}$ ,  $^{232}\text{Th}$  and  $^{40}\text{K}$  to absorbed dose rate in every sample from Gharib City.

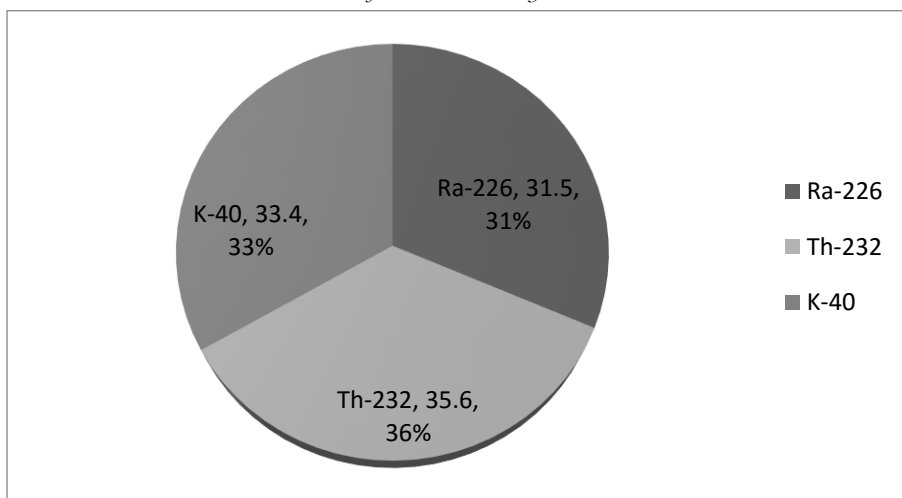
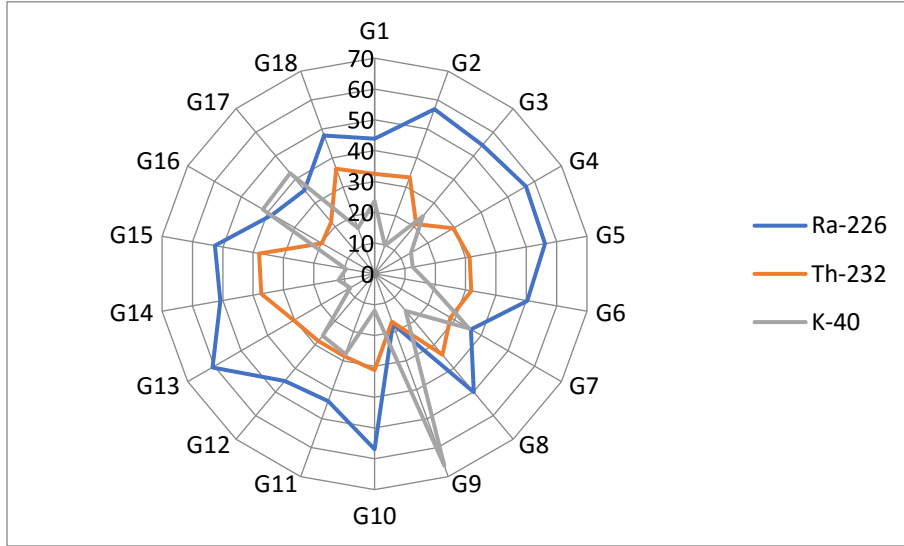


**Figure 3.68:** The average relative contribution to absorbed dose rate (D) due to  $^{226}\text{Ra}$ ,  $^{232}\text{Th}$  and  $^{40}\text{K}$  in sediment samples from Gharib city.

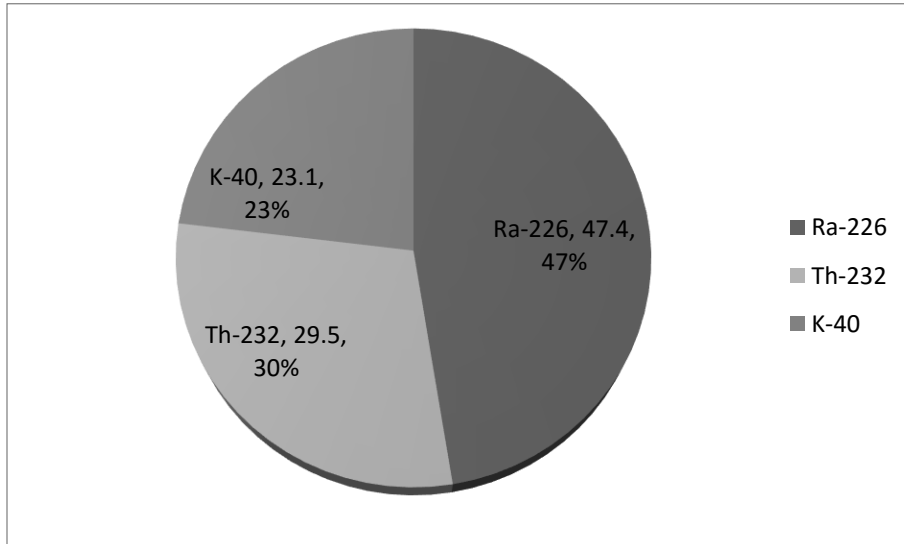
Figure (3.68), shows the average relative contribution to (D) owing to  $^{226}\text{Ra}$ ,  $^{232}\text{Th}$  and  $^{40}\text{K}$  are 31%, 36% and 33%, respectively. It is evident that the contribution from  $^{232}\text{Th}$  is the highest one where the contribution from  $^{226}\text{Ra}$  is the smallest; these indicate that the contribution to (D) is owing to  $^{232}\text{Th}$  followed by  $^{40}\text{K}$  followed by  $^{226}\text{Ra}$ .

**2.4.3 Internal radiation hazard ( $H_{in}$ )**

Values of internal hazard index ( $H_{in}$ ), ranged from 0.1 to 0.8 with average value 0.3 as given in Table 3.12, for samples under investigation, which were lower than the unity, acceptable level (Beretka, and Mathew, 1985). Figure 3.69, shows the relative contribution of ( $H_{in}$ ) owing to  $^{226}\text{Ra}$ ,  $^{232}\text{Th}$  and  $^{40}\text{K}$  in all measured samples. The contribution to ( $H_{in}$ ) owing to  $^{226}\text{Ra}$ ,  $^{232}\text{Th}$  and  $^{40}\text{K}$  ranged from 17% to 61%, from 16% to 38% and from 9% to 66% for sediment samples under investigation respectively.



**Figure 3.69:** The relative contribution (%) of  $^{226}\text{Ra}$ ,  $^{232}\text{Th}$  and  $^{40}\text{K}$  to internal hazard index ( $H_{in}$ ) in every sample from Gharib City.



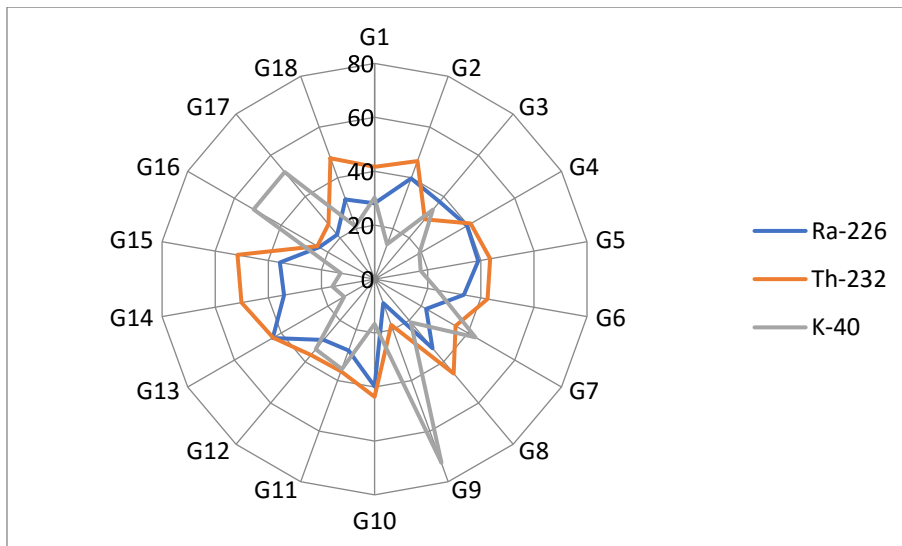
**Figure 3.70:** The average relative contribution to internal hazard index ( $H_{in}$ ) due to  $^{226}\text{Ra}$ ,  $^{232}\text{Th}$  and  $^{40}\text{K}$  in sediment samples from Gharib city.

Figure (3.70), shows the average relative contribution to ( $H_{in}$ ) owing to  $^{226}\text{Ra}$ ,  $^{232}\text{Th}$  and  $^{40}\text{K}$  are 47%, 30% and 23%, respectively. It is evident that the contribution from  $^{226}\text{Ra}$  is the highest one where the contribution from  $^{40}\text{K}$  is the smallest; these indicate that the contribution to ( $H_{in}$ ) is owing to  $^{226}\text{Ra}$  followed by  $^{232}\text{Th}$  and  $^{40}\text{K}$ .

#### 2.4.4 External radiation hazard ( $H_{ex}$ )

The External hazard index ( $H_{ex}$ ), values ranged from 0.1 to 0.7 with average value 0.2 as given in Table 3.12, for samples under investigation, which were lower than the unity, acceptable level (Beretka, and Mathew, 1985).

Figure (3.71), shows the relative contribution of ( $H_{ex}$ ) owing to  $^{226}\text{Ra}$ ,  $^{232}\text{Th}$  and  $^{40}\text{K}$  in all measured samples. The contribution to ( $H_{in}$ ) owing to  $^{226}\text{Ra}$ ,  $^{232}\text{Th}$  and  $^{40}\text{K}$  ranged between (9% to 44%), (18% to 52%) and (13% to 72%) for sediment samples under investigation respectively.



**Figure 3.71:** The relative contribution (%) of  $^{226}\text{Ra}$ ,  $^{232}\text{Th}$  and  $^{40}\text{K}$  to External hazard index ( $H_{ex}$ ) in every sample from Gharib City.

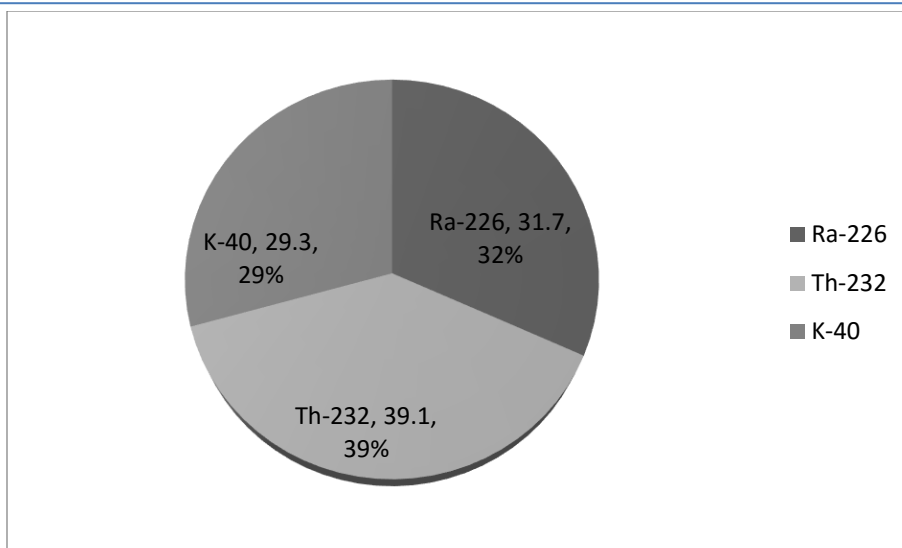


**Figure 3.72:** The average relative contribution to External hazard index ( $H_{ex}$ ) due to  $^{226}\text{Ra}$ ,  $^{232}\text{Th}$  and  $^{40}\text{K}$  in sediment samples from Gharib city

Figure (3.72), shows the average relative contribution to ( $H_{ex}$ ) owing to  $^{226}\text{Ra}$ ,  $^{232}\text{Th}$  and  $^{40}\text{K}$  are 32%, 39% and 29%, respectively. It is evident that the contribution from  $^{232}\text{Th}$  is the highest one where the contribution from  $^{40}\text{K}$  is the smallest; these indicate that the contribution to ( $H_{ex}$ ) is owing to  $^{232}\text{Th}$  followed by  $^{226}\text{Ra}$  followed by  $^{40}\text{K}$ .

#### 2.4.5 Annual effective dose

Table 3.12, shows the annual effective doses outdoors from measured sediment samples. It can be seen that the annual outdoor effective dose of samples under investigation from Gharib city varied from 18 to 146  $\mu\text{Svy}^{-1}$ , with an average value of 53  $\mu\text{Svy}^{-1}$ . It is evident that the obtained average annual effective doses for outdoor in this study are smaller than the world average 70  $\mu\text{Svy}^{-1}$  reported in UNSCEAR (2000).

The distribution patterns of (AEDE) at Ras Ghareb City Figure 3. (73-a,b and c) divided into three stations from south to north the first one; El-Sakala area, which is characterized by the existence of a narrow intertidal zone. In the beach area and intertidal zone, the sands are accumulated in the form of small dunes covered by some vegetation. These dunes separate between the shore zone and sabkha evaporates. AEDE increases at the center toward the beach and decreases on both sides, perhaps due to the formation of a lagoon that allows the entry of water and does not allow it to get out as shown in Figure 3. (73-a). While in the General Beach area, we can see an increase in (AEDE) in the southern part, which may be the result of terrigenous sediments that have been transported to the marine environment by some wadis, especially in the southern part, which may contain natural radioactive materials Figure 3. (73-b). But in the General Company of Petroleum Figure 3. (73-c). The (AEDE) recorded high values compared with other stations, this is due to the existing of a big part of the intertidal zone is covered by heavy

oil spills as a result of exploration and extraction activities of crude oil and flooding of some oil wells. Generally, the beach area of Ras Ghareb is affected by oil spills.

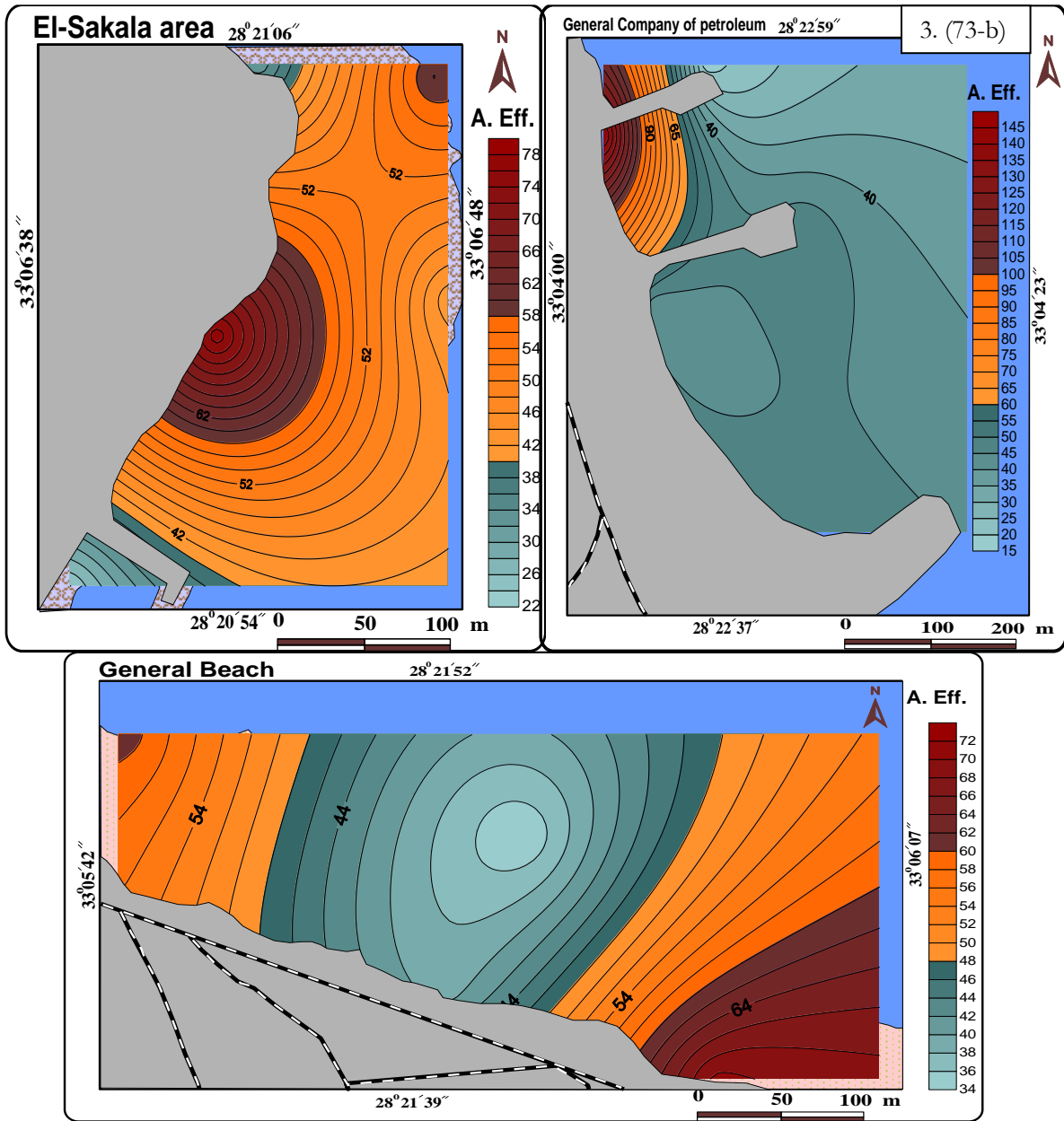
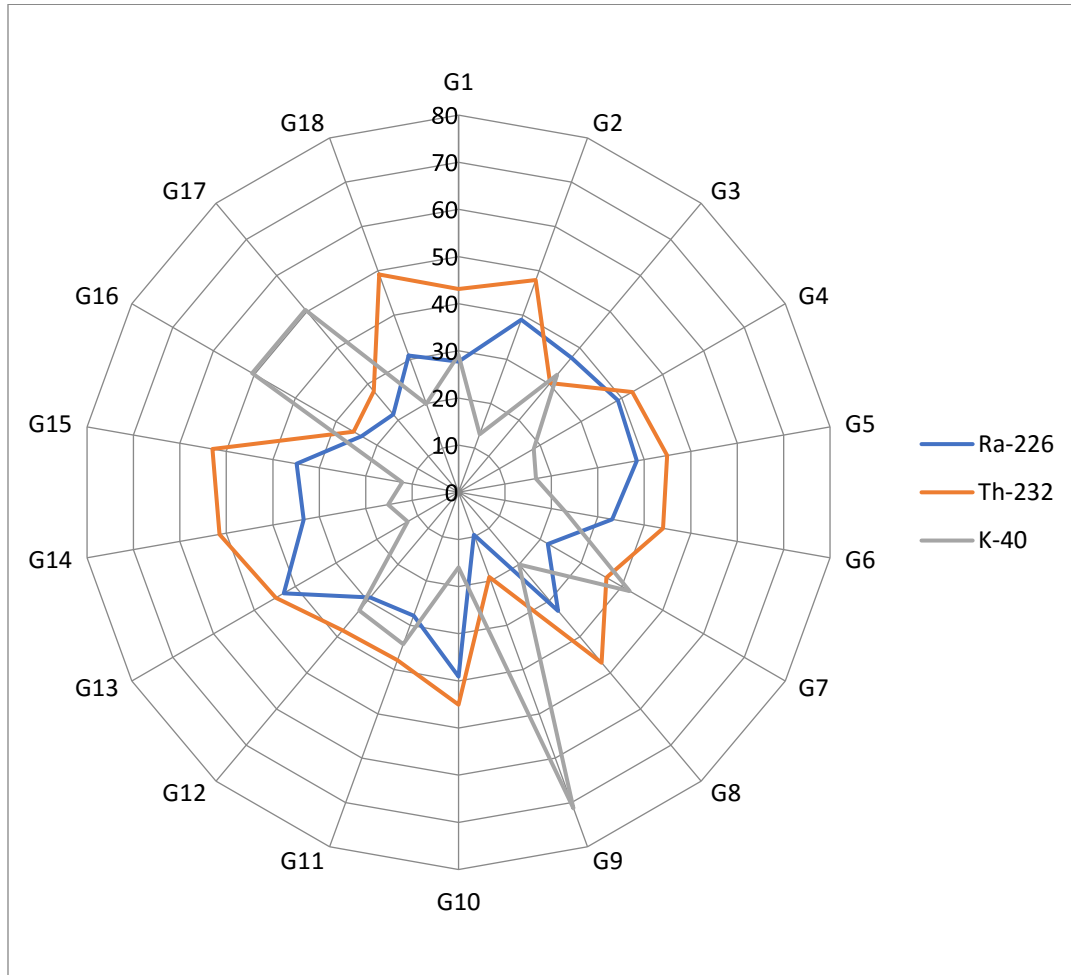


Figure 3.73: The distribution patterns of AEDE at Ras Gharib city

### 2.4.6 Gamma index ( $I_\gamma$ )

Gamma index ( $I_\gamma$ ) was estimated for sediments under test and the derived values are presented in Table (3.12). It can be seen that, gamma activity index values were ranged from 0.1 to 0.8 with average value of 0.3. It is observed that, all samples have gamma index  $I_\gamma < 2$  which indicates gamma dose contribution from these sediment samples was not exceed  $0.3 \text{ mSv.y}^{-1}$



**Figure 3.74:** The relative contribution (%) of  $^{226}\text{Ra}$ ,  $^{232}\text{Th}$  and  $^{40}\text{K}$  to Gamma activity index ( $I_\gamma$ ) in every sample from Gharib City.

Figure (3.74), shows the relative contribution to gamma index  $I_\gamma$  owing to  $^{226}\text{Ra}$ ,  $^{232}\text{Th}$  and  $^{40}\text{K}$ , where they ranged between (10% to 43%), (19% to 53%) and (12% to 71%) for sediment samples under investigation respectively. Figure 3.75, shows the average relative contribution to  $I_\gamma$  owing to  $^{226}\text{Ra}$ ,  $^{232}\text{Th}$  and  $^{40}\text{K}$  are 31%, 41% and 28%, respectively. It is evident that the contribution from  $^{232}\text{Th}$  is the highest one where the contribution from  $^{40}\text{K}$  is the smallest; these indicate that the contribution to  $I_\gamma$  is owing to  $^{232}\text{Th}$  followed by  $^{226}\text{Ra}$  and  $^{40}\text{K}$ .

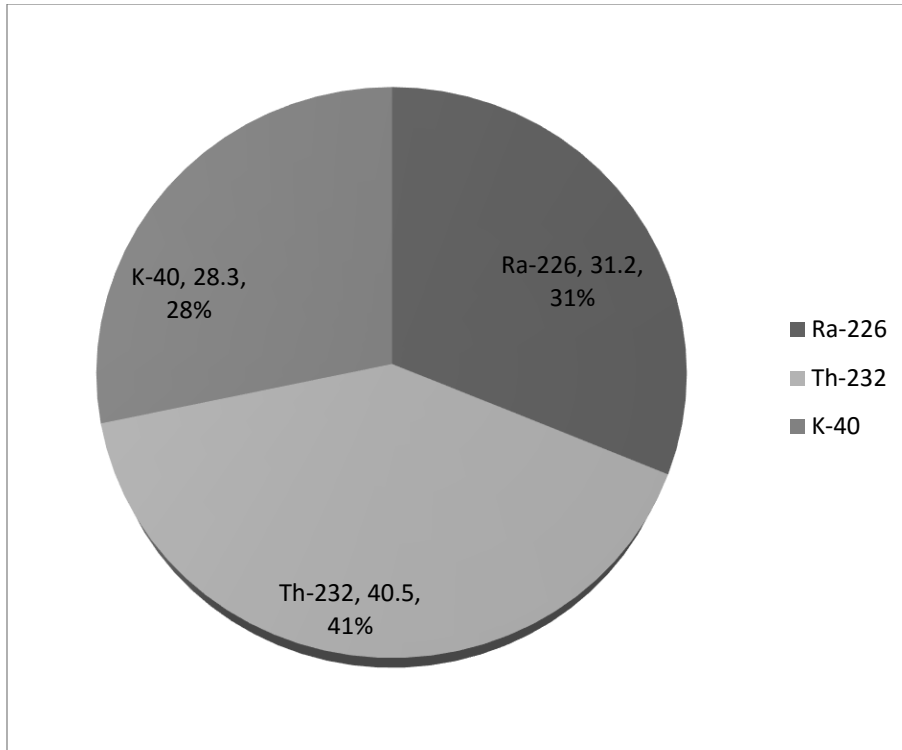


**Figure 3.75:** The average relative contribution to Gamma activity index ( $I_\gamma$ ) due to  $^{226}\text{Ra}$ ,  $^{232}\text{Th}$  and  $^{40}\text{K}$  in sediment samples from Gharib city

#### 2.4.7 Excess lifetime cancer risk (ELCR)

The obtained values of ELCR for the studied samples are summarized in Table 3.12. As we shown in Table (3.12), ELCR values ranged from  $63 \times 10^{-6}$  to  $510 \times 10^{-6}$  with average value of  $185 \times 10^{-6}$ . It evident that the obtained average ELCR in this study are smaller than the world average  $2900 \times 10^{-6}$  reported in UNSCEAR (2000).

The distribution patterns of (ELCR) at Ras Ghareb city show three patterns (Figure3.76). The first one for, El-Sakala area we can see that the (ELCR) increasing at the center and decreases on both sides as shown in Figure3. (76-a), while (ELCR) in General Beach area Increase at the southern region and decreases in the direction of the north as illustrated in figure 3. (76-b). In General Company of Petroleum are the (ELCR) recorded high value especially around the marine as shown in figure 3. (64-c). The reasons we have explained previously in (AEDE).

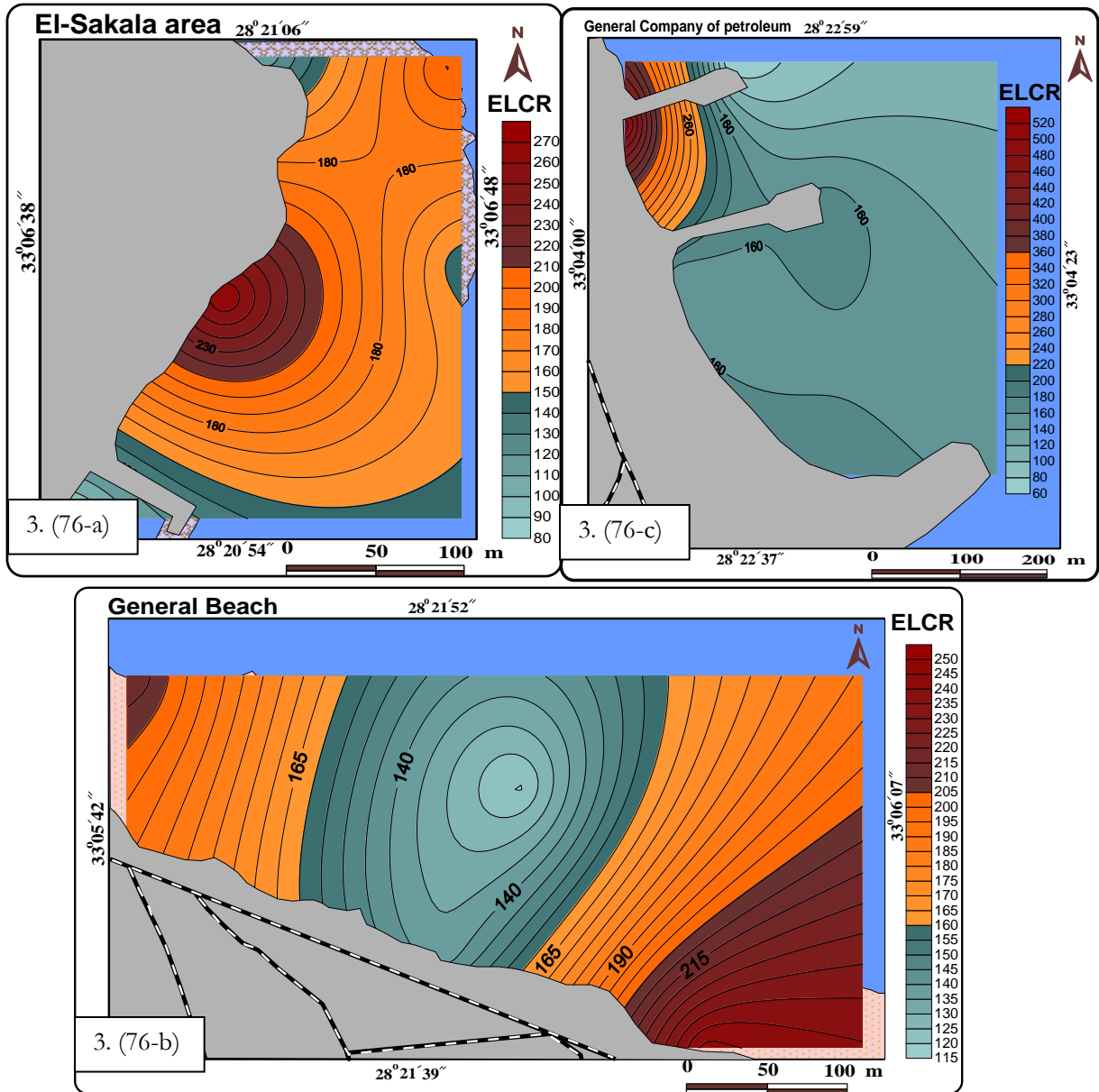


Figure 3.76: The distribution patterns of ELCR at Ras Gharib city

#### 2.4.8 Annual gonadal dose equivalent (AGDE)

The obtained values of AGDE for the studied samples are summarized in Table (3.12). As we shown in Table (3.12), AGDE values ranged from 102 to 866 with average value of  $306 \mu\text{Sv} \cdot \text{y}^{-1}$ , the average AGDE value is higher than the world average values for soil  $0.298 \text{ mSv} \cdot \text{y}^{-1}$  (Zaidi et al., 1999). The annual gonadal dose equivalent results exceed the permissible recommended limits, indicating that the hazardous effects of the radiation are serious.



### **3 Geochemical characteristics OF MARINE SEDIMENTS.**

The major threat to the health, productivity and biodiversity of the marine environment result from human activities on land in coastal areas and further inland. Most of the pollution load of the marine environment, including municipal (scrap metal, wood, plastics, miscellaneous garbage and a variety of construction materials) industrial and other wastes and run-off, as well as atmospheric deposition, emanates from land-based activities and affects the most productive areas of the marine environment, including estuaries and near shore coastal water. These areas are likewise threatened by physical alteration of the coastal environment, including destruction of habitats of vital importance for ecosystem health. Moreover, contaminants which pose risks to human health and living resources are transported long distances by watercourses, coastal currents and atmospheric processes.

This study discusses the Sediment types; the total organic matter and organic carbon content, carbonates and concentration of heavy metals in order to explain their distribution and inter-relations to detect the effect of human activities in marine environment to identify and characterize impacted areas. The results of the geochemical analyses of marine sediments in Qusier city, Safaga city, Hurghada city and Ras Ghareb city are listed in in Table (3.13) and Table (3.14) in form Min, Max and Average.

#### **3.1 Sediment Texture**

The purpose of the mechanical analysis for sediments is not only to obtain the nature of sediments but also:

1. Understanding the physical characteristics of these sediments,
2. Revealing the relation and the influence of grain size and source material and depositional environment, and
3. Illustrating the correlation between concentration of radioactive materials and sediments type.

The areas under investigation receive sediments from two different sources; the terrigenous rock fragments from the hinter land mountains (i.e.,siliclastic) and skeletal carbonates from the sea (carbonate sediments).In these mixed environments ,the terrigenous components are introduced from outside the depositional basin, whereas the skeletal carbonates originates mainly from near the depositional basin (Mansour,1995).The skeletal carbonates have a remarkably limited history of transportation and deposition. However, it is not easy to reveal the hydrodynamic behavior of the skeletal fragments, which is dependent on shape, density and size (Maiklem, 1968; Braithwaite, 1973). Generally, the particle size of the sediments changes from coarse sand near the beach to fine sand with increasing distance from the beach towards the deeper water.

**Table 3.13:** Minimum, Maximum and Average of Sediment types (Gravel, Sand and Mud) and heavy metals of marine sediments from shoreline for all samples.

area	Division	Sediment types			Fe	Mn	Zn	Cu	Pb	Ni	Cd	
		Gravel	Sand	Mud								
Quseir City	El-Edua area	Min	1	68	0	4987	188	12	4	2	5	0
		Max	32	99	2	8925	390	32	13	8	33	0
		Avg.	14	86	1	6918	273	20	9	5	16	0
	Quseir Harbor	Min	0	69	0	9500	500	38	20	24	25	1
		Max	31	99	9	16000	1000	110	60	75	65	3
		Avg.	8	90	2	12190	740	78	37	49	49	2
	north Flamiko Village	Min	0	69	0	3245	99	8	4	6	5	0
		Max	31	97	3	6543	457	24	16	18	26	1
		Avg.	12	87	1	4908	255	15	10	12	14	0
Safaga City	Mangrove area	Min	2	77	1	64720	378	38	10	7	5	0
		Max	23	96	8	76277	531	53	15	24	15	0
		Avg.	10	87	3	70499	447	45	13	16	11	0
	Abu-Tartour Harbour	Min	0	65	1	78589	281	52	10	4	1	0
		Max	34	98	2	90146	578	117	22	28	12	1
		Avg.	9	90	1	84367	387	78	14	15	6	1
	Touristic Harbour	Min	0	79	0	92457	200	40	10	22	0	0
		Max	21	98	3	104014	620	361	756	81	5	1
		Avg.	8	91	1	98236	401	138	199	41	3	0
Hurghada City	north Safer Hotel	Min	1	90	0	106326	77	21	5	14	2	0
		Max	10	99	2	117883	245	110	37	35	22	1
		Avg.	5	95	1	112104	153	50	15	23	9	1
	Hurghada Harbor	Min	1	57	0	120194	164	10	6	18	7	0
		Max	40	96	7	129440	353	82	58	52	10	1
		Avg.	18	79	3	124817	257	42	25	31	8	1
	NIOF area	Min	0	78	0	43917	162	17	7	5	2	0
		Max	20	99	3	62409	534	39	14	32	9	1
		Avg.	13	86	1	53163	326	29	10	17	5	1
Ras Gharib City	General Beach	Min	0	85	0	16180	68	14	5	12	2	0
		Max	15	100	0	27737	218	50	12	15	8	2
		Avg.	7	93	0	21959	121	26	7	13	5	1
	El-Sakala area	Min	0	74	0	2311	81	16	5	8	1	1
		Max	26	100	1	13869	108	46	12	67	8	1
		Avg.	11	88	0	8090	96	27	9	30	5	1
	General Company of	Min	0	72	0	30049	96	20	5	8	3	1
		Max	28	100	2	41606	181	37	17	29	10	1
		Avg.	11	88	1	35827	129	25	9	16	4	1

Sediments of the investigated beach and intertidal bottoms facies are composed of over 83% sand Table (3.13). Very fine sand, fine sand and medium sand are the most dominant the beach sediments, whereas coarse sand and very coarse sand are the most abundant fractions in the intertidal sediment. While the gravel and mud reach up to an average 13% in gravel. Mud is less in the beach samples than in the intertidal sediments reach up to an average 2%

### 3.2 Carbonates (Carb.)

The average carbonates content in the studied sediments varies from 13.4 % at Touristic Harbor to 75.6 % at north Flminko Village Table, (3.14). North Flaminko Village area recorded the highest values of carbonat contents compared with the studied areas. It is due to terrestrial materials from erosion boundary limestone rock and biogenic from accumulation of skeletal grains. On the other hand, the principal sources of carbonate in marine sediment are:

- 1- Inorganic chemical precipitation.
- 2- Residual from weathering of limestone rock on the sea floor.
- 3- Terrestrial rock. and
- 4- Biogenic from accumulation of skeletal grains

**Table 3.14:** Geochemical characteristics (Carb. %, TOM % and O.C. %) of marine sediments from shoreline for all samples.

	El Edua area				Quseir Harbor				N. Flaminko Village		
Sa. No.	Carb. %	TOM %	O.C. %	Sa. No.	Carb. %	TOM %	O.C. %	Sa. No.	Carb. %	TOM %	O.C. %
<b>Min</b>	12.1	15.8	8.8	<b>Min</b>	17.5	4.9	2.7	<b>Min</b>	67.4	5.2	2.9
<b>Max</b>	61.5	34.4	19.1	<b>Max</b>	83.3	22.0	12.2	<b>Max</b>	81.0	7.5	4.2
<b>Avg.</b>	32.7	24.3	13.5	<b>Avg.</b>	50.8	13.3	7.4	<b>Avg.</b>	75.6	6.5	3.6
Km 17 Mangrove area				Abu Tartour Harbor				Touristic Harbor			
Sa. No.	Carb. %	TOM %	O.C. %	Sa. No.	Carb. %	TOM %	O.C. %	Sa. No.	Carb. %	TOM %	O.C. %
<b>Min</b>	35.7	4.7	2.6	<b>Min</b>	24.4	2.4	1.3	<b>Min</b>	7.0	2.3	1.3
<b>Max</b>	90.8	13.7	7.6	<b>Max</b>	44.4	4.8	2.7	<b>Max</b>	21.3	4.9	2.7
<b>Avg.</b>	60.5	8.4	4.7	<b>Avg.</b>	36.1	3.8	2.1	<b>Avg.</b>	13.4	3.6	2.0
North Safier Hotel				Hurghada Harbor				NIOF area			
Sa. No.	Carb. %	TOM %	O.C. %	Sa. No.	Carb. %	TOM %	O.C. %	Sa. No.	Carb. %	TOM %	O.C. %
<b>Min</b>	14.6	6.9	3.8	<b>Min</b>	27.9	4.0	2.2	<b>Min</b>	36.0	3.1	1.7
<b>Max</b>	66.1	14.4	8.0	<b>Max</b>	63.9	63.5	35.3	<b>Max</b>	60.9	42.4	23.5
<b>Avg.</b>	40.2	11.3	6.3	<b>Avg.</b>	47.9	23.0	12.8	<b>Avg.</b>	48.8	18.7	10.4
El Sakala area				General Beach				General Company of petroleum			
Sa. No.	Carb. %	TOM %	O.C. %	Sa. No.	Carb. %	TOM %	O.C. %	Sa. No.	Carb. %	TOM %	O.C. %
<b>Min</b>	36.5	4.6	2.6	<b>Min</b>	37.6	2.8	1.6	<b>Min</b>	32.3	13.8	7.6
<b>Max</b>	54.4	24.5	13.6	<b>Max</b>	64.5	4.7	2.6	<b>Max</b>	63.5	27.9	15.5
<b>Avg.</b>	47.6	12.3	6.8	<b>Avg.</b>	53.1	3.9	2.1	<b>Avg.</b>	52.0	22.8	12.7

### 3.3 Total Organic Matter(TOM) And Organic Carbon(OC)

Organic matter affects the aquatic ecosystem by interacting with inorganic matter to form complex compounds, which include in its structure several other elements. It also serves as a source of food for several animal groups (Beltagy and Mussa, 1984). In general, the beach sediments of this area have average values of organic carbon that range from 1.3 % in (Abu Tartour Harbor) to 12.8% in (Hurghada Harbor) and total organic matter content which varies from 3.6% in (Touristic Harbor) to 30 %. The content of organic matter in intertidal sediment varies from 6.84 % at north Flaminko Village area to 24.3 % in (El Edua area) Table (3.14). El-Edua area and Hurghada Harbour recorded the highest values of organic matter content compared with other area. The aerial distribution of the organic matter shown a general decrease toward the north. (Mansour, 1999 and Mansour et al.,2000) attributed the high content of the organic matter in tidal flat sediments to the terrigenous flux. Also, they recorded that the terrestrial materials rich in organic matter and the high organic productivity are the two main reasons for the higher organic matter content.

### 3.4 Heavy Metals Distribution

In the present work, marine sediments from area under investigation analyzed to detect the concentration and distribution of Seven metals (Fe, Mn, Ni, Zn, Cu, Pb and Cd) in order to understand the effect of human action and natural unputs on the quality of marine sediments, and the relation between it and radionuclides of  $^{226}\text{Ra}$  and  $^{232}\text{Th}$  and  $^{40}\text{K}$  Table (3.13).

The Seven heavy metals (Fe, Mn, Zn, Cu, Pb, Ni and Cd) showed a wide range of concentrations. Average Fe concentration in marine sediments varies between 4908  $\mu\text{g g}^{-1}$  at (north Flaminko area) and 124817  $\mu\text{g g}^{-1}$  at (Hurghada Harbor). In the same manner Mn level ranges from average 96  $\mu\text{g g}^{-1}$  at El-Sakala area to 740  $\mu\text{g g}^{-1}$  at Quseir Harbour. The association of iron and manganese is well known; (Jeffery, 1975) reported that in the igneous silicate rocks, Mn is present in divalent state associated with ferromagnesium and accessory iron minerals. There are many sources for iron and manganese transfer to the marine environment. Fe and Mn transfer to the marine environment naturally by Wadis (Madkour, 2005). Quseir Harbour recorded the highest values compared with the other studied area due to shipment of mineral products from phosphate mines in the Eastern Desert in the past time.

Obviously, the concentration of heavy metals (Zn and Cu) recorded high values in Touristic Harbour compared with the studied areas. Obviously, the concentration of heavy metals (Pb, Ni and Cd) recorded high average values in Quseir Harbour compared with the studied areas as we shown in Table (3.13). A number of anthropogenic activities in Touristic Harbour and Quseir Harbour are the main reasonable sources for the high heavy metals contents.

From the Permissible Levels of heavy metals ( $\mu\text{g g}^{-1}$ ) for marine Sediments Quality Guidelines according to Canadian, Ontario and Florida Guidelines Table (3.15) (Bennet and Cubbage,

1991; Persaud et al., 1990; MacDonald et al., 1996) we found Fe exceed the Severe Effect Level (SEL) in almost study areas. Also Cu is exceed the (SEL) in Touristic Harbour, while Pb, Cd and Ni are reach the Probable Effect Level (PEL) in Quseir Harbour, while in the rest stations in the Threshold Effect Level (TEL).

**Table 3.15:** Permissible Levels of heavy metals ( $\mu\text{g g}^{-1}$ ) for Marine Sediments Quality Guidelines according to Canadian, Ontario and Florida Guidelines (Bennet and Cubbage, 1991; Persaud et al., 1990; MacDonald et al., 1996)

Metals	Levels of heavy metals ( $\mu\text{g g}^{-1}$ )		
	TEL	PEL	SEL
Cd	0.6 - 0.7	4.21	10
Cu	16 - 18.7	108	110
Ni	15.9 – 16	42.8	75
Zn	120 – 124	271	820
Pb	30.2 - 46.7	112	250
Mn	460	–	1110
Fe	20000	–	40000

Where: **TEL:** The Threshold Effect Level, **PEL:** The Probable Effect Level, **SEL:** The Severe Effect Level

The correlation coefficient between  $^{226}\text{Ra}$ ,  $^{232}\text{Th}$  and  $^{40}\text{K}$  with Gravel, in all cities have been calculated and listed in Table (3.16). we can see there is positive correlation except Qusier. While we see negative correlation between radioactive material with sand, mud and OC% except in Gharib city we found positive correlation between  $^{226}\text{Ra}$  and  $^{232}\text{Th}$  and  $^{40}\text{K}$  with Gravel, mud and OC%. This indicated that there is contaminations by oil industries in Ras Ghareb as it appear in Table (3.16).

**Table 3.16:** Correlation coefficients between Natural Radioactive Materials and sediments type and geochemical analyses in marine sediments at the study areas.

	$^{226}\text{Ra}$	$^{232}\text{Th}$	$^{40}\text{K}$	Gravel	Sand	Mud	Carb.%	OC%
<b>Quseir City</b>								
$^{226}\text{Ra}$	1							
$^{232}\text{Th}$	0.706	1						
$^{40}\text{K}$	0.008	0.278	1					
Gravel	-0.055	-0.216	-0.218	1				
Sand	0.063	0.244	0.210	-0.988	1			
Mud	-0.027	-0.078	0.133	-0.470	0.328	1		
Carb.%	0.261	0.147	-0.240	0.071	-0.060	-0.091	1	
OC%	-0.144	-0.067	0.162	0.015	-0.017	0.009	-0.654	1
	$^{226}\text{Ra}$	$^{232}\text{Th}$	$^{40}\text{K}$	Gravel	Sand	Mud	Carb.%	OC%
<b>Safaga City</b>								
$^{226}\text{Ra}$	1							
$^{232}\text{Th}$	0.540	1						
$^{40}\text{K}$	0.062	0.252	1					

Gravel	0.163	0.045	0.115	1				
Sand	-0.128	-0.043	-0.089	-0.983	1			
Mud	-0.197	-0.015	-0.151	-0.191	0.007	1		
Carb.%	-0.164	-0.215	-0.663	0.180	-0.206	0.124	1	
OC%	-0.337	-0.092	-0.495	-0.086	0.030	0.303	0.468	1
	<sup>226</sup> Ra	<sup>232</sup> Th	<sup>40</sup> K	Gravel	Sand	Mud	Carb.%	OC%
<b>Hurghada City</b>								
<sup>226</sup> Ra	1							
<sup>232</sup> Th	0.589	1						
<sup>40</sup> K	0.542	0.323	1					
Gravel	0.056	-0.039	0.125	1				
Sand	-0.031	0.088	-0.084	-0.989	1			
Mud	-0.148	-0.331	-0.237	0.182	-0.328	1		
Carb.%	-0.170	-0.127	-0.048	-0.085	0.037	0.294	1	
OC%	-0.027	0.201	0.189	-0.015	0.012	0.017	0.346	1
	<sup>226</sup> Ra	<sup>232</sup> Th	<sup>40</sup> K	Gravel	Sand	Mud	Carb.%	OC%
<b>Ras Gharib City</b>								
<sup>226</sup> Ra	1							
<sup>232</sup> Th	0.878	1						
<sup>40</sup> K	0.477	0.519	1					
Gravel	0.094	0.158	-0.110	1				
Sand	-0.106	-0.180	0.089	-0.998	1			
Mud	0.169	0.349	0.318	-0.137	0.080	1		
Carb.%	-0.082	0.071	0.271	-0.418	0.380	0.673	1	
OC%	0.237	0.153	0.198	-0.115	0.085	0.563	0.292	1

The comparison includes for every two-size parameters, in order to use the grain size characters as a tool discriminates between different environments. The correlation coefficients of the studied localities are computed Table (3.16) in order to clarify the parameters studied some give positive and other give negative correlation's, with variable order of magnitude in both cases. The correlation coefficients of the sediments of study areas indicates that radiation elements (<sup>226</sup>Ra, <sup>232</sup>Th and <sup>40</sup>K) are observed weak correlated with carbonate, TOM and gravel, sand and mud fractions

In Qusier city we see from Table (3.17) significant negative correlation between radioactivity and (Mn), while we see positive correlation between Natural radioactive materials with (Fe, Zn, Cu, Pb, Ni and Cd)

In Safaga city Table (3.17), we can find positive correlation between <sup>226</sup>Ra and <sup>40</sup>K with all heavy metals except Mn have a negative correlation with <sup>226</sup>Ra. Now we can say <sup>40</sup>K has the highest value in safaga city. In case of <sup>232</sup>Th, it negatively correlated with (Fe, Mn and Ni) and positively correlated with (Zn, Cu, Pb and Cd)

In Hurghada city Table (3.17) the relationships showed that <sup>226</sup>Ra is positively correlated with all heavy metals except (Fe and Zn) also <sup>232</sup>Th is positively correlated with all heavy metals except (Fe and Pb), while <sup>40</sup>K negatively correlated with all heavy metals except (Pb), So we can say this indicated that, <sup>226</sup>Ra and <sup>232</sup>Th concentration are almostly high in Hurghada city.

**Table 3.17:** Correlation coefficients between Natural Radioactive Materials and heavy metals in marine sediments at the study areas.

	$^{226}\text{Ra}$	$^{232}\text{Th}$	$^{40}\text{K}$	$\text{Fe}$	$\text{Mn}$	$\text{Zn}$	$\text{Cu}$	$\text{Pb}$	$\text{Ni}$	$\text{Cd}$
<b>Quseir City</b>										
$^{226}\text{Ra}$	1									
$^{232}\text{Th}$	0.706	1								
$^{40}\text{K}$	0.008	0.278	1							
$\text{Fe}$	0.008	-0.227	0.308	1						
$\text{Mn}$	-0.019	-0.042	0.477	0.769	1					
$\text{Zn}$	0.112	0.084	0.506	0.850	0.922	1				
$\text{Cu}$	0.147	0.004	0.278	0.815	0.737	0.815	1			
$\text{Pb}$	0.226	0.089	0.307	0.825	0.802	0.854	0.893	1		
$\text{Ni}$	0.056	-0.015	0.337	0.870	0.863	0.943	0.883	0.842	1	
$\text{Cd}$	0.058	0.129	0.572	0.720	0.880	0.922	0.809	0.774	0.874	1
	$^{226}\text{Ra}$	$^{232}\text{Th}$	$^{40}\text{K}$	$\text{Fe}$	$\text{Mn}$	$\text{Zn}$	$\text{Cu}$	$\text{Pb}$	$\text{Ni}$	$\text{Cd}$
<b>Safaga City</b>										
$^{226}\text{Ra}$	1									
$^{232}\text{Th}$	0.540	1								
$^{40}\text{K}$	0.062	0.252	1							
$\text{Fe}$	0.204	0.102	0.586	1						
$\text{Mn}$	-0.216	0.115	0.009	-0.243	1					
$\text{Zn}$	0.423	0.313	-0.137	0.462	-0.262	1				
$\text{Cu}$	0.275	0.153	-0.200	0.399	-0.412	0.952	1			
$\text{Pb}$	0.394	0.241	0.103	0.524	-0.350	0.798	0.833	1		
$\text{Ni}$	-0.304	-0.111	-0.525	-0.756	0.478	-0.272	-0.271	-0.479	1	
$\text{Cd}$	0.105	0.128	0.047	0.220	0.212	0.142	-0.007	-0.268	-0.040	1
	$^{226}\text{Ra}$	$^{232}\text{Th}$	$^{40}\text{K}$	$\text{Fe}$	$\text{Mn}$	$\text{Zn}$	$\text{Cu}$	$\text{Pb}$	$\text{Ni}$	$\text{Cd}$
<b>Hurghada City</b>										
$^{226}\text{Ra}$	1									
$^{232}\text{Th}$	0.589	1								
$^{40}\text{K}$	0.542	0.323	1							
$\text{Fe}$	-0.499	-0.201	0.054	1						
$\text{Mn}$	0.467	0.174	-0.017	-0.441	1					
$\text{Zn}$	-0.015	0.067	-0.157	0.269	0.128	1				
$\text{Cu}$	0.139	0.123	-0.035	0.317	0.100	0.226	1			
$\text{Pb}$	0.062	-0.067	0.218	0.429	-0.030	0.140	0.770	1		
$\text{Ni}$	0.056	0.341	-0.004	0.379	0.045	0.710	0.604	0.383	1	
$\text{Cd}$	0.030	0.155	-0.195	-0.048	0.077	-0.067	0.264	0.274	0.126	1
	$^{226}\text{Ra}$	$^{232}\text{Th}$	$^{40}\text{K}$	$\text{Fe}$	$\text{Mn}$	$\text{Zn}$	$\text{Cu}$	$\text{Pb}$	$\text{Ni}$	$\text{Cd}$
<b>Ras Gharib City</b>										
$^{226}\text{Ra}$	1									
$^{232}\text{Th}$	0.878	1								
$^{40}\text{K}$	0.477	0.519	1							
$\text{Fe}$	0.111	0.040	0.073	1						
$\text{Mn}$	0.423	0.237	-0.039	0.286	1					
$\text{Zn}$	0.386	0.132	0.243	0.023	0.489	1				
$\text{Cu}$	0.147	0.028	0.051	0.042	0.235	0.690	1			
$\text{Pb}$	-0.087	-0.147	-0.219	-0.300	-0.140	0.300	0.485	1		
$\text{Ni}$	-0.100	-0.170	-0.036	-0.071	0.229	0.183	0.290	0.057	1	
$\text{Cd}$	-0.046	0.314	0.153	-0.102	-0.311	-0.252	-0.092	0.171	-0.148	1

In Ras Ghareb city the relationships showed that  $^{226}\text{Ra}$  and  $^{232}\text{Th}$  are positively correlated with (Fe, Mn, Zn and Cu) and negatively correlated with (Pb and Ni) while we can see  $^{40}\text{K}$  positively correlated with (Fe, Zn, Cu and Cd) and negatively correlated with (Mn, Pb and Ni) as we can see in Table (3.17)

The results of correlation coefficient illustrated in Table (3.17) show weak positive and negative correlation between ( $^{226}\text{Ra}$ ,  $^{232}\text{Th}$  and  $^{40}\text{K}$ ) and heavy metals except with Mn observed high positive correlation in Hurghada and Ras Ghareb but shows weak positive correlation in Safaga and Quseir Cities. This is due to the total heavy metals concentrations in the surface sediments of the studied localities appears to be controlled primarily by variations in lithogenic and biogenic admixtures of sediments.

#### 4 Conclusions

The Red Sea recourses contribute substantially to Egypt's economy, particularly in the areas of oil production, tourism, and navigation by Suez Canal and fisheries. The purpose of this work is to provide a baseline map of radioactivity background levels in the investigated area along the Egyptian Red Sea coast due to their importance in assessing potential environmental hazards resulting from natural inputs and the irrational human activities. In this study, Eighty four sediment samples have been collected from four selected localities; Quseir City, Safaga City, Hurghada City and Ras Ghareb City. Each area divided into three stations. Each station divided into number of transects nearly perpendicular to the shoreline where cover the areas under study. The conclusions of our study can be summarized in the following points

- 1) The average activities of  $^{226}\text{Ra}$ ,  $^{232}\text{Th}$  and  $^{40}\text{K}$  in Quseir harbors are higher than those in north and south Quseir.
- 2) The results in Safaga city show that, the average activity of  $^{226}\text{Ra}$  and  $^{232}\text{Th}$  (22 and 19 Bqkg<sup>-1</sup>) are less than the compared worldwide average, while  $^{40}\text{K}$  (478 Bqkg<sup>-1</sup>) is higher than the compared worldwide average value of these radionuclides in the sediment (UNSCEAR, 2000).
- 3) The average activities of  $^{226}\text{Ra}$ ,  $^{232}\text{Th}$  (19 and 15 Bqkg<sup>-1</sup>) in Hurghada city lower than the worldwide average values, while average activity of  $^{40}\text{K}$  (432 Bqkg<sup>-1</sup>) in this city is closed to the worldwide average (UNSCEAR, 2000).
- 4) The average activities of  $^{226}\text{Ra}$ ,  $^{232}\text{Th}$  (28 and 24 Bqkg<sup>-1</sup>) in Gharib city lower than the worldwide average values, while average activity of  $^{40}\text{K}$  (381 Bqkg<sup>-1</sup>) in this city is closed to the worldwide average (UNSCEAR, 2000).
- 5) All maximum values of activities of  $^{226}\text{Ra}$ ,  $^{232}\text{Th}$  and  $^{40}\text{K}$  in twelve station under investigation are higher than the worldwide average allowed, this indicate to significant radiation hazards arising in these stations.



- 6) There are a pollution in each of the stations (Abu Tartour Harbor, Touristic Harbor, Hurghada Harbor, NIOF area, General Beach and General Company of petroleum) ,because the average activity of  $^{40}\text{K}$  is higher than the worldwide average value of these radionuclides in the sediment (UNSCEAR, 2000)
- 7) Generally, Ras Gharib coast along Red Sea is relatively contaminated.
- 8) The Average results of the radiological hazard indices indicate that the radiological characteristics of the sediments samples do not present a significant radiological risk.
- 9) Qusier Harbor recoded the highest average value concentration of heavy metals (Mn=740, Pb=49, Ni=49 and Cd=2  $\mu\text{gg}^{-1}$ ) and the highest value of activity concentration of  $^{226}\text{Ra}$  and  $^{232}\text{Th}$  (58, 47)  $\text{BqKg}^{-1}$ , respectively.
- 10) Touristic Harbor recorded the highest average value of (Zn=138 and Cu=199  $\mu\text{gg}^{-1}$ ).
- 11) Hurghada Harbor recorded the highest average value of (Fe=124817  $\mu\text{gg}^{-1}$ ). And highest average values of Mud=3%, Gravel=18% and the highest value of activity concentration of  $^{40}\text{K}$  (950  $\text{Bq kg}^{-1}$ ) respectively.

## References

- Abbadly G.E Adel., M.A.M. Uosif and A. El-Taher, (2005). Natural radioactivity and dose assessment for phosphate rocks from Wadi El-Mashash and El-Mahamid Mines, Egypt. *Journal of Environmental Radioactivity* 84, 65-78
- Abd El Raoof, A., (2004). Geoenvironmental map of the Red Sea coast from Hurghada to Halayeb. Report No. 2, the Egyptian Mineral Resources Authority.
- Adloff, J.-P. and Guillaumont, R., (1993). *Fundamentals of Radiochemistry*, London: CRC Press Inc.
- Allisy, A., (1996). "Henri Becquerel: The discovery of radioactivity", *Becquerel's Legacy: A Century of Radioactivity*. Proceedings of a Conference, London: Nuclear Technology Publishing, pp. 3-10.
- Anon, (1980). *Red Sea and Gulf of Aden Pilot*. 12<sup>th</sup> (ed.), Publ. Hydrographic of the navy, Somerset, England, p. 284.
- ASTM, (1983). American Society for Testing Materials Standard method for sampling surface soils for radionuclides. Report No. C (Philadelphia, PA: ASTM) pp. 983–998.
- ASTM, (1986). American Society for Testing Materials. Recommended practice for investigation and sampling soil and rock for engineering purposes. Report No. D (Philadelphia, PA: ASTM) Ann. Book of ASTM Standards (04.08) 420; pp. 109–113
- Behairy, A. K. A.; Sheppard, C. R. C., and El-Sayed, M. K., (1992). A review of the geology of coral reefs in the Red Sea. *UNEP Regional Seas Reports and Studies*, 152, 1-32.
- Bennet, J. B.; and Cabbage, J., (1991). *Summary of Criteria and Guidelines for Contaminated Freshwater Sediments*. Washington State Department of Ecology, Olympia, WA.
- Beretka, J., Mathew, P.J., (1985), *Natural Radioactivity of Australian Building Materials, Industrial Wastes and By-products*. *Health Physics* 48, 87–95.
- Braithwaite, C.J.R., (1973). Setting behavior related to sieve analysis of skeletal sands. *Sedimentology* 20, 251–262.
- Brenner M, Binford, MW., (1988). Relationships between concentrations of sedimentary variables and tropic state in Florida lakes. *Can J Fish Aquat Sci.*; 45, 294–300.
- Burcham, W.E. (1973). *Nuclear Physics: An Introduction* (2nd edition), Harlow: Longman.
- Carver, R. E., (1971). *Procedures in sedimentary petrology*. John Wiley and Sons, p. 653.
- Cember, H. and Johnson, T.E., (2009). *Introduction to Health Physics* (4th edition), New York: McGraw-Hill Companies, Inc.
- Chester, R., Lin, F.G., Basaham, A.S., (1994). Trace metals solid state speciation changes associated with the down-column fluxes of oceanic particulates. *Geol. Soc. London* 151, 351–360.
- Choppin, G., Liljenzin, J. and Rydberg, J., (2002). *Radiochemistry and Nuclear Chemistry* (3rd edition), USA: Butterworth-Heinemann.
- Curie, M., Debierne, A., Eve, A.S., Geiger, H., Hahn, O., Lind, S.C., Meyer, St., Rutherford, E. and Schweidler, E., (1931). "The Radioactive Constants as of 1930 Report of the International Radium-Standard Commission", *Review of Modern Physics* 3, 427-445.

- Curve Expert 1.3, (1995-2003): A comprehensive curve fitting system for Windows Copyright (c), Daniel Hyams
- Das, A. and Ferbel, T., (2003). Introduction to Nuclear and Particle Physics (2nd edition), London: World Scientific.
- Dean Jr EW., (1974). Determination of carbonate and organic matter in calcareous sediments and sedimentary rocks by loss in ignition: comparison with other methods. *J Sediment Petrol.*; 44, 242–248.
- Debertin, K. and Helmer, R.G., (1988). Gamma and X-Ray Spectrometry with Semiconductor Detectors, Amsterdam: Elsevier Science Publishers B.V.
- Edwards, A. J., and Head, S. M., (1987). Red Sea. Pergamon Press, Oxford, p. 441.
- Eisenbud, M. and Gesell, T., (1997). Environmental Radioactivity from Natural, Industrial, and Military Sources (4th edition), London: Academic Press.
- El-Gezeery, M. V., and Marsouk, I. M., (1974). Miocene rock stratigraphy of Egypt. *Egypt. J. Geol.*, 18, 1–59.
- El-Mamoney, M.H., (1995). Evaluation of terrestrial contribution to the Red Sea sediments, Egypt, Ph. D. Thesis, Faculty of science, Alex. Univ., p. 146.
- El-Sabh, M. I., and Beltagy, A. I., (1983). Hydrography and chemistry of the Gulf of Suez during September 1966. *Bull. Inst Oceanogr. And Fish. Egypt*, 9, 73-78.
- El-Sayed, M. Kh., (1984). Reefal sediments of Al-Ghardaqa, Northern Red Sea Egypt. *Mar. Geol.*, 56, 259-271.
- El-Taher, A., and Madkour, H. A., (2011). Distribution and environmental impacts of metals and natural radionuclides in marine sediments in-front of different wadies mouth along the Egyptian Red Sea coast. *Applied Radiation and Isotopes*, 69, 550-558
- European Commission, (2000). Radiological Protection Principles Concerning the Natural Radioactivity of Building Materials (Radiation Protection 112). Office for Official Publications of the EC.
- Faires, R.A. and Boswell, G.G.J., (1981). Radioisotope Laboratory Techniques (4<sup>th</sup> edition), London: Butterworth & Co (Publishers) Ltd.
- Flannery SM, Snodgrass DR, Whitmore JT., (1982). Deepwater sediments and tropic conditions in Florida lakes. *Hydrobiologia*. 92, 597–602.
- Friedman, G. M., and Krumbein, W. C., (1985). Hypersalins ecosystems. *The Gavish sabkha*. X., Berlin-Heidelberg, p. 484.
- Gass, I. G., (1977). The evolution of the pan african crystalline basement in NE africa and arabia. *Journal of the geological society*, London, 134, 129-38.
- GENIE-2000 Basic Spectroscopy (Standalone), (1997). Canberra Industries, Inc., V1.2A Copyright (c).
- G. Suresh, V. Ramasamy, V. Meenakshisundaram, R. Venkatachalapathy and V. Ponnusamy, (2011). Relationship between the natural radioactivity and mineralogical composition of the Ponnaiyar river sediments, India. *Journal of Environmental Radioactivity* 102, 370-377.

- Gilmore, G.R., (2008). *Practical Gamma-ray Spectrometry* (2<sup>nd</sup> edition), Chichester: John Wiley & Sons Ltd.
- Grasshof K., (1969). A simultaneous multiple channel system for nutrient analysis in sea water with analog and digital data record. In: *Advances in automated analysis, Technicon symposia*, 1970, 133-145.
- Groeneveld, R.A., Meeden, G., (1984). Measuring skewness and kurtosis. *The Statistician*. 33, (4), 391–399.
- Halliday, D. (1955), *Introductory Nuclear Physics* (2nd edition), New York: Johnson Wiley & Sons Inc.
- Hanna, R. G.; Saad, M. A., and Kandeel, M. M., (1988). Hydrographical studies on the Red Sea water in front of Hurghada. *Marine Mesopotamica*, 3/2, 139-156.
- Harvey, B.G., (1969). *Introduction to Nuclear Physics and Chemistry* (2nd edition), New Jersey: Prentice-Hall Inc.
- Hastings S., Doug R., Ensslin N. and Kreiner S., (1991). *Passive Nondestructive assay of Nuclear Materials*, LANL, Los Alamos, pp. 27-63.
- Head, S. M., (1987). Corals and coral reefs of the Red Sea. In: Edwards, A.J. & Head, S.M., (eds.), *Key Environments: Red Sea*. Pergamon Press (Oxford: England), p. 128-151.
- Hamed, M. A. F., (1992). *Seawater quality at the northern part of the Gulf of Suez and the nearby area of the Suez Canal*, M.Sc. Thesis, Faculty of Science, El-Mansoura University.
- Huy, N.Q. and Luyen, T.V., (2006). “Study in external exposure doses from terrestrial radioactivity in Southern Vietnam.” *Radiation protection Dosimetry Journal*, 118 (3), 331-336.
- IAEA, (2005). International Atomic Energy Agency, “IAEA-TECDOC-1472”, *Proceedings of an international Conference on Naturally Occurring Radioactive Materials (NORM IV)*, Poland: IAEA, Vienna.
- IAEA, (2003). International Atomic Energy Agency. “Extent of Environmental Contamination by Naturally Occurring Radioactive Material (NORM) and Technological Options for Mitigation”, *Technical Reports Series No.419*, IAEA, Vienna.
- ICRP-60, (1991). International Commission on Radiological Protection *Recommendations of the International Commission on Radiological Protection*. *Annals of the ICRP* 21, 1–3.
- International Commission on Radiological Protection, (1991). “Radiation Protection”, ICRP Publication 60. Elmsford, NY: Pergamon Press, Inc.
- Issa, S.A.M., (2013). Radiometric assessment of natural radioactivity levels of agricultural soil samples collected in Dakahlia, Egypt. *Radiation Protection Dosimetry*, 156, 59-67.
- Issawi, B.; Francis, M.; Mehanna, A. and El-Deftar, T., (1971). Geology of Safaga – Quseir coastal plain and of Mohamed Rabah area. *Ann. Geol. Surv. Egypt*, 1, 1-20.
- James, P. M., (1991). *Principles, methods, and applications of particle size analysis*. Cambridge University Press. Cambridge, 3/5, p. 229.
- Jeffery, P. G., (1975). *Chemical methods of rock analysis*. (2<sup>nd</sup> edition), pergamon press, Oxford, p. 525
- Kaplan, I., (1962). *Nuclear Physics* (2<sup>nd</sup> edition), USA: Addison-Wesley Publishing Company, Inc.

- Khedr, E. S., (1989). Recent coastal sabkhas from the Red Sea: a model of sabkhaization. *Egypt. J. Geol.*, 33/ (1-2), 87-120.
- Klement, A.W., (1982). *CRC Handbook of Environmental Radiation*, Florida: CRC Press, Inc.
- Knoll, G. F., (2000). *Radiation Detection and Measurement* (3<sup>rd</sup> edition), USA: John Wiley & Sons Inc.
- Krane, K. S., (1988). *Introductory Nuclear Physics*, Chichester: John Wiley & Sons Inc.
- Lapp, R.E. and Andrews, H.L., (1972). *Nuclear Radiation Physics* (4<sup>th</sup> edition), London: Sir Isaac Pitman and Sons Ltd.
- Larsson staffan, (2002). "Issue-based Dialogue Management." PhD Thesis, Goteborg University.
- Lilley, J., (2001). *Nuclear Physics: Principles and Applications*, Chichester: John Wiley & Sons, Ltd.
- L'Annunziata, M. F., (2007). *Radioactivity: Introduction and History*, Amsterdam: Elsevier B.V.
- Madkour, H. A. and Dar, M., (2007). The anthropogenic effects of the human activities on the Red Sea coast at Hurghada harbour (case study). *Egyptian Journal of Aquatic Research*. Vol. 33 (1), 43-58.
- Madkour, H. A. and Ahmed, N. A., (2006). The environmental impacts of the Red Sea coast at Quseir District, Red Sea, Egypt. *The 3<sup>rd</sup>. Int. Conf. for Develop. and the Env. in the Arab World*, March, 21 (23), p. 733-757.
- Madkour, H. A., (2005). Geochemical and environmental studies of recent marine sediments and some hard corals of Wadi El-Gemal area of the Red Sea, Egypt. *Egyptian Journal of Aquatic Research*, 31/1, 69-91.
- Madkour, H. A., (2004). Geochemical and environmental studies of recent marine sediments and some invertebrates of the Red Sea, Egypt. Ph. D. Thesis, Fac., of Sci., South Valley University, p. 33.
- MacDonald, D. D.; Carr, R. S.; Calder, F. D.; Long, E. R. and Ingersoll, C. G., (1996). Development and evaluation of sediment quality guidelines for Florida coastal waters. *Ecotoxicology*, 5, 253-278
- Maiklem, W.R., (1968). Some hydraulic properties of bioclastic carbonate grains. *Sedimentology* 10, 101-109.
- Mamont-Ciesla, K., Gwiazdowski, B., Biernacka, M. and Zak, A., (1982). Radioactivity of building materials in Poland. In: Vohra, G., Pillai, K. C. and Sadavisan, S., Eds. *Natural Radiation Environment*. Halsted Press, p. 551.
- Mansour, A. M; Nawar, A. H., and Mohamed, A W., (2000). Geochemistry of coastal marine sediments and their contaminant metals, Red Sea, Egypt: A legacy for the future and a tracer to modern sediment dynamics. *Sedimentology of Egypt*, 8, 231-242.
- Mansour, A.M., (1999). Changes of sediment nature by environmental impacts of Sharm Abu Makkdeg area, Red Sea, Egypt. *Sedimentology of Egypt*. V. 7, 25-36.
- Mansour, A.M., (1995). Sedimentary facies and carbonate-siliciclastic transition of Sharm El Bahari and Sharm El Qibli, Red Sea, Egypt. *Egypt. Jour. Geol.* 39/1, 57-76.

- Merdanoğlu B. and Altinsoy N., (2006). "Radioactivity concentration and Dose Assessment for Soil Samples from Kestanbol Granite Area, Turkey", *Radiation Protection Dosimetry*, 121, 399-405.
- Meshal, A. H., (1970). Water pollution in Suez Bay. *Bull. Inst. Oceanogr. Fish., Egypt*, 1, 463–473.
- Mohammed, E. E., (1988). Circulation patterns and hydrographic structure of the southern Red Sea and Gulf of Aden. Ph. D. Thesis, Alex. Univ., p. 220.
- Morcos, S. A., (1970). Physical and chemical oceanography of the Red Sea. *Oceanogr. Mar. Bial. Ann. Rev.*, 8, 73-202.
- Morsy, Z., El-Wahab., Magda Abd., El-Faramawy., Nabil., (2012). Determination of natural radioactive elements in Abo Zaabal, Egypt by means of gamma spectroscopy. *Ann. Nucl. Energy*, 44, 8-11
- Moussa, A. A., Moussa, K. A. and El-Mamony, A. H., (1986). Beach sediments and littoral processes along the Red Sea coast of Egypt. *Bull. Inst. Oceanogr. and Fish. Egypt*, 12, 301-313.
- Murty, T.S., El Sabh, M.I., (1984). Storm tracks, storm surges and sea state in the Arabian Gulf, Strait of Hormuz and the Gulf of Oman. *UNESCO Report Mar Sci* 28,12-24.
- NCRP, (1985). National Council on Radiation Protection and Measurements, "A Handbook of Radioactivity Measurements Procedures (2nd edition)", NCRP Report No.58. NCRP, Maryland.
- NCRP, (1977). National Council on Radiation Protection and Measurements, "Environmental Radiation Measurement", NCRP Report No.50.
- NCRP, (1975). National Council on Radiation Protection and Measurements, "Natural Background Radiation in the United States", NCRP Report No.45. NCRP, Washington, D.C.
- NEA-OECD, (1979). Nuclear Energy Agency. Exposure to radiation from natural radioactivity in building materials. Report by NEA Group of Experts. OECD, Paris.
- Noorddin Ibrahim, (1999). Natural activities of  $^{238}\text{U}$ ,  $^{232}\text{Th}$  and  $^{40}\text{K}$  in building materials. *Journal of Environmental Radioactivity* 43, 255-258.
- Noz, M. E. and Maguire Jr., G. Q., (2007). *Radiation Protection in the Health Sciences*, London: World Scientific Publishing Co. Pte. Ltd.
- Ormond, R. and Edwards, A., (1987). Red Sea fishes. Key environments – Red Sea (ed. by A.J. Edwards and S.M. Head), pp. 251–287. Pergamon Press, Oxford.
- Persaud, D.; Jaagumagi, R. and Hayton, A., (1990). The provincial sediment quality guidelines. Ontario Ministry of the Environment.
- Piller, W. E. and Pervesler, P., (1989). The Northern Bay of Safaga (Red Sea, Egypt): an actuopalaeontoloical approach. I. Topography and Bottom Facies. *Beitr. Palaöntologie, Österr*, 15, 103-147, Wien.
- Prince, J.H., (1979). "Comments on Equilibrium, Transient Equilibrium, and Secular Equilibrium in Serial Radioactive Decay", *Journal of Nuclear Medicine* 20, 162-164.
- Ravisankar, R., Vanasundari, K., Suganya, M., Raghu, Y., Rajalakshmi, A., Chandrasekaran, A., Sivakumar, S., Chandramohan, J., Vijayagopal, P., Venkatraman, B., (2014). Multivariate

- statistical analysis of radiological data of building materials used in Tiruvannamalai, Tamilnadu, India. *Appl. Radiat. Isot.* 85, 114–127.
- Red Sea Governorate web site, (2015). (<http://www.redsea.gov.eg/t/default.aspx>) on 01/01/2015.
- Reuss U., W. Westmeier, (1983). *At. Data Nucl. Data Tables* 29
- Robinson, J., Herbert, D., (2002). “Integrating Climate change and Sustainable Development.” *Climate Change and Its Linkages with Development, Equity, and Sustainability*, Colombo, Sri Lanka, Intergovernmental Panel on climate Change.
- Ross, D. A., (1983). The Red Sea. In: B. H. Ketchum (Eds), *Estuaries and enclosed seas*, 293-308. Elsevier, Amsterdam
- Saad, M. A. H., (1978). A study on the mixed waters between lake Idku and the Mediterranean Sea. *Bull. Off. Natu. Peche Tunisie*, 2 (1-2): 347-354.
- Said, R., (1962). *Geology of Egypt*. Elsevier, Amsterdam, p 377.
- S. Tavernier, (2010). *Experimental Techniques in Nuclear and Particle Physics*. DOI 10.1007/978-3-642-00829-0\_3, Springer-Verlag Berlin Heidelberg
- Said, R., (1970). General stratigraphy of the adjacent land area of the Red Sea: *Royal Soc. London Philos. Trans.*, A267, 71-81.
- Shams A. M. Issa, M. A. M. Uosif, Mahmoud Tammam, and Reda Elsaman, (2014). A comparative study of the radiological hazard in sediments samples from drinking water purification plants supplied from different sources. *Journal of Radiation Research and Applied Sciences* 7(1), 80-94.
- Shams A. M Issa and A.M.A. Mostafa, (2014). Distribution of natural radionuclide and radiation hazards of building materials used in Assiut, Egypt. *Isotopes in Environmental & Health Studies*,
- Shams ISSA, Mohamed UOSIF and Reda ELSAMAN, (2013). Gamma radioactivity measurements in Nile River sediment samples, *Turkish Journal of Engineering & Environmental Sciences* 37 (1), 109 – 122.
- Sheppard, C.; Price, A., and Roberts, C., (1992). *Marine ecology of the Arabian region: patterns and processes in the extreme tropical environments*. London, UK, Academic press, p. 359.
- Shukri, N. M., (1945). Bottom deposits of the Red Sea. *Nature* 155, 306.
- Siedler, G., (1969). General circulation of water masses in the Red Sea. In: Degenes and Davied A. Ross “Hot brines and recent heavy metal deposits in the Red Sea”. Edited by Egont.. Springer-Verlag New York Inc., 131-138.
- Soliman, G. F., (1996). Simulation of water circulation in the Suez Bay and its hydrographic features during winter and summer. The 6<sup>th</sup> Conf. of the Envi. Prot. is a Must. Nat. Oceanogr. And Fish., Euro-Arab Cooperation Center, Inter. Sci. Asso. and Soci. Fund for Development, 400– 433.
- Smith, W. H. F., and Sandwell, D. T., (1997). Global seafloor topography from satellite altimetry and ship depth soundings, *Science*, 277, 1957-1962.
- Stampfli, G. M.; Mosar, J.; Favre, P.; Pillecuit, A., and Vannay, J. C., (2001). Permo-Mesozoic evolution of the western Tethys realm: the Neo- Tethys East Mediterranean Basin connection. In P.A. Ziegler, W. Cavazza, A.H.F. Robertson, and S. Crasquin-Soleau.



- PeriTethys memoir 6: Peritethyan rift/wrench basins and passive margins. IGCP 369. Mém. Museum Nat. Hist. Nat. 186, 51–108.
- Tsoufanidis, N., (1995). Measurement and detection of radiation, 2nd Ed. Taylor & Francis, London, pp. 211-232
- Turner, J.E., (2007). Atoms, Radiation, and Radiation Protection (3rd edition), Weinheim: Wiley-VCH.
- UNSCEAR, (2000). United Nations Scientific Committee on the Effects of Atomic Radiation. “Sources and Effects of Ionizing Radiation”, UNSCEAR 2000 Report Vol.1 to the General Assembly, with scientific annexes, United Nations Sales Publication, United Nations, New York.
- UNSCEAR, (1993). United Nations Scientific Committee on the Effects of Atomic Sources and Effects of Ionizing Radiation. Report to General Assembly, with Scientific Annexes. United Nations, New York
- UNSCEAR, (1988). United Nations Scientific Committee on the Effects of Atomic Radiation, Sources, Effects and Risks of Ionizing Radiation. United Nations, New York.
- Uosif M. A. M., Mahmoud Tammam, Shams A. M. Issa and Reda Elsaman, (2012). Naturally Occurring Radionuclides in Sludge Samples from Some Egyptian Drinking Water Purification Stations. International Journal of Advanced Science and Technology 42, 69-81.
- Uosif, M. A. M., (2007). Gamma-Ray spectroscopic Analysis Of Selected Samples From Nile River Sediments In Upper Egypt. Radiation protection dosimetry 123, No.2, 215-220.
- Uosif M. A. M., and A. El-Taher, (2005). Comparison of Total Experimental and Theoretical Absolute  $\gamma$ -ray Detection Efficiencies of a Cylindrical NaI(Tl) Crystal. Arab Journal of Nuclear Science and Applications 38, 27- 30.
- Wafaa Rashed, (2012). “Radiation Measurements and Radiological Effects of Some Environments and Radiological Effects of Some Environmental Samples from Tushka Area-South Egypt.” PhD Thesis, Assiut University.
- Watson, S. J., Jones, A. L., Oatway, W. B. and Hughes, J. S., (2005). “Ionising Radiation Exposure of the UK population, Health Protection Agency, Centre for Radiation, Chemical and Environmental Hazards, Radiation Protection Division, Chilton, Didcot, Oxfordshire, OX11 0RQ, UK
- Wattenberg, H., (1933). Das chemische Beobachtungsmaterial – Kalziumkarbonate’ und kohlenzureichhalt des Meer Wassers. Wissensch. Ergbn. D.” deutschen Atlantischen Exped.” Auf des Forsch. Undvermessungsschiff “Meteor” (1925-1927).
- William, B.; Philippe, H., and Ken, M., (2005). The Red Sea and Gulf of Aden basins. Journal of African Earth Sciences, 43: 334–378.
- Wilson, A. J. and L. M. Scott, (1992). Characterization of Radioactive Petroleum Piping Scale with an Evaluation of Subsequent Land Contamination. Health physics, 63 (6), 681-685.
- Wilson, W. F. (1994). A Guide to Naturally Occurring Radioactive Material, Oklahoma: Pennwell Books.
- World Nuclear Association, (2011). “Radiation and Nuclear Energy”,



<http://www.world-nuclear.org/info/inf30.html> [Updated August 2011]

Yu, K.N., Guan, Z.J., Stokes, M.J., Young, E.C.M., (1992). The assessment of natural radiation dose committed to Hong Kong people. *Journal of Environmental Radioactivity*, 17, 31.

Zaidi, J.H., Arif, M., Ahmed, S., Fatima, I. and Qureshi, I. H., (1999). "Determination of natural radioactivity in Building materials used in the Rawalpindi/ Islamabad area by  $\gamma$ -ray spectrometry and instrumental neutron activation analysis." *Applied Radiation and Isotopes Journal*, 51, 559-564.